High-Frequency Scattering by an Impenetrable Sphere[*]

H. M. NUSSENZVEIG[†]

Courant Institute of Mathematical Sciences, New York University, New York, New York

The scattering of a scalar plane wave by a totally reflecting sphere (hard-core potential) at high frequencies is treated by a modified Watson transformation. The behavior of the solution both in the near and far regions of space is discussed, as well as the accuracy and domain of applicability of the WKB approximation and classical diffraction theory. It is shown that different transformations are required in the forward and backward half-spaces, and corresponding integral representations for the primary wave are derived. The transformations are rigorously proved and the convergence of the residue series is discussed. In the shadow region, the physical interpretation of the complex angular momentum poles in terms of surface waves is in agreement with Keller's geometrical theory of diffraction. In the lit region, sufficiently far from the shadow boundary, the WKB expansion for the wave function is confirmed up to the second order. On the surface of the sphere, Kirchhoff's approximation is accurate, except in the penumbra region, where the behavior is described by Fock's function. The diffraction effects in the neighborhood of the shadow boundary are investigated and the corrections to classical diffraction theory are obtained. The shift of the shadow boundary is evaluated. The expression for the wave function in the Fresnel-Lommel region is derived and applied to the discussion of the Poisson spot and the behavior near the axis. The total scattering amplitude is evaluated for all angles, including the neighborhood of the forward and backward directions. The corrections to the forward diffraction peak and the transition to the region of geometrical reflection are discussed. The modified Watson transformation is also applied directly to the scattering amplitude. The connection between representations valid in different regions is established.

I. INTRODUCTION

The problem to be considered is the scattering of a scalar plane wave by a totally reflecting sphere at high frequencies. This means not only that $ka \gg 1$, but also that $(ka)^{1/3} \gg 1$, where k is the wave number and a is the radius of the

sphere. It will be attempted to make the treatment both rigorous and compre-
hensive, including a discussion of the near and far regions and a comparison of
the results with the WKB approximation and classical diffraction theory.

The wave function can be interpreted either as the velocity potential of sound
waves, corresponding to an acoustically soft sphere, or as the Schrödinger wave
function in nonrelativistic quantum mechanics, in which case it corresponds to
a hard-core potential. In both cases, the boundary condition is the vanishing of
the wave function on the surface of the sphere. There is no difficulty in extending
the treatment to a vector wave field, so as to represent electromagnetic scattering
from a perfectly conducting sphere.

This is perhaps the simplest problem involving a finite size scatterer, and its
exact solution in the form of a partial-wave series has been known for a long
time. It is also well known that this form of the solution becomes useless at high
frequencies, because of the large number of terms one would have to keep in
order to get a good approximation.

The way out of this difficulty was proposed by Watson (1), who transformed
the partial-wave series into a "residue series," which is rapidly convergent at
high frequencies. Several applications of this transformation to the theory of
radio wave propagation around the Earth were made by Van der Pol and Brem-
mer (2).

Watson's procedure applies only to the shadow region behind the sphere, and
not to the lit region. An extension of the treatment to the lit region was made
by Fock (3) and later reformulated by Franz (4, 5).

As will be shown in Section VI, this treatment is also incomplete, for it does
not apply to the backward half-space. A certain amount of confusion seems to
exist in the literature concerning the application of Watson's transformation in
the lit region.

Recently, interest in Watson's transformation has been renewed, in connection
with Regge's work on complex angular momentum in potential scattering and
its applications to elementary-particle physics (6).

In view of this, as well as of its intrinsic interest, a reexamination of the
totally reflecting sphere problem seems warranted. Since this is the simplest
problem of its kind, it should also serve as a model for the extension to more
complicated situations, such as different refractive indices and different shapes.
The case of a transparent sphere, which has numerous applications to optics
and nuclear physics, will be treated in a subsequent paper.

In the present work, Watson's transformation will be reformulated in such a
way that it becomes applicable both in the forward and in the backward half-
space, and in particular in the neighborhood of the forward and backward
directions. For this purpose, new integral representations of the primary wave
will be derived in Section II.

A rigorous proof of Watson's transformation and the convergence of the residue series will be given in Sections III and IV. The physical interpretation of the results in the shadow region will be discussed in Section V. In Section VI, the nearby lit region, excluding the neighborhood of the shadow boundary, will be considered. It will be shown that the solution in this region agrees with the WKB approximation up to the second order.

The diffraction effects arising in the transition between lit and shadow regions will be examined in Section VII, where the results derived from the exact solution will be compared with classical diffraction theory. The shift of the shadow boundary will also be investigated.

At greater distances from the sphere, but still in the near region, the wave function resembles the classical solution to the problem of diffraction by a circular disc, as will be shown in Section VIII. The well-known Poisson spot effect, as well as the behavior near the axis, will also be studied. Finally, in Section IX, expressions for the scattering amplitude in all directions will be derived.

The main results and conclusions derived from the present treatment will be summarized in Section X. Some of them are not new, but have been included here for completeness. The basic mathematical tools employed will be presented in Appendices A to F.

II. WATSON'S TRANSFORMATION

A. THE TOTAL WAVE FUNCTION

Let the incident plane wave be given by

$$\psi_i(r, \theta) = \exp\ (ikr\cos\theta) = \sum_{l=0}^{\infty}\ (2l + 1)i^l j_l(kr)P_l(\cos\theta), \qquad (2.1)$$

where j_l is the spherical Bessel function of order l and $P_l(\cos\theta)$ is the lth Legendre polynomial.

The solution of our problem is given by the well-known partial-wave expansion

$$\psi(r, \theta) = \frac{1}{2}\sum_{l=0}^{\infty}\ (2l + 1)i^l[h_l^{(2)}(\rho) + S_l(\beta)h_l^{(1)}(\rho)]P_l(\cos\theta), \qquad (2.2)$$

where the S-function $S_l(\beta)$ is determined by the boundary condition $\psi(a, \theta) = 0$:

$$S_l(\beta) = -h_l^{(2)}(\beta)/h_l^{(1)}(\beta), \qquad (2.3)$$

and we have introduced the notations

$$\rho = kr, \qquad \beta = ka. \qquad (2.4)$$

It is well known that at high frequencies one can associate with the lth par-

tial wave an "impact parameter"

$$p_l = (l + \tfrac{1}{2})/k \tag{2.5}$$

and all partial waves with $p_l \lesssim a$ are strongly affected by the scatterer. Thus, the number of terms one has to keep in the partial-wave expansion is of the order of $\beta \gg 1$, so that (2.2) becomes useless at high frequencies.

Watson's transformation is based upon the following formula:

$$\sum_{l=0}^{\infty} f\left(l + \frac{1}{2}\right) = \frac{1}{2} \int_C f(\lambda)\, \frac{\exp\,(-i\pi\lambda)}{\cos\,\pi\lambda}\, d\lambda, \tag{2.6}$$

where C is the contour shown in Fig. 1. This formula can easily be checked by taking the residues of the integrand at the physical (half-integral) values of λ.

Clearly, there is a large degree of arbitrariness in (2.6). For instance, the factor $(\cos\,\pi\lambda)^{-1}$ might have been replaced by any analytic function having poles with the same residues as this factor at the physical points. The only restrictions to which the "interpolating" function $f(\lambda)$ is subject are that it must reproduce $f(l + \tfrac{1}{2})$ at the physical points and that it must be regular in a neighborhood of the real axis, so that the integral can be computed by residues in the indicated manner. There is usually a wide class of functions satisfying these conditions.

The choice of $f(\lambda)$ is dictated in practice by the requirement of appropriate behavior at infinity in the λ plane, since the next step in Watson's transformation will consist in the deformation of contour C away from the real axis. In Field Theory, this leads to a unique continuation, with the help of Carlson's theorem (6).

This result does not apply in the present case. However, only two alternative
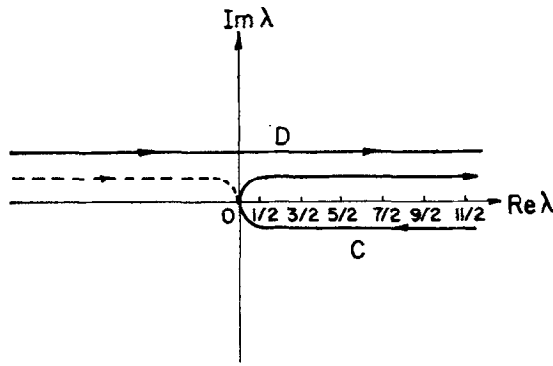

Fig. 1. Paths of integration in the λ plane.

choices of $f(\lambda)$ will be required. The first one leads to

$$\psi(r, \theta) = \int_C f(\lambda, \beta, \rho) P_{\lambda-1/2}(\cos \theta) e^{-i\lambda\pi/2} \frac{\lambda \, d\lambda}{\cos \pi\lambda}, \qquad (2.7)$$

where

$$\begin{aligned} f(\lambda, \beta, \rho) &= \frac{1}{2} \left(\frac{\pi}{2\rho}\right)^{1/2} e^{-i\pi/4} \left[H_\lambda^{(2)}(\rho) - \frac{H_\lambda^{(2)}(\beta)}{H_\lambda^{(1)}(\beta)} H_\lambda^{(1)}(\rho) \right] \\ &= \frac{1}{2} \left(\frac{\pi}{2\rho}\right)^{1/2} e^{-i\pi/4} \frac{g(\lambda, \beta, \rho)}{H_\lambda^{(1)}(\beta)}, \end{aligned} \qquad (2.8)$$

with

$$g(\lambda, \beta, \rho) = H_\lambda^{(1)}(\beta)H_\lambda^{(2)}(\rho) - H_\lambda^{(2)}(\beta)H_\lambda^{(1)}(\rho). \qquad (2.9)$$

In this expression, $P_{\lambda-1/2}$ is Legendre's function of the first kind and we have employed the relation $h_l(x) = (\pi/2x)^{1/2}H_{l+1/2}(x)$ between spherical and cylindrical functions.

The other choice is based on the relation

$$P_l(-\cos \theta) = (-1)^l P_l(\cos \theta), \qquad (2.10)$$

which holds for integral l, and leads to

$$\psi(r, \theta) = -i \int_C f(\lambda, \beta, \rho) P_{\lambda-1/2}(-\cos \theta) e^{i\lambda\pi/2} \frac{\lambda \, d\lambda}{\cos \pi\lambda}. \qquad (2.11)$$

B. POISSON'S SUM FORMULA

We shall now consider an alternative transformation,[1] based on Poisson's sum formula (7), which, for our purposes, may be written as follows:

$$\sum_{l=0}^{\infty} f\left(l + \frac{1}{2}\right) = \sum_{m=-\infty}^{\infty} (-1)^m \int_0^{\infty} f(\lambda) e^{2im\pi\lambda} \, d\lambda. \qquad (2.12)$$

Applying this to (2.2), we get

$$\psi(r, \theta) = 2 \sum_{m=-\infty}^{\infty} (-1)^m \int_0^{\infty} f(\lambda, \beta, \rho) P_{\lambda-1/2}(\cos \theta)$$
$$\exp\left[i\pi\lambda \left(2m + \frac{1}{2}\right)\right] \lambda \, d\lambda. \qquad (2.13)$$

Substituting λ by $-\lambda$ in the integrals for $m = -1$ to $-\infty$ and making use

---

[1] This transformation seems to have been first employed by Bremmer (2, p. 210). It was subsequently adopted by several authors.

of the properties

$$P_{-\lambda-1/2}(\cos\,\theta)\ =\ P_{\lambda-1/2}(\cos\,\theta), \tag{2.14}$$

$$H^{(1)}_{-\lambda}(x)\ =\ e^{i\pi\lambda}H^{(1)}_{\lambda}(x), \qquad H^{(2)}_{-\lambda}(x)\ =\ e^{-i\pi\lambda}H^{(2)}_{\lambda}(x), \tag{2.15}$$

we find that (2.13) can be rewritten as

$$\psi(r,\,\theta)\ =\ \sum_{m=0}^{\infty}\,\psi_m(r,\,\theta), \tag{2.16}$$

where

$$\psi_m(r,\,\theta)\ =\ 2(-1)^m\int_{-\infty}^{\infty}f(\lambda,\,\beta,\,\rho)P_{\lambda-1/2}(\cos\,\theta)\,\exp\,[i\pi\lambda\,(2m\,+\,\tfrac{1}{2})]\,\lambda\;d\lambda. \tag{2.17}$$

This result is equivalent to (2.7). In fact, according to (2.14) and (2.15), the integrand of (2.7) is an odd function of λ, so that the lower half of contour C may be replaced by its reflection about the origin, shown in broken line in Fig. 1. Accordingly, contour C is equivalent to the straight line D located above the real axis. On D, the following expansion is valid:

$$\frac{e^{-i\lambda\pi/2}}{\cos\,\pi\lambda}\ =\ 2e^{i\lambda\pi/2}\sum_{m=0}^{\infty}\,(-1)^m e^{2im\pi\lambda}. \tag{2.18}$$

Substituting this result in (2.7), we are led to (2.16). It will be seen later that (2.16) is a more convenient form for several purposes.

C. The Incident Wave

We shall now apply Watson's transformation to the incident wave (2.1). The resulting expressions will play an important role later on.

A derivation similar to that of (2.7) and (2.11) leads to the representations

$$e^{i\rho\cos\theta}\ =\ \left(\frac{\pi}{2\rho}\right)^{1/2}e^{-i\pi/4}\int_C\,J_\lambda(\rho)G_1(\lambda,\,\theta)\;d\lambda, \tag{2.19}$$

$$e^{i\rho\cos\theta}\ =\ \left(\frac{\pi}{2\rho}\right)^{1/2}e^{-i\pi/4}\int_C\,J_\lambda(\rho)G_2(\lambda,\,\theta)\;d\lambda, \tag{2.20}$$

where

$$G_1(\lambda,\,\theta)\ =\ \lambda e^{-i\lambda\pi/2}P_{\lambda-1/2}(\cos\,\theta)/\cos\,\pi\lambda, \tag{2.21}$$

$$G_2(\lambda,\,\theta)\ =\ -i\lambda e^{i\lambda\pi/2}P_{\lambda-1/2}(-\cos\,\theta)/\cos\,\pi\lambda. \tag{2.22}$$

The next step is to deform contour C into a contour that is symmetrical about the origin. For this purpose, we must find the asymptotic behavior of the integrand at infinity in the λ-plane.

The asymptotic behavior of the cylindrical and Legendre functions is discussed

in Appendices A and C, respectively. According to (A.6),

$$J_\lambda(\rho) \approx \left(\frac{1}{2\pi\lambda}\right)^{1/2} \left(\frac{e\rho}{2\lambda}\right)^\lambda \qquad (\mid \lambda \mid \to \infty) \quad (2.23)$$

and, according to (C.8),

$$G_1(\lambda, \theta) \approx (2\lambda/\pi \sin \theta)^{1/2} \exp\left[i\lambda\left(\frac{\pi}{2} - \theta\right) + i\frac{\pi}{4}\right] \quad (\mid \lambda \mid \to \infty \text{ in } I_+),$$

$$\approx (2\lambda/\pi \sin \theta)^{1/2} \exp\left[-i\lambda\left(\frac{3\pi}{2} - \theta\right) - i\frac{\pi}{4}\right] \qquad (2.24)$$

$$(\mid \lambda \mid \to \infty \text{ in } I_-),$$

$$G_2(\lambda, \theta) \approx (2\lambda/\pi \sin \theta)^{1/2} \exp\left[i\lambda\left(\frac{\pi}{2} + \theta\right) - i\frac{\pi}{4}\right] \quad (\mid \lambda \mid \to \infty \text{ in } I_+),$$

$$\approx -(2\lambda/\pi \sin \theta)^{1/2} \exp\left[i\lambda\left(\frac{\pi}{2} - \theta\right) + i\frac{\pi}{4}\right] \quad (\mid \lambda \mid \to \infty \text{ in } I_-), \qquad (2.25)$$

where I_+ and I_- denote the upper and the lower half of the λ-plane, respectively.

It follows from these results that contour C may be freely deformed in the right half-plane, except possibly along directions approaching that of the imaginary axis. To study the behavior along such directions, let us introduce the notations

$$\sigma = i \exp (i\epsilon) = \exp\left[i\left(\frac{\pi}{2} + \epsilon\right)\right], \qquad (2.26)$$

$$\eta = \epsilon \ln \mid 2\lambda/e\rho \mid \qquad (2.27)$$

and let us consider the behavior of the integrand when $\lambda \to \pm\sigma\infty$ and simultaneously $\epsilon \to 0$ in such a way that η approaches a constant value.

The curves $\lambda = \sigma\mid\lambda\mid$, $\eta \to -\pi/2$ and $\lambda = -\sigma\mid\lambda\mid$, $\eta \to \pi/2$ for large $\mid\lambda\mid$ are shown in broken lines in Fig. 2 and Fig. 3. According to Appendix A, the function $J_\lambda(\rho)$ approaches zero to the right of these curves, and so do the integrands of (2.19) and (2.20), so that it suffices to consider their behavior to the left of the curves. In this region, (2.23) to (2.25) imply

$$\frac{\pi}{2} (\sin \theta)^{1/2} \mid J_\lambda(\rho)G_1(\lambda, \theta) \mid \approx \exp\left[\mid \lambda \mid(\eta + \theta)\right] \text{ for } \lambda \to \sigma\infty,$$

$$\approx \exp\left[-\mid \lambda \mid (\eta - \theta + \pi)\right] \text{for} \lambda \to -\sigma\infty, \qquad (2.28)$$

and

$$\frac{\pi}{2} (\sin \theta)^{1/2} \mid J_\lambda(\rho)G_2(\lambda, \theta)\mid \approx \exp\left[\mid \lambda \mid(\eta - \theta)\right] \text{ for } \lambda \to \sigma\infty,$$

$$\approx \exp\left[-\mid \lambda \mid(\eta + \theta - \pi)\right] \text{for} \lambda \to -\sigma\infty. \qquad (2.29)$$

FIG. 2. The path of integration in (2.19) must begin and end at infinity to the right of
the shaded regions. A possible path that is symmetrical about the origin is shown $(\theta < \pi/2)$.
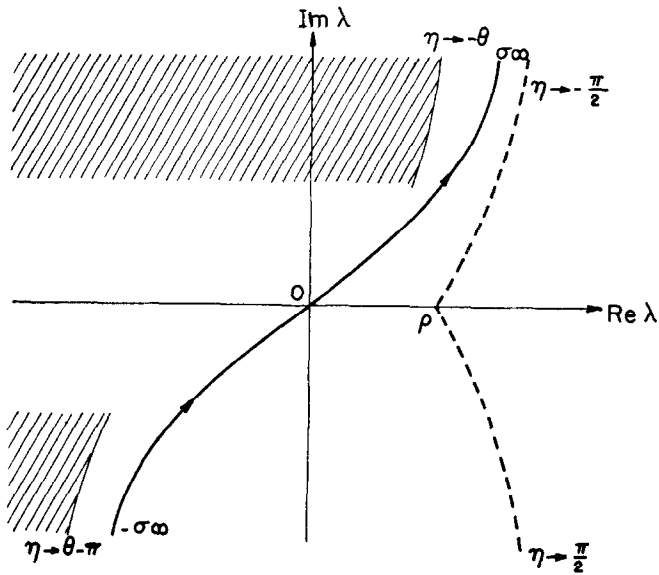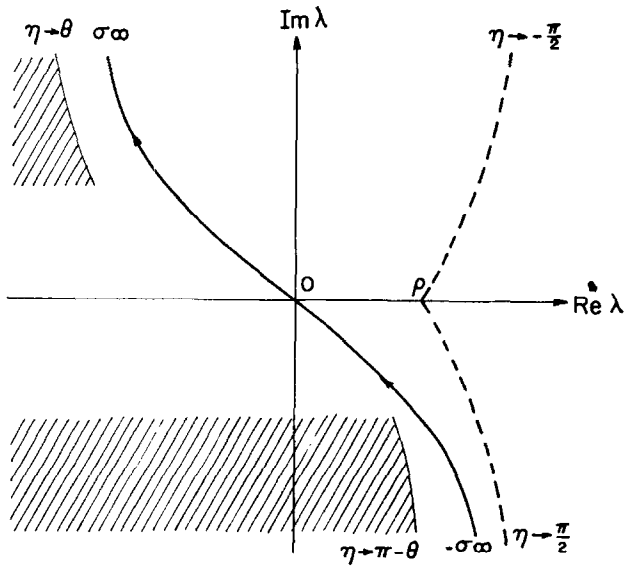

FIG. 3. The path of integration in (2.20) must begin and end at infinity to the right of
the shaded regions. A possible path that is symmetrical about the origin is shown $(\theta > \pi/2)$.

It follows from these results that the path of integration in (2.19) may be deformed at will, provided that it stays asymptotically to the right of the shaded regions in Fig. 2. A symmetric path of integration can be found, as shown in Fig. 2, provided that the corresponding η satisfies

$$\theta - \pi < \eta < -\theta, \tag{2.30}$$

which is only possible for $\theta < \pi/2$.

Similarly, as shown in Fig. 3, a symmetric path of integration can be found in (2.20), provided that the corresponding η satisfies

$$\pi - \theta < \eta < \theta, \tag{2.31}$$

which is only possible for $\theta > \pi/2$.

We shall therefore take (2.19) with the path of Fig. 2 for $\theta < \pi/2$, and (2.20) with the path of Fig. 3 for $\theta > \pi/2$. Making the substitution $\lambda \rightarrow -\lambda$ in the integrals from $-\sigma\infty$ to 0 and employing (2.14) as well as the identities

$$J_\lambda(\rho) - e^{i\pi\lambda}J_{-\lambda}(\rho) = -ie^{i\pi\lambda} \sin \pi\lambda H_\lambda^{(1)}(\rho), \tag{2.32}$$

$$J_\lambda(\rho) - e^{-i\pi\lambda}J_{-\lambda}(\rho) = ie^{-i\pi\lambda} \sin \pi\lambda H_\lambda^{(2)}(\rho), \tag{2.33}$$

we finally get the integral representations[2]

$$e^{i\rho\cos\theta} = -\left(\frac{\pi}{2\rho}\right)^{1/2} e^{i\pi/4} \int_0^{\sigma\infty} H_\lambda^{(1)}(\rho)P_{\lambda-1/2}(\cos \theta)e^{i\lambda\pi/2} \tan(\pi\lambda)\lambda \, d\lambda$$
$$\cdot \left(\theta < \frac{\pi}{2}\right), \tag{2.34}$$

$$e^{i\rho\cos\theta} = \left(\frac{\pi}{2\rho}\right)^{1/2} e^{-i\pi/4} \int_0^{\sigma\infty} H_\lambda^{(2)}(\rho)P_{\lambda-1/2}(-\cos \theta) \, e^{-i\lambda\pi/2} \tan (\pi\lambda)\lambda \, d\lambda$$
$$\cdot \left(\theta > \frac{\pi}{2}\right), \tag{2.35}$$

the corresponding paths of integration being those shown in Fig. 2 and in Fig. 3, respectively.

III. THE POLES OF THE S-FUNCTION

In order to deform the path of integration in (2.7) and (2.11) away from the real axis, we need information about the singularities of the integrand in the λ-plane. The integrand is a meromorphic function of λ, and its poles are the poles of the S-function

$$S(\lambda, \beta) = -H_\lambda^{(2)}(\beta)/H_\lambda^{(1)}(\beta), \tag{3.1}$$

[2] An integral representation related to (2.34), but involving trigonometric instead of Legendre functions, was given by Franz and Galle (8).

which are the roots $\lambda_n(\beta)$ of the equation

$$H_\lambda^{(1)}(\beta) = 0. \tag{3.2}$$

They might be called the Regge poles for the hard sphere problem, although they do not show the typical Regge behavior characteristic of Yukawa-type potentials.

The roots of (3.2) have been discussed by several authors (2, 4, 9, 10). We are only interested in their behavior for large values of β.

It follows from (2.15) that the roots are symmetrically distributed with respect to the origin, so that it suffices to consider them in the right half-plane. In this region, there exists an infinite number of roots, all located in the first quadrant, close to the curve h_1 defined by (cf. Appendix A):

$$\text{Re} \, [(\lambda^2 - \beta^2)^{1/2} - \lambda \cosh^{-1} (\lambda/\beta)] = 0. \tag{3.3}$$

This curve is shown in broken line in Fig. 4. It cuts the real λ axis at $\lambda = \beta$, at an angle of $\pi/3$, and tends to become parallel to the imaginary axis as $|\lambda| \to \infty$. All the roots are simple (9).

The roots of greatest physical importance are those closest to the real axis, which are located in the neighborhood of $\lambda = \beta$. In this region, we can use the expansion (A.17):

$$H_\lambda^{(1)}[\lambda - xe^{i\pi/3}(\lambda/2)^{1/3}] = 2e^{-i\pi/3}(2/\lambda)^{1/3}Ai(-x) + O(\lambda^{-1}). \tag{3.4}$$

Since the zeros of the Airy function are all located on the negative real axis, we get (4)

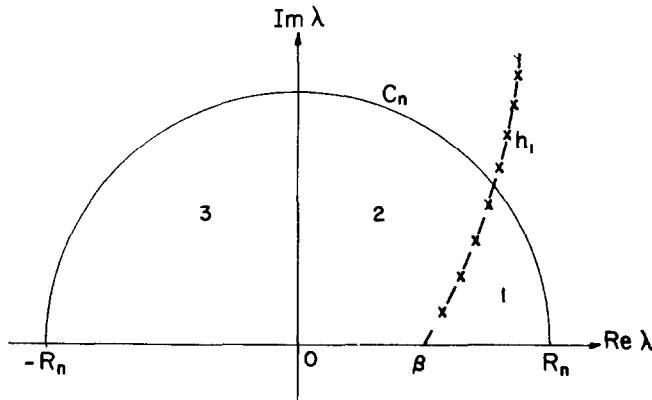$$\lambda_n(\beta) = \beta + (\beta/2)^{1/3}x_ne^{i\pi/3} + O(\beta^{-1/3}), \tag{3.5}$$

FIG. 4. $\times \times \times$—Poles of the S-function, located on curve h_1. The contour C_n passes half-way between consecutive poles.

where $-x_n$ is the nth zero of the Airy function. A table of the first five zeros is given in Appendix D. According to (D.7), we have, for large n,

$$\lambda_n(\beta) \approx \beta + \tfrac{1}{2}[3\pi(n - \tfrac{1}{4})]^{2/3} e^{i\pi/3}\beta^{1/3} \qquad (n \gg 1). \quad (3.6)$$

Let us finally consider the asymptotic behavior of the roots for $|\lambda| \to \infty$. In this region, the behavior of $H_\lambda^{(1)}$ in the neighborhood of h_1 is given by (A.7):

$$\begin{aligned}
H_\lambda^{(1)}(\beta) &\approx 2(2/\pi)^{1/2}(\lambda^2 - \beta^2)^{-1/4} e^{i\pi/4} \sinh\left[(\lambda^2 - \beta^2)^{1/2} \right. \\
&\left. -\lambda \ln\left(\frac{\lambda + (\lambda^2 - \beta^2)^{1/2}}{\beta}\right) - i\frac{\pi}{4}\right],
\end{aligned} \quad (3.7)$$

so that the roots are given by

$$\lambda_n \ln\left[\frac{\lambda_n + (\lambda_n^2 - \beta^2)^{1/2}}{\beta}\right] - (\lambda_n^2 - \beta^2)^{1/2} = i\left(n - \frac{1}{4}\right)\pi. \quad (3.8)$$

Let

$$\lambda_n = \rho_n \exp\left[i\left(\frac{\pi}{2} - \epsilon_n\right)\right], \qquad \rho_n \gg \beta^2. \quad (3.9)$$

Then, (3.8) gives

$$\epsilon_n \ln\left(2\rho_n/e\beta\right) \approx \pi/2, \quad (3.10)$$

where

$$\rho_n \ln\left(2\rho_n/e\beta\right) \approx (n - \tfrac{1}{4})\pi. \quad (3.11)$$

This equation may be solved by iteration. We find

$$\rho_n = \left(n - \frac{1}{4}\right)\pi \left\{\ln\left[\frac{2\pi(n - \tfrac{1}{4})}{e\beta}\right]\right\}^{-1} \left[1 + O\left(\frac{\ln \ln n}{\ln n}\right)\right], \quad (3.12)$$

so that (10)

$$\begin{aligned}
\lambda_n(\beta) &\approx \frac{i\pi(n - \tfrac{1}{4})}{\ln\,[2\pi(n - \tfrac{1}{4})/e\beta]} \exp\left\{\frac{-i\pi}{2\,\ln\,[2\pi(n - \tfrac{1}{4})/e\beta]}\right\} \\
&\cdot \left[1 + O\left(\frac{\ln \ln n}{\ln n}\right)\right] \qquad (|\lambda_n| \gg \beta^2).
\end{aligned} \quad (3.13)$$

Thus, both Re λ_n and Im λ_n approach infinity with n, but Re λ_n does so more slowly by an inverse logarithmic factor. Note also that $\lambda_n - \lambda_{n-1} = O[(\ln n)^{-1}]$, so that the roots cluster closer together as $n \to \infty$.

The residues of the S-function at its poles will also be required. According to

(3.1),

$$r_n(\beta) = \text{residue } S(\lambda, \beta)|_{\lambda=\lambda_n} = -H^{(2)}_{\lambda_n}(\beta) \left/ \frac{\partial}{\partial \lambda} H^{(1)}_{\lambda}(\beta)\right|_{\lambda=\lambda_n}. \qquad (3.14)$$

In the neighborhood of $\lambda = \beta$ we have, by (A.17),

$$H^{(2)}_{\lambda}[\lambda - xe^{i\pi/3}(\lambda/2)^{1/3}] = 2e^{i\pi/3}(2/\lambda)^{1/3}Ai(-xe^{2i\pi/3}) + O(\lambda^{-1}). \qquad (3.15)$$

It follows from (3.14), (3.15), (3.4), and (D.2) that

$$r_n(\beta) \approx \frac{e^{-i\pi/6}}{2\pi}\left(\frac{\beta}{2}\right)^{1/3}\frac{1}{[Ai'(-x_n)]^2} \qquad (3.16)$$

at the poles (3.5). Asymptotically, for $n \gg 1$, we may employ (D.8), which leads to

$$r_n \approx \frac{1}{2}e^{-i\pi/6}\beta^{1/3}[3\pi(n - \frac{1}{4})]^{-1/3} \qquad (n \gg 1). \quad (3.17)$$

Finally, let us consider the residues at the poles (3.13). In this region, $H^{(2)}_{\lambda}$ is given by (cf. Appendix A)

$$H^{(2)}_{\lambda}(\beta) \approx i\left(\frac{2}{\pi}\right)^{1/2}(\lambda^2 - \beta^2)^{-1/4}$$
$$\cdot \exp\left\{-(\lambda^2 - \beta^2)^{1/2} + \lambda\ln\left[\frac{\lambda + (\lambda^2 - \beta^2)^{1/2}}{\beta}\right]\right\} \qquad (3.18)$$

so that, according to (3.8),

$$H^{(2)}_{\lambda}(\beta) \approx (-1)^n e^{i\pi/4}(2/\pi)^{1/2}(\lambda_n^2 - \beta^2)^{-1/4}. \qquad (3.19)$$

Similarly, according to (3.7) and (3.8),

$$\partial H^{(1)}_{\lambda}(\beta)/\partial\lambda|_{\lambda=\lambda_n} \approx (-1)^{n+1}2e^{i\pi/4}(2/\pi)^{1/2}(\lambda_n^2 - \beta^2)^{-1/4}\ln\left[\frac{\lambda_n + (\lambda_n^2 - \beta^2)^{1/2}}{\beta}\right]. \quad (3.20)$$

It follows from these results that

$$r_n(\beta) \approx \frac{1}{2}\left\{\ln\left[\frac{2\pi(n - \frac{1}{4})}{e\beta}\right]\right\}^{-1}$$
$$\cdot \exp\left\{-\frac{i\pi}{2\ln[2\pi(n - \frac{1}{4})/e\beta]}\right\} \quad (|\lambda_n| \gg \beta^2), \qquad (3.21)$$

so that $r_n \to 0$ like $(\ln n)^{-1}$ for $n \to \infty$.

IV. THE RESIDUE SERIES

Let us consider the integral that appears in (2.17). We already know that the integrand has an infinite number of simple poles in the upper half-plane. Let

us now inquire under what conditions the integral is reducible to a series of residues taken at these poles. For this purpose, we must find a sequence of paths C_n passing between the poles and such that

$$\lim_{n\to\infty} \int_{C_n} f(\lambda, \beta, \rho) P_{\lambda-1/2}(\cos\theta) \exp\left[i\pi\lambda(2m + \tfrac{1}{2})\right] \lambda \, d\lambda = 0. \quad (4.1)$$

Let us consider the behavior of the integrand as $|\lambda| \to \infty$ in I_+. It is shown in Appendix B that

$$g(\lambda, \beta, \rho) \approx \frac{2i}{\pi\lambda}\left[\left(\frac{a}{r}\right)^\lambda - \left(\frac{r}{a}\right)^\lambda\right](|\lambda| \to \infty), \quad (4.2)$$

where g is given by (2.9).

According to Appendix A, the behavior of $H_\lambda^{(1)}(\beta)$ differs on the right and left of the curve h_1 (cf. (3.3)) where the poles are located. In regions 2 and 3 of Fig. 4, we have

$$H_\lambda^{(1)}(\beta) \approx \left(\frac{2}{\pi\lambda}\right)^{1/2}\left(\frac{e\beta}{2\lambda}\right)^\lambda, \quad (4.3)$$

whereas, in region 1,

$$H_\lambda^{(1)}(\beta) \approx -i\left(\frac{2}{\pi\lambda}\right)^{1/2}\left(\frac{2\lambda}{e\beta}\right)^\lambda. \quad (4.4)$$

In the neighborhood of h_1, according to (A.7), we must take the sum of both estimates:

$$H_\lambda^{(1)}(\beta) \approx 2\left(\frac{2}{\pi\lambda}\right)^{1/2} e^{i\pi/4} \sinh\left[\lambda \ln\left(\frac{e\beta}{2\lambda}\right) - i\frac{\pi}{4}\right]. \quad (4.5)$$

Let us exclude, for the moment, the directions $\theta = 0$ and $\theta = \pi$. Then, according to (C.8),

$$P_{\lambda-1/2}(\cos\theta) \approx (2\pi\lambda \sin\theta)^{-1/2} \exp\left(-i\lambda\theta + i\pi/4\right) (|\lambda| \to \infty \text{ in } I_+). \quad (4.6)$$

It follows from these results that, for $|\lambda| \to \infty$, the integrand of (4.1) behaves like

$$\exp\left[\lambda \ln\left(\frac{2\lambda}{e\rho}\right) + i\lambda\left(\frac{\pi}{2} - \theta\right) + 2im\pi\lambda\right] \text{ in region 3}, \quad (4.7)$$

$$\exp\left[\lambda \ln\left(\frac{2\lambda r}{eka^2}\right) + i\lambda\left(\frac{\pi}{2} - \theta\right) + 2im\pi\lambda\right] \text{ in region 2}, \quad (4.8)$$

$$\exp\left[-\lambda \ln\left(\frac{2\lambda}{e\rho}\right) + i\lambda\left(\frac{\pi}{2} - \theta\right) + 2im\pi\lambda\right] \text{ in region 1}, \quad (4.9)$$

except in the neighborhood of curve h_1, where it behaves like

$$K(\lambda) = \frac{\exp\left[\lambda \ln(r/a) + i\lambda\{(\pi/2) - \theta\} + 2im\pi\lambda\right]}{\sinh\left[\lambda \ln(2\lambda/e\beta) + i\,\pi/4\right]}. \tag{4.10}$$

It is readily seen that (4.7) approaches zero at least exponentially for all θ, $0 < \theta < \pi$; the same is true for (4.8) and (4.9) if $m \geqq 1$. However, for $m = 0$, (4.8) and (4.9) go to zero everywhere if and only if $\theta < \pi/2$.

Finally, near h_1, we have to avoid the poles, which are the zeros of the denominator of (4.10) (cf. (3.8)). For this purpose, we shall choose C_n as a half-circle of radius R_n passing half-way between consecutive poles, so that, for large n, we have, according to (3.11),

$$R_n \ln\left(\frac{2R_n}{e\beta}\right) + \frac{\pi}{4} = n\pi + \frac{\pi}{2}. \tag{4.11}$$

Then, in the neighborhood of h_1,

$$\lambda = R_n \exp\left[i\left(\frac{\pi}{2} - \epsilon\right)\right] \tag{4.12}$$

and, since

$$|\sinh(a + ib)| = (\sinh^2 a \cos^2 b + \cosh^2 a \sin^2 b)^{1/2} \geqq \cosh a |\sin b|, \tag{4.13}$$

it follows from (4.10) that

$$\begin{aligned}
|K(\lambda)| &\leqq \frac{\exp\left[-R_n[2m\pi + (\pi/2) - \theta - \epsilon \ln(r/a)]\right]}{\cosh\{R_n[\epsilon \ln(2R_n/e\beta) - (\pi/2)]\}} \\
&\leqq \exp\left[-R_n[2m\pi + (\pi/2) - \theta - \epsilon \ln(r/a)]\right].
\end{aligned} \tag{4.14}$$

Since $\epsilon \to 0$ along h_1 and its neighborhood,[3] we see that $K(\lambda)$ approaches zero exponentially for $0 < \theta < \pi$, $m \geqq 1$ and for $0 < \theta < \pi/2$ if $m = 0$.

Since $P_{\lambda-1/2}(1) = 1$, it is readily verified that all the above results remain true if $\theta = 0$. However, near $\theta = \pi$, we can no longer employ (2.17), since $P_{\lambda-1/2}(\cos\theta)$ has a logarithmic singularity at this point.

In conclusion, we see that (4.1) is valid for all $m \geqq 1$, $0 \leqq \theta < \pi$, but it is only valid for $0 \leqq \theta < \pi/2$ if $m = 0$. It then follows from (2.17) that

$$\begin{aligned}
\psi_m(r, \theta) = &(-1)^m\, 2\pi e^{i\pi/4}\left(\frac{\pi}{2\rho}\right)^{1/2} \\
&\cdot \sum_{n=1}^{\infty} \lambda_n\, r_n \exp\left[i\pi\lambda_n(2m + \tfrac{1}{2})\right] H_{\lambda_n}^{(1)}(\rho) P_{\lambda_n-1/2}(\cos\theta)
\end{aligned} \tag{4.15}$$

[3] For a discussion of the width of this neighborhood, see Appendix A.

provided that

$$m = 0, \quad 0 \leqq \theta < \frac{\pi}{2} \quad \text{or} \quad m \geqq 1, \quad 0 \leqq \theta < \pi, \tag{4.16}$$

where $\lambda_n(\beta)$ are the poles of $S(\lambda, \beta)$ and $r_n(\beta)$ is defined by (3.14).

One can verify directly, with the help of (3.13) and (3.21), that, for $n \to \infty$, the nth-order term of (4.15) behaves, in absolute value, like

$$\exp\left\{-\frac{n\pi}{2\ln(2n\pi/e\beta)}\left[2m\pi + \frac{\pi}{2} - \theta - \frac{\pi\ln(r/a)}{2\ln(2n\pi/e\beta)}\right]\right\},$$

so that the conditions for the convergence of the residue series are exactly those stated in (4.16).

A rigorous discussion of Watson's transformation and the convergence of the residue series in the shadow region was apparently first given by Pflumm (*11*).

V. THE SHADOW REGION

We shall begin the discussion of the solution with the simplest case, namely, the behavior in the shadow region.

According to geometrical optics, the shadow region is the whole cylinder

$$0 \leqq \theta < \theta_0 \leqq \pi/2, \tag{5.1}$$

where

$$\theta_0 = \sin^{-1}(a/r) \tag{5.2}$$

is the shadow boundary angle. Actually, as will be seen later, the shadow of the sphere does not extend beyond distances $\sim\beta a$, and the transition to the illuminated region already starts at much smaller distances, of the order of $\beta^{1/3}a$.

Since $\theta < \pi/2$ in the shadow region, (4.15) is valid for all $m \geqq 0$, so that (2.16) becomes

$$\psi(r, \theta) = 2\pi e^{i\pi/4}\left(\frac{\pi}{2\rho}\right)^{1/2}\sum_{m=0}^{\infty}(-1)^m$$

$$\cdot \sum_{n=1}^{\infty}\lambda_n r_n \exp\left[i\pi\lambda_n\left(2m + \frac{1}{2}\right)\right]H_{\lambda_n}^{(1)}(\rho)P_{\lambda_n-1/2}(\cos\theta) \tag{5.3}$$

$$= \pi e^{i\pi/4}\left(\frac{\pi}{2\rho}\right)^{1/2}\sum_{n=1}^{\infty}\lambda_n r_n \frac{\exp(-i\pi\lambda_n/2)}{\cos\pi\lambda_n}H_{\lambda_n}^{(1)}(\rho)P_{\lambda_n-1/2}(\cos\theta),$$

where we have employed (2.18). The last form of this result could also have been obtained directly from (2.7).

Equation (5.3) is formally similar to an "eigenfunction" expansion in terms

of the functions $H_{\lambda_n}^{(1)}(\rho)$, which satisfy the boundary condition on the surface of the sphere (cf. (3.2)) and the radiation condition at infinity. The latter implies a nonself-adjoint problem, explaining why the "eigenvalues" are complex. It was remarked by Sommerfeld (12) that the "eigenfunctions" are even orthogonal in a certain sense, and he proposed to derive (5.3) on this basis. However, as was shown by Pflumm (11), the set of "eigenfunctions" is by no means complete, and no general characterization of the class of functions for which the expansion is applicable has so far been given.

In practice, even though (5.3) converges for all $\theta < \pi/2$, its usefulness is restricted to the domain where its terms are rapidly decreasing from the beginning, so that only the first few terms have to be considered. This happens only within the shadow region, as will now be seen.

Let us consider the first few terms of (5.3), corresponding to poles of the type (3.5), located near $\lambda = \beta$. We shall restrict ourselves to points within the shadow region, not too close to the surface of the sphere, so that

$$r - a \gg \beta^{-2/3}a. \tag{5.4}$$

Under these conditions, we have $kr - |\lambda_n| \gg |\lambda_n|^{1/3}$, so that we may employ the expansion (A.16) for $H_{\lambda_n}^{(1)}(\rho)$. Furthermore, assuming that

$$\theta \gg \beta^{-1}, \tag{5.5}$$

we have $|\lambda_n|\theta \gg 1$, so that we may employ expansion (C.8) for $P_{\lambda_n-1/2}(\cos\theta)$.

Substituting these expansions in (5.3), and taking into account (3.5) and (3.16), we get

$$\psi(r,\theta) \approx \frac{e^{-i\pi/6}}{(2\pi)^{1/2}}\left(\frac{\beta}{2}\right)^{1/3}\left(\frac{a^2}{r^2-a^2}\right)^{1/4}\frac{\exp\left[ik(r^2-a^2)^{1/2}\right]}{(kr\sin\theta)^{1/2}}\sum_{m=0}^{\infty}(-1)^m$$
$$\cdot\sum_n\frac{1}{[Ai'(-x_n)]^2}\left[\exp\left(i\lambda_n\gamma_m+i\frac{\pi}{4}\right)+\exp\left(i\lambda_n\delta_m-i\frac{\pi}{4}\right)\right], \tag{5.6}$$

where

$$\gamma_m = \theta_0 - \theta + 2m\pi, \tag{5.7}$$

$$\delta_m = \theta_0 + \theta + 2m\pi, \tag{5.8}$$

and θ_0 is given by (5.2).

In writing (5.6), we have already assumed that only the first few terms of the series give a significant contribution, since the approximations employed correspond to the poles (3.5). Thus,

$$|\exp(i\lambda_n\gamma_0)| = \exp\left[-\frac{\sqrt{3}}{2}x_n\left(\frac{\beta}{2}\right)^{1/3}(\theta_0-\theta)\right] \tag{5.9}$$

must be a rapidly decreasing function of n. This will be true provided that

$$\gamma_0 = \theta_0 - \theta \gg \beta^{-1/3},\tag{5.10}$$

so that (5.6) is valid in this region.

The physical interpretation of (5.6) is well known (13). At short wavelengths, one may employ the concept of propagation along rays. The incident rays that are tangent to the sphere at T_1 and T_2 (Fig. 5) excite a series of surface waves emanating from these points. These waves travel along the surface with phase velocity slightly smaller than that in free space, due to the delay in overcoming the curvature of the sphere. As they travel along the surface, they shed radiation along tangential directions, leading to the angular damping factor (5.9).

A point P within the geometrical shadow is reached by two rays emanating from the points T_1' and T_2' where the tangents to the sphere from P meet the surface (Fig. 5). The corresponding angles travelled along the surface are, according to Fig. 5,

$$\gamma_0 = (\pi/2) - \cos^{-1}(a/r) - \theta = \theta_0 - \theta,$$

$$\delta_0 = (\pi/2) - \cos^{-1}(a/r) + \theta = \theta_0 + \theta,$$

in agreement with (5.7) and (5.8) for $m = 0$. The paths $T_1T_1'P$ and $T_2T_2'P$ are called "diffracted rays" in Keller's geometrical theory of diffraction (13).

The terms with $m \geqq 1$ in (5.6) correspond to rays which have encircled the sphere m times before leaving the surface, so that the corresponding angular paths are increased by $2m\pi$. This interpretation is corroborated by the solution to the problem of diffraction of a pulse (14), where one can follow the diffracted wave front around the sphere. In each encirclement, the rays go through the
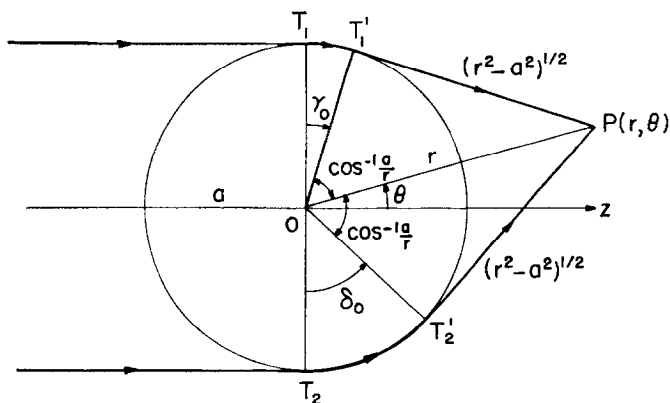

FIG. 5. Diffracted rays $T_1T_1'P$ and $T_2T_2'P$ reaching a point P in the geometrical shadow region.

points T_1 and T_2, where all diffracted rays meet. As is well known, passage through a focal point leads to a phase decrease by $\pi/2$. This explains the factor $[\exp(-i\pi/2)]^{2m} = (-1)^m$ in (5.6).

The phase factor

$$\exp\{ik(r^2 - a^2)^{1/2} + ik[1 + x_n(4\beta)^{-2/3}]a\gamma_m\}$$

also corresponds to the described optical path (and similarly for the term in δ_m). Note the decrease of the phase velocity along the surface.

The denominator $(r^2 - a^2)^{1/4}(r \sin \theta)^{1/2}$ can also be obtained from the law of conservation of the intensity along a pencil of rays (13). This denominator would vanish at $r = a$, which is a caustic of diffracted rays, but, according to (5.4), (5.6) is not valid there (the actual value, of course, is $\psi(a, \theta) = 0$). It would also vanish at $\theta = 0$, but this is excluded by (5.5).

The direction $\theta = 0$ is a focal line of diffracted rays. In fact, an observation point P on the axis is reached by a whole cone of diffracted rays tangent to the sphere, instead of by two rays only. This focusing effect, which is responsible for the well-known Poisson spot (cf. Section VIII), leads to an enhancement of intensity near the axis.

In fact, for $\theta \lesssim \beta^{-1}$, we must employ (C.9) instead of (C.8), so that (5.6) is replaced by

$$\psi(r, \theta) \approx e^{-i\pi/6} \left(\frac{\beta}{2}\right)^{1/3} \left(\frac{a}{r}\right)^{1/2} \left(\frac{a^2}{r^2 - a^2}\right)^{1/4} \exp[ik(r^2 - a^2)^{1/2}]$$
$$\cdot \sum_{m=0}^{\infty} (-1)^m \sum_n \frac{\exp[i\lambda_n(2m\pi + \theta_0)]}{[4i'(-x_n)]^2} J_0(\lambda_n \theta). \tag{5.11}$$

The surface waves associated with the poles λ_n are also known as "creeping modes" (5). It should be emphasized, however, that the above physical interpretation applies only to the lowest-order modes. As soon as the damping within a single wavelength becomes appreciable, the above concepts lose their validity. In practice, of course, only the lowest-order modes give a significant contribution.

VI. THE NEARBY LIT REGION AND THE WKB APPROXIMATION

We shall now consider the behavior of the solution in the lit region, not too close to the surface, so that (5.4) is assumed valid, but still not in the far field region, which will be treated in Section IX. We shall also stay away from the neighborhood of the shadow boundary, which will be discussed in Sections VII and VIII.

A. THE FORWARD HALF-SPACE

For $\theta > \theta_0$, we have $\gamma_0 < 0$ in (5.6). According to (5.9), this implies that the residue series containing γ_0 starts out with exponentially increasing terms.

It does not follow that the residue series representation becomes incorrect, for, as we have seen in Section IV, it still converges for $\theta < \pi/2$. What happens, however, is that it becomes useless for all practical purposes. The physical reason for this behavior is that the wave function is no longer exponentially damped, but contains additional contributions corresponding to the incident and reflected waves in geometrical optics.

A modification of Watson's transformation to take into account these contributions in the lit region was first proposed by Fock (3). As reformulated by Franz $(4, 5)$, the basic idea is to substitute in (2.7), taken over the alternative contour D in Fig. 1, the identity $(C.5)$

$$P_{\lambda-1/2}(\cos \theta) = -ie^{i\pi\lambda}[P_{\lambda-1/2}(-\cos \theta) + 2i \cos \pi\lambda Q^{(1)}_{\lambda-1/2}(\cos \theta)]. \qquad (6.1)$$

The integral of the first term on the right-hand side of this expression is then reduced to a residue series, which gives, as we shall see later, the continuation of (5.3) into the lit region. The second term cancels the denominator $\cos \pi\lambda$ in (2.7), so that the integrand no longer has poles at the positive half-integers, and the integral can be evaluated by the saddle-point method, yielding the contributions from the incident and reflected waves. We shall see, however, that the proposed contour of integration can only be employed in the forward half-space $(\theta < \pi/2)$. In this region, we shall derive essentially the same results by a different method, which has the advantage of greater simplicity, as well as of showing more clearly the connection between the lit and shadow regions. This method does not require the re-evaluation of the whole residue series, but only of that part of the term $m = 0$ in (5.6) that "goes wrong" for $\theta > \theta_0$.

In fact, for $m \geq 1$, not only is the transformation that led to the residue series allowed for $0 \leq \theta < \pi$ (cf. (4.16)), but also the corresponding residue series in (5.6) are all rapidly convergent, so that we need only be concerned with the term $m = 0$. The corresponding term in (2.17) is

$$\psi_0(r, \theta) = 2 \int_{-\infty}^{\infty} f(\lambda, \beta, \rho) P_{\lambda-1/2}(\cos \theta)e^{i\lambda\pi/2}\lambda \, d\lambda. \qquad (6.2)$$

Let us make the splitting (cf. $(C.2)$)

$$P_{\lambda-1/2}(\cos \theta) = Q^{(1)}_{\lambda-1/2}(\cos \theta) + Q^{(2)}_{\lambda-1/2}(\cos \theta). \qquad (6.3)$$

Then, according to $(C.7)$, the term in γ_0 in (5.6) arises from $Q^{(1)}_{\lambda-1/2}$, while that in δ_0 arises from $Q^{(2)}_{\lambda-1/2}$.

The residue series containing δ_0 remains rapidly convergent in the lit region, provided that (cf. (5.8))

$$\beta^{1/3}(\theta_0 + \theta) \gg 1, \qquad (6.4)$$

which will be assumed throughout this section. The vicinity of the forward direction, where this assumption is not fulfilled, will be considered in Section VIII.

Thus, we finally have to consider only the expression

$$\psi_0^{(1)}(r, \theta) = 2 \int_{-\infty+i\epsilon}^{\infty+i\epsilon} f(\lambda, \beta, \rho) Q_{\lambda-1/2}^{(1)}(\cos \theta) e^{i\lambda\pi/2} \lambda \, d\lambda, \qquad (6.5)$$

where the path of integration has to be taken slightly above the real axis in order to avoid the poles of $Q_{\lambda-1/2}^{(1)}$ at the negative half-integers. This is done before the splitting (6.3). We shall see that the geometrical-optics approximation to the solution is entirely contained in this integral.

The behavior of the integrand of (6.5) as $|\lambda| \to \infty$ in I_+ is similar to that of (4.1) with $m = 0$. In fact, according to (4.6) and (C.7), the behavior of $P_{\lambda-1/2}(\cos \theta)$ in I_+ is the same as that of $Q_{\lambda-1/2}^{(1)}(\cos \theta)$. The discussion given in Section IV implies that the path of integration in (6.5) may be deformed at will in I_+, for $\theta < \pi/2$.

Following Franz's method (5), we shall deform it into the path Γ shown in Fig. 6, going around the poles of $S(\lambda, \beta)$, and beginning and ending at infinity in the region between the curves $\eta \to 3\pi/2$ and $\eta \to -\pi/2$, where η is defined by (2.27). According to Appendix A, $H_\lambda^{(2)}(\rho) \to 0$ as $|\lambda| \to \infty$ in this region. It follows that we may split (6.5) into two integrals, corresponding to the two terms in the second member of (2.8), since each of the integrands will separately go to zero as $|\lambda| \to \infty$ in this region. The integral containing $H_\lambda^{(2)}(\rho)$
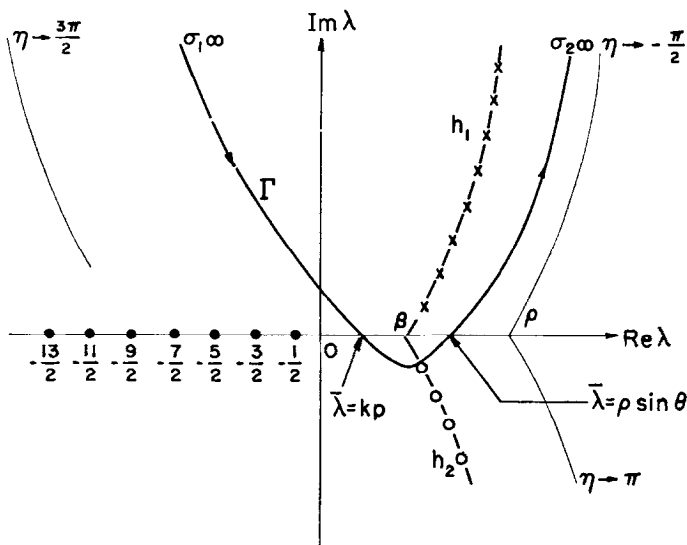

FIG. 6. $\times$ $\times$ $\times$—Poles of the S-function; $\bigcirc$ $\bigcirc$ $\bigcirc$—zeros of the S-function; $\bullet$ $\bullet$ $\bullet$—poles of $Q_{\lambda-1/2}^{(1)}(\cos \theta)$. The path of integration Γ goes through the saddle points $\lambda = k\rho$ and $\bar{\lambda} = \rho \sin \theta (\theta < \pi/2)$.

identically vanishes, since the contour may be closed at infinity and the integrand has no singularities within it. Finally, we get

$$\psi_0^{(1)}(r, \theta) = -\left(\frac{\pi}{2\rho}\right)^{1/2} e^{-i\pi/4} \int_\Gamma \frac{H_\lambda^{(2)}(\beta)}{H_\lambda^{(1)}(\beta)} H_\lambda^{(1)}(\rho) Q_{\lambda-1/2}^{(1)}(\cos\theta) e^{i\lambda\pi/2} \lambda \, d\lambda \tag{6.6}$$

$$(\theta < \pi/2).$$

The path Γ crosses the real axis twice: first between 0 and β and then between β and ρ. We shall see that there is one saddle point of the integrand in each of these intervals, and Γ will be taken through both saddle points. In the lower half-plane, to the left of the curve $\eta \to \pi$ (Fig. 6), the integrand increases exponentially for $|\lambda| \to \infty$. However, the steepest descent paths corresponding to the two saddle points can be joined by an arc going through the neighborhood of the first zero of $H_\lambda^{(2)}(\beta)$, where the integrand is small (5).

To the right of the curves h_1 and h_2 in Fig. 6, we have, according to Appendix A,

$$H_\lambda^{(2)}(\beta)/H_\lambda^{(1)}(\beta) \approx -1. \tag{6.7}$$

Furthermore, we can employ the expansion (A.16) for $H_\lambda^{(1)}(\rho)$ and the expansion (C.7) for $Q_{\lambda-1/2}^{(1)}(\cos\theta)$. Making the change of variable

$$\lambda = \rho \sin w, \tag{6.8}$$

we find that the portion of the contour Γ to the right of h_1 and h_2 contributes

$$\psi_1 = \left(\frac{\rho}{2\pi \sin\theta}\right)^{1/2} e^{-i\pi/4} \int A(w, \rho, \theta) \exp\left[i\rho\alpha(w, \theta)\right] dw, \tag{6.9}$$

where the path of integration crosses the real w axis between $w = 0$ and $w = \pi/2$, and

$$\alpha(w, \theta) = \cos w + (w - \theta)\sin w, \tag{6.10}$$

$$A(w, \rho, \theta) = (\sin w \cos w)^{1/2} \left\{ 1 + \frac{i}{4\rho}\left(\frac{\cot\theta}{2\sin w} - \frac{3 + 2\sin^2 w}{6\cos^3 w}\right) \right. $$
$$\left. + O(\rho^{-2}) \right\}. \tag{6.11}$$

In this approximation, (6.9) is independent of the radius of the sphere, so that ψ_1 should correspond to the incident wave. This is indeed so, as will now be seen.

The exponent (6.10) gives rise to a saddle point at

$$\bar{w} = \theta$$

corresponding to $\bar{\lambda} = \rho \sin\theta$, as shown in Fig. 6. The corresponding steepest descent path crosses the real axis at an angle of $\pi/4$.

Taking into account not only the main term, but also the first correction term in the saddle-point method, the behavior of (6.9) for large values of ρ is found to be given by

$$
\psi_1 = \frac{A e^{i\rho\alpha}}{(\alpha'' \sin \theta)^{1/2}} \left\{ 1 + \frac{i}{2\alpha''\rho} \left[\frac{A''}{A} - \frac{A'}{A} \frac{\alpha'''}{\alpha''} \right. \right.
$$
$$
\left. \left. + \frac{5}{12} \left(\frac{\alpha'''}{\alpha''} \right)^2 - \frac{1}{4} \frac{\alpha^{IV}}{\alpha''} \right] + O(\rho^{-2}) \right\}, \tag{6.12}
$$

where A, α and all their derivatives (denoted by A', α'', $\cdots$) are to be taken at the saddle point.

Substituting A and α by (6.10) and (6.11), it is found that the expression within square brackets identically vanishes, so that

$$
\psi_1 = e^{i\rho\cos\theta} + O(\rho^{-2}) \qquad\qquad (\rho \gg 1). \quad (6.13)
$$

Thus, the contribution from the right-hand saddle point is essentially identical to the incident wave.

To the left of the curves h_1 and h_2 (Fig. 6) we have, according to (A.16),

$$
H_\lambda^{(2)}(\beta)/H_\lambda^{(1)}(\beta) = \exp\left\{ -2i \left[(\beta^2 - \lambda^2)^{1/2} - \lambda \cos^{-1}\left(\frac{\lambda}{\beta}\right) - \frac{\pi}{4} \right] \right\}
$$
$$
\cdot \left[1 + \frac{i}{4(\beta^2 - \lambda^2)^{1/2}} \left(1 + \frac{5}{3} \frac{\lambda^2}{\beta^2 - \lambda^2} \right) + \cdots \right] \tag{6.14}
$$

and, again making the change of variable (6.8), we find that the contribution from the portion of the contour Γ to the left of h_1 and h_2 is

$$
\psi_r = -\left(\frac{\rho}{2\pi \sin \theta} \right)^{1/2} e^{i\pi/4} \int B(w, \rho, \theta, \gamma) \exp\left[i\rho\delta(w, \theta, \gamma) \right] dw, \quad (6.15)
$$

where

$$
\gamma = a/r, \tag{6.16}
$$

$$
\delta(w, \theta, \gamma) = \cos w - 2(\gamma^2 - \sin^2 w)^{1/2}
$$
$$
+ \sin w \left[w - \theta + 2 \cos^{-1}\left(\frac{\sin w}{\gamma} \right) \right], \tag{6.17}
$$

$$
B(w, \rho, \theta, \gamma) = (\sin w \cos w)^{1/2} \left\{ 1 + \frac{i}{4\rho} \left[\frac{\cot \theta}{2 \sin w} \right. \right.
$$
$$
\left. \left. + \frac{(2 \sin^2 w + 3\gamma^2)}{3(\gamma^2 - \sin^2 w)^{3/2}} - \frac{(3 + 2 \sin^2 w)}{6 \cos^3 w} \right] + O(\rho^{-2}) \right\}. \tag{6.18}
$$

The saddle point is determined by the condition

$$\sin \bar{w} = \gamma \cos \left(\frac{\theta - \bar{w}}{2} \right)$$

or

$$p = r \sin \bar{w} = a \cos \left(\frac{\theta - \bar{w}}{2} \right). \tag{6.19}$$

The corresponding value of λ is $\bar{\lambda} = \rho \sin \bar{w} = kp$ (cf. Fig. 6). The steepest descent path crosses the real axis at an angle of $-\pi/4$.

The physical interpretation of (6.19) is shown in Fig. 7. According to (2.5), $p = \bar{\lambda}/k$ may be interpreted as the impact parameter associated with an incident ray. As shown in Fig. 7, this is precisely the incident ray AB that reaches the observation point P after being reflected at the surface according to the laws of geometrical optics. The angle

$$\zeta = \tfrac{1}{2}(\theta - \bar{w}) \tag{6.20}$$

is the complement of the angle of incidence.

A saddle-point evaluation of (6.15), including the first correction term, yields, similarly to (6.12),

$$\psi_r = -\frac{Be^{i\rho\delta}}{(|\delta''| \sin \theta)^{1/2}} \left\{ 1 - \frac{i}{2\rho |\delta''|} \left[\frac{B''}{B} + \frac{B'}{B} \frac{\delta'''}{|\delta''|} \right. \right.$$
$$\left. \left. + \frac{5}{12} \left(\frac{\delta'''}{\delta''} \right)^2 + \frac{1}{4} \frac{\delta^{IV}}{|\delta''|} \right] + O(\rho^{-2}) \right\}, \tag{6.21}$$

where B, δ, and their derivatives are to be evaluated at the saddle point.

It is convenient to express the result in terms of the parameters ζ and

$$s = r \cos \bar{w} - \frac{a}{2} \sin \zeta, \tag{6.22}$$

which measures the distance (taken along the ray) from the observation point to the caustic of the reflected rays. Substituting (6.17), (6.18), and (6.19) in (6.21), it is found that

$$\psi_r = -\left[\frac{a^2 \sin 2\zeta}{4s(s \sin 2\zeta + a \cos^3 \zeta)} \right]^{1/2} \exp \left[ik \left(s - \frac{3}{2} a \sin \zeta \right) \right]$$
$$\cdot \left\{ 1 + \frac{i}{2\beta} \left[\frac{1}{\sin^3 \zeta} + \frac{1}{2^4 \sin^2 \zeta \cos^2 \zeta} \frac{a}{s} + \frac{3}{2^5} \left(\frac{2}{\sin \zeta} - 5 \sin \zeta \right) \left(\frac{a}{s} \right)^2 \right. \right. \tag{6.23}$$
$$\left. \left. - \frac{15}{2^6} \cos^2 \zeta \left(\frac{a}{s} \right)^3 - \frac{1}{2^3 \sin \zeta \cos \zeta} \cdot \frac{a}{(s \sin 2\zeta + a \cos^3 \zeta)} \right] + O(k^{-2}) \right\}.$$

This asymptotic expansion in inverse powers of k corresponds to the well-
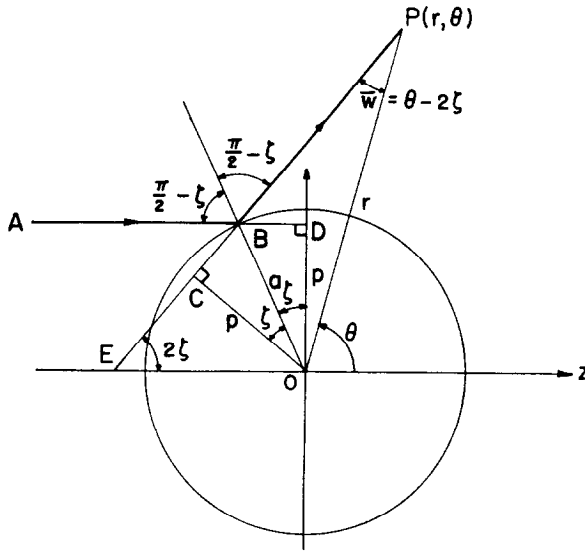
FIG. 7. Physical interpretation of the left saddle point: p is the impact parameter of the incident ray AB which reaches point P after geometrical reflection at the surface.

known WKB approximation, which has been investigated by Luneburg (*15*) and Kline (*16*) in connection with Maxwell's equations.

The first term of (6.23) represents the reflected wave according to geometrical optics (first-order WKB approximation). The amplitude of this term takes into account the divergence of the rays after reflection at the surface.

The remainder of (6.23) represents the correction to geometrical optics. It contains the main correction term, which is proportional to k^{-1}, corresponding to the second-order WKB approximation. This term has also been computed by Keller, Lewis, and Seckler (*17*), directly by the WKB method. Equation (6.23) agrees with their result.[4]

The complete expression for the wave function in this region, according to the above results, is

$$
\psi = \psi_1 + \psi_r + \frac{e^{-i\pi/6}}{(2\pi)^{1/2}} \left(\frac{\beta}{2}\right)^{1/3} \left(\frac{a^2}{r^2 - a^2}\right)^{1/4} \frac{\exp\left[ik(r^2 - a^2)^{1/2}\right]}{(kr \sin \theta)^{1/2}}
$$

$$
\times \left\{ e^{-i\pi/4} \sum_n \frac{\exp\left(i\lambda_n \delta_0\right)}{[Ai'(-x_n)]^2} + \sum_{m=1}^{\infty} (-1)^m \sum_n \frac{1}{[Ai'(-x_n)]^2} \right. \tag{6.24}
$$

$$
\left. \times \left[\exp\left(i\lambda_n \gamma_m + i\frac{\pi}{4}\right) + \exp\left(i\lambda_n \delta_m - i\frac{\pi}{4}\right)\right] \right\},
$$

[4] Actually, the expression within square brackets in the second term of (6.23) differs from Keller, Lewis, and Seckler's by the powers of 2 in the denominators, which are all less by one unit. However, it can be verified that this is due to a misprint in their paper.

where ψ_l and ψ_r are given by (6.13) and (6.23), respectively. From the point of view of a strict asymptotic expansion, the residue series should not appear in this expression, since it is exponentially small as compared with the other two terms, and even with respect to higher-order correction terms not taken into account in (6.23). However, from a physical point of view, this term is meaningful, since it represents the continuation of the surface waves (5.6) that were found in the shadow region. Note also that the residue series in δ_0 becomes significant near the shadow boundary, when condition (6.4) is no longer satisfied.

B. The Backward Half-Space

The above treatment is no longer valid for $\theta > \pi/2$. According to (4.8) and (4.9), the integrand of (6.5) blows up exponentially for $|\lambda| \to \infty$ in the region between the imaginary axis and the curve $\eta \to -\pi/2$ in Fig. 6. Thus, the transformation that led to (6.6) can no longer be performed. Furthermore, the integrand of (6.6) no longer has a saddle point on the real axis between β and ρ; rather, it is the other term in (6.5), containing $H_\lambda^{(2)}(\rho)$, that has such a saddle point.

It is therefore necessary to modify the above procedure in the whole backward half-space. For this purpose, we shall again start from (6.5), but now taking the path of integration symmetrically about the origin, from $-\infty + i\epsilon$ to $+\infty - i\epsilon$ (note that there are no poles on the *positive* real axis), and we make the substitution $\lambda \to -\lambda$ in the integral from 0 to $+\infty - i\epsilon$. Taking into account (2.15) and the relation

$$Q_{\lambda-1/2}^{(1)}(\cos\theta) - e^{-2i\pi\lambda}Q_{-\lambda-1/2}^{(1)}(\cos\theta) = -e^{-i\pi\lambda}\tan\pi\lambda P_{\lambda-1/2}(-\cos\theta), \quad (6.25)$$

which follows from (2.14) and (C.5), we find

$$\psi_0^{(1)}(r,\theta) = 2\int_0^{-\infty+i\epsilon} f(\lambda,\beta,\rho)P_{\lambda-1/2}(-\cos\theta)e^{-i\lambda\pi/2}\lambda\tan\pi\lambda\,d\lambda. \quad (6.26)$$

The behavior of the integrand in region 3 of Fig. 4 differs from (4.7) (with $m = 0$) only by the replacement

$$\exp\left[i\lambda\left(\frac{\pi}{2} - \theta\right)\right] \to \exp\left[-i\lambda\left(\frac{3\pi}{2} - \theta\right)\right],$$

so that, for $\lambda \to \sigma\infty$ (cf. (2.26)), it behaves like

$$\exp\left[-|\lambda|(\eta + \theta - \pi)\right],$$

where η is given by (2.27). It follows that the path of integration in (6.26) may be deformed into the path from 0 to $\sigma\infty$ shown in Fig. 3, with

$$\eta > \pi - \theta. \quad (6.27)$$

Thus,

$$\psi_0^{(1)}(r, \theta) = \left(\frac{\pi}{2\rho}\right)^{1/2} e^{-i\pi/4} \int_0^{\sigma\infty} \left[H_\lambda^{(2)}(\rho) - \frac{H_\lambda^{(2)}(\beta)}{H_\lambda^{(1)}(\beta)} H_\lambda^{(1)}(\rho) \right]$$

$$\times P_{\lambda-1/2}(-\cos\theta) e^{-i\lambda\pi/2} \tan(\pi\lambda)\lambda \, d\lambda. \tag{6.28}$$

In particular, for $\theta > \pi/2$, we may subject η to the additional restriction (2.31). Under these conditions, (2.35) applies and (6.28) becomes

$$\psi_0^{(1)}(r, \theta) = e^{i\rho\cos\theta} + \psi_r, \tag{6.29}$$

where

$$\psi_r = -\left(\frac{\pi}{2\rho}\right)^{1/2} e^{-i\pi/4} \int_0^{\sigma\infty} \frac{H_\lambda^{(2)}(\beta)}{H_\lambda^{(1)}(\beta)} H_\lambda^{(1)}(\rho) P_{\lambda-1/2}(-\cos\theta)$$

$$\times e^{-i\lambda\pi/2} \tan(\pi\lambda)\lambda \, d\lambda. \tag{6.30}$$

We may now apply again (6.25) and the converse of the transformation that led from (6.5) to (6.26). The result is

$$\psi_r = -\left(\frac{\pi}{2\rho}\right)^{1/2} e^{-i\pi/4} \int_{\sigma\infty}^{-\sigma\infty} \frac{H_\lambda^{(2)}(\beta)}{H_\lambda^{(1)}(\beta)} H_\lambda^{(1)}(\rho) Q_{\lambda-1/2}^{(1)}(\cos\theta) e^{i\lambda\pi/2}\lambda \, d\lambda \tag{6.31}$$

$$(\theta > \pi/2),$$

where the path of integration is that of Fig. 3 taken in the opposite sense.

This integral may be evaluated by the saddle-point method. There is now a single saddle point on the real axis, at $\bar{\lambda} = kp$, where p is again given by (6.19). In fact, the integrand is identical to that of (6.6), the only difference being that the path of integration now goes over only one saddle point. Thus, the result of the saddle-point calculation is identical to (6.23).

In spite of the fact that the solution in the backward half-space is just the continuation of the solution in the forward half-space, it does not seem possible to extend the representation (6.6) to $\theta > \pi/2$, or to extend (6.31) to $\theta < \pi/2$. The reason for this is that $P_{\lambda-1/2}(x)$ becomes singular at $x = -1$, so that one cannot find a single representation that remains valid both for $\theta = 0$ and for $\theta = \pi$. One needs a representation in terms of $P_{\lambda-1/2}(\cos\theta)$ (cf. (6.2)) near $\theta = 0$, and one in terms of $P_{\lambda-1/2}(-\cos\theta)$ (cf. (6.28)) near $\theta = \pi$. The appearance of two saddle points in the forward half-space is also related to the diffraction effects that arise, as will be seen in Section VII, when these points approach each other.

We must still see what happens to the residue series near $\theta = \pi$, because both the term $\psi_0^{(2)}$ containing $Q_{\lambda-1/2}^{(2)}(\cos\theta)$ in (6.2) and the terms ψ_m with

$m \geqq 1$ in (2.17) become singular at this point. However, we can write

$$
\psi_0^{(2)} + \sum_{m=1}^{\infty} \psi_m = 2 \int_{-\infty+i\epsilon}^{\infty+i\epsilon} f(\lambda, \beta, \rho) Q_{\lambda-1/2}^{(2)}(\cos \theta) e^{i\lambda\pi/2} \lambda \, d\lambda
$$

$$
+ 2 \sum_{m=1}^{\infty} (-1)^m \int_{-\infty+i\epsilon}^{\infty+i\epsilon} f(\lambda, \beta, \rho) [Q_{\lambda-1/2}^{(1)}(\cos \theta) + Q_{\lambda-1/2}^{(2)}(\cos \theta)]
$$

$$
\times \exp\left[i\pi\lambda \left(2m + \frac{1}{2} \right) \right] \lambda \, d\lambda = 2 \sum_{m=0}^{\infty} (-1)^m \int_{-\infty+i\epsilon}^{\infty+i\epsilon} f(\lambda, \beta, \rho)
$$

$$
\times [Q_{\lambda-1/2}^{(2)}(\cos \theta) - e^{2i\pi\lambda} Q_{\lambda-1/2}^{(1)}(\cos \theta)] \exp\left[i\pi\lambda \left(2m + \frac{1}{2} \right) \right] \lambda \, d\lambda,
$$

$$(6.32)$$

and employ the identity (cf. (C.5) and (C.6))

$$
Q_{\lambda-1/2}^{(2)}(\cos \theta) - e^{2i\pi\lambda} Q_{\lambda-1/2}^{(1)}(\cos \theta) = -i e^{i\pi\lambda} P_{\lambda-1/2}(-\cos \theta) \qquad (6.33)
$$

to get

$$
\psi_0^{(2)} + \sum_{m=1}^{\infty} \psi_m = 2i \sum_{m=1}^{\infty} (-1)^m \int_{-\infty}^{\infty} f(\lambda, \beta, \rho) P_{\lambda-1/2}(-\cos \theta)
$$

$$
\cdot \exp\left[i\pi\lambda \left(2m - \frac{1}{2} \right) \right] \lambda \, d\lambda.
$$

$$(6.34)$$

The contour of integration may be closed in the upper half-plane, leading to the residue series

$$
\psi_{\mathrm{res}}(r, \theta) = 2\pi e^{-i\pi/4} \left(\frac{\pi}{2\rho} \right)^{1/2} \sum_{m=0}^{\infty} (-1)^m \sum_{n=1}^{\infty} \lambda_n \, r_n \exp\left[i\pi\lambda_n \left(2m + \frac{3}{2} \right) \right]
$$

$$
\times H_{\lambda_n}^{(1)}(\rho) P_{\lambda_n-1/2}(-\cos \theta) \qquad (6.35)
$$

$$
= \pi e^{-i\pi/4} \left(\frac{\pi}{2\rho} \right)^{1/2} \sum_{n=1}^{\infty} \lambda_n \, r_n \frac{\exp (i\pi\lambda_n/2)}{\cos \pi\lambda_n} H_{\lambda_n}^{(1)}(\rho) P_{\lambda_n-1/2}(-\cos \theta),
$$

which differs from (5.3) only by the substitution

$$
P_{\lambda_n-1/2}(\cos \theta) \to -i \exp (i\pi\lambda_n) P_{\lambda_n-1/2}(-\cos \theta). \qquad (6.36)
$$

If

$$
\pi - \theta \gg \beta^{-1}, \qquad (6.37)
$$

we may employ the expansion (C.8) for $P_{\lambda_n-1/2}(-\cos \theta)$ and we find that (6.35) is equivalent to the residue series appearing in (6.24), so that (6.24) may be continued to $\theta > \pi/2$.

Note that

$$
\gamma_1 = 2\pi + (\pi/2) - \cos^{-1}(a/r) - \theta
$$

no longer corresponds to one complete encirclement of the sphere, but rather to the smallest angle described by a surface wave excited at T_1 before leaving the surface (Fig. 8).

If, instead of (6.37), we have $\pi - \theta \lesssim \beta^{-1}$, we must employ (C.9), which leads to

$$\psi_{\text{res}}(r, \theta) \approx e^{-2i\pi/3} \left(\frac{\beta}{2}\right)^{1/3} \left(\frac{a}{r}\right)^{1/2} \left(\frac{a^2}{r^2 - a^2}\right)^{1/4} \exp\left[ik(r^2 - a^2)^{1/2}\right]$$

$$\times \sum_{m=0}^{\infty} (-1)^m \sum_n \frac{1}{[A_i'(-x_n)]^2} \exp\{i\lambda_n[(2m + 1)\pi + \theta_0]\} J_0[\lambda_n(\pi - \theta)]. \tag{6.38}$$

This expression should be compared with (5.11). The same focusing effect already discussed there leads to an enhancement of the radiation from the surface waves in the backward direction.

The approximations employed in the present section fail when the correction terms appearing in (6.23) become large. This happens near the forward and the backward directions. The behavior near the backward direction will be discussed in Section IX, in connection with the scattering amplitude. The behavior near the forward direction and the corresponding diffraction effects will be investigated in the next two sections.

VII. DIFFRACTION EFFECTS IN THE NEAR REGION

A. The Normal Derivative on the Surface

According to Huygens' Principle, the wave function at any point in space can be expressed in terms of its normal derivative on the surface of the sphere (where the wave function vanishes).
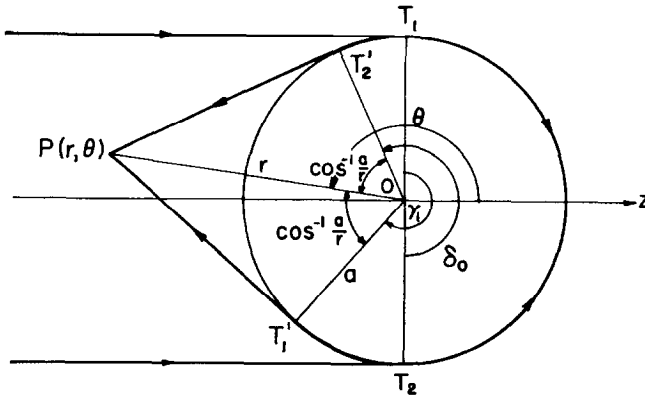

FIG. 8. Diffracted rays $T_1T_1'P$ and $T_2T_2'P$ reaching a point P in the lit region.

The analogue of Kirchhoff's approximation in classical diffraction theory would be to replace the exact values of the normal derivative by the geometrical optics approximation:

$$\chi = 0 \qquad (\theta < \pi/2), \tag{7.1}$$

$$\chi = \frac{2}{k} \left[\frac{\partial}{\partial r} \left(e^{ikr \cos \theta} \right) \right]_{r=a} = 2i \cos \theta e^{i\beta \cos \theta} \left(\theta > \frac{\pi}{2} \right), \tag{7.2}$$

where we have introduced the notation

$$\chi(\beta, \theta) = \frac{1}{k} \left(\frac{\partial \psi}{\partial r} \right)_{r=a}. \tag{7.3}$$

The expression (7.1) corresponds to the geometrical shadow region and (7.2) to the geometrically lit region on the surface. The factor 2 in (7.2) arises from joining the contributions of the incident and geometrically reflected waves.

Substituting (7.1) and (7.2) in the Huygens-Kirchhoff integral, one can easily derive the corresponding approximation for the scattering amplitude (18). It is found to be the sum of two terms, one of which corresponds to the geometrically reflected wave, while the other one corresponds to the diffracted wave in the classical theory of diffraction by a circular disc of radius a. The latter term, which is also known as the "shadow-forming wave," depends only on the shadow contour of the obstacle, so that it is the same for a sphere or for a disc.

Since we are later going to compare our results with classical diffraction theory, it is of interest to discuss the accuracy of Kirchhoff's approximation by evaluating χ. The only significant contribution arises from (6.5):

$$\chi_0^{(1)} = -\frac{2}{\beta} \left(\frac{2}{\pi \beta} \right)^{1/2} e^{i\pi/4} \int_{-\infty+i\epsilon}^{\infty+i\epsilon} \frac{Q_{\lambda-1/2}^{(1)}(\cos \theta)}{H_\lambda^{(1)}(\beta)} e^{i\lambda\pi/2} \lambda \, d\lambda, \tag{7.4}$$

where we have employed (2.8) and the Wronskian relation

$$W[H_\lambda^{(1)}(\beta), H_\lambda^{(2)}(\beta)] = -(4i/\pi\beta). \tag{7.5}$$

For $\theta > \pi/2$, the main contribution to (7.4) arises from a saddle point on the real axis, to the left of $\lambda = \beta$, where, according to (A.16) and (C.7),

$$\lambda e^{i\lambda\pi/2} Q_{\lambda-1/2}^{(1)}(\cos \theta)/H_\lambda^{(1)}(\beta) \approx \frac{i}{2} (\lambda/\sin \theta)^{1/2} (\beta^2 - \lambda^2)^{1/4}$$

$$\times \exp\left[-i(\beta^2 - \lambda^2)^{1/2} + i\lambda \left(\frac{\pi}{2} - \theta + \cos^{-1}(\lambda/\beta) \right) \right], \tag{7.6}$$

so that the saddle-point is at

$$\cos^{-1} (\bar{\lambda}/\beta) = \theta - (\pi/2) \rightarrow \bar{\lambda} = \beta \sin \theta. \tag{7.7}$$

The saddle-point evaluation gives

$$\chi_0^{(1)} \approx 2i \cos \theta e^{i\beta \cos \theta} \qquad (\theta - \pi/2 \gg \beta^{-1/3}), \quad (7.8)$$

in agreement with the geometrical optics approximation (7.2).

The condition in parentheses arises from the fact that (A.16) is valid only for $\beta - \lambda \gg \beta^{1/3}$. As θ approaches $\pi/2$, the saddle point (7.7) moves towards $\lambda = \beta$ and, if $|\theta - (\pi/2)| \lesssim \beta^{-1/3}$, we have to employ the approximation (A.17):

$$H_\lambda^{(1)}(\beta) \approx 2(2/\beta)^{1/3} e^{-i\pi/3} Ai(xe^{2i\pi/3}) \qquad (|\lambda - \beta| \lesssim \beta^{1/3}), \quad (7.9)$$

where

$$x = (2/\beta)^{1/3}(\lambda - \beta). \tag{7.10}$$

Since the main contribution to the integral in this case arises from $|x| \lesssim 1$, we may extend the range of integration where (7.9) is employed to infinity, with the following result:

$$\chi_0^{(1)} \approx \frac{e^{-i\pi/6}}{\pi(\sin\theta)^{1/2}} \frac{\exp\{i\beta[(\pi/2) - \theta)]\}}{(4\beta)^{1/3}} \mathfrak{F}(\tau) \qquad (|\theta - (\pi/2)| \lesssim \beta^{-1/3}), \quad (7.11)$$

where

$$\tau = (\beta/2)^{1/3}[(\pi/2) - \theta] \tag{7.12}$$

and

$$\begin{aligned}
\mathfrak{F}(\tau) &= \int_0^\infty \frac{e^{i\tau x}}{Ai(xe^{i\pi/3})} dx + \int_0^\infty \frac{e^{-i\tau x}}{Ai(xe^{-i\pi/3})} dx \\
&= -e^{i\pi/3} \int_{\infty \exp(-i\pi/3)}^{\infty \exp(2i\pi/3)} \frac{\exp(e^{-i\pi/6}\tau w)}{Ai(w)} dw.
\end{aligned} \tag{7.13}$$

Finally, if $(\pi/2) - \theta \gg \beta^{-1/3}$, we may evaluate (7.4) by closing the path of integration in the upper half-plane, where the integrand is exponentially decreasing at infinity. This leads to a residue series at the poles of $[H_\lambda^{(1)}(\beta)]^{-1}$. The terms in the series are then rapidly decreasing and the main contribution arises from the poles (3.5):

$$\chi_0^{(1)} \approx \left(\frac{2}{\beta}\right)^{1/3} \frac{e^{-i\pi/3}}{(\sin\theta)^{1/2}} \sum_n \frac{\exp\{i\lambda_n[(\pi/2) - \theta]\}}{Ai'(-x_n)} \left(\frac{\pi}{2} - \theta \gg \beta^{-1/3}\right). \quad (7.14)$$

This corresponds to the surface waves associated with γ_0 in (5.6). The normal derivative is exponentially damped in the shadow region $\frac{\pi}{2} - \theta \gg \beta^{-1/3}$, in good agreement with (7.1).

Thus, the only domain where Kirchhoff's approximation (7.1) — (7.2) fails to be accurate is the penumbra region

$$|\theta - (\pi/2)| \lesssim \beta^{-1/3} \tag{7.15}$$

where the normal derivative is given by (7.11). The function $\mathfrak{F}(\tau)$, which gives the transition from light to shadow, was introduced by Fock (*3*).

There remains to be shown that (7.11) goes over smoothly into (7.8) or (7.14) for $|\theta - (\pi/2)| \gg \beta^{-1/3}$. The asymptotic behavior of the integrand of (7.13) in the w-plane follows from Appendix D. It is found that the path of integration, represented by the straight line D in Fig. 9, may be deformed at will, provided that it begins and ends at infinity outside of the shaded sector.

If $\tau \gg 1$, we may evaluate (7.13) by moving the path of integration to infinity in the left half-plane, which leads to a residue series at the poles $-x_n$:

$$\mathfrak{F}(\tau) = 2\pi e^{-i\pi/6} \sum_n \frac{\exp\left(-e^{-i\pi/6}\tau x_n\right)}{Ai'(-x_n)} \qquad (\tau \gg 1). \tag{7.16}$$

On the other hand, if $\tau \ll -1$, we may evaluate (7.13) by the saddle-point method. For this purpose, D is deformed to the right over the region where $|w| \gg 1$, so that the expansion (D.4) can be employed. The saddle point is located at

$$\bar{w} = e^{-i\pi/3}\tau^2 \tag{7.17}$$
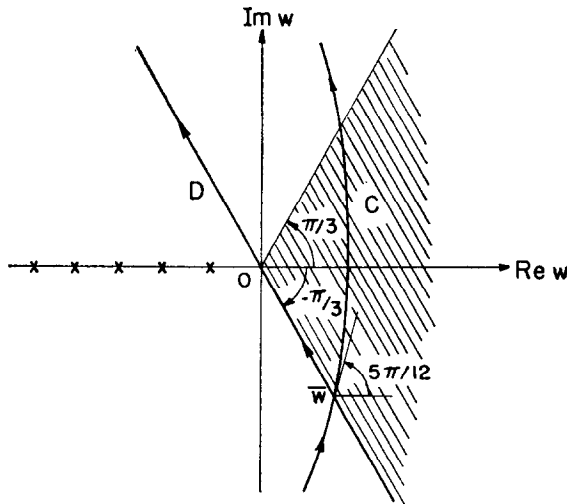

FIG. 9. Paths of integration for (7.13); $\bar{w}$ is the saddle point. $\times \times \times$—Poles of $[Ai(w)]^{-1}$. The path must begin and end at infinity outside of the shaded sector.

and the corresponding path of integration C is shown in Fig. 9. The result of the saddle-point evaluation is

$$\mathfrak{F}(\tau) \approx 4\pi e^{-i\pi/3} \mid \tau \mid \exp (i \mid \tau \mid^3/3) \quad (\tau \ll -1) \quad (7.18)$$

Substituting (7.16) in (7.11), we get (7.14). Substituting (7.18) in (7.11), we find

$$\chi_0^{(1)} \approx 2i \frac{[(\pi/2) - \theta]}{(\sin \theta)^{1/2}} \exp \left\{ i\beta \left[\left(\frac{\pi}{2} - \theta \right) - \frac{1}{3!} \left(\frac{\pi}{2} - \theta \right)^3 \right] \right\}, \quad (7.19)$$

which agrees with (7.8) for $\theta - (\pi/2) \gg \beta^{-1/3}$ (but still not too large, so that $\beta \cos \theta$ is well approximated by the expansion within curly brackets in (7.19)).

Thus, Fock's function indeed interpolates smoothly between the shadow and lit regions on the surface of the sphere. However, it cannot be employed in the lit region too far beyond $\theta - (\pi/2) \sim \beta^{-1/3}$.

B. THE NEIGHBORHOOD OF THE SHADOW BOUNDARY

Let us now consider the behavior of the wave function in the neighborhood of the geometrical shadow boundary, $\theta \approx \theta_0$ (cf. (5.2)), at not too large a distance from the sphere,

$$r \ll \beta^{1/3}a. \quad (7.20)$$

Under these conditions it follows from (5.8) and (5.9) that

$$\mid \exp (i\lambda_n\delta_0) \mid \ll 1, \quad (7.21)$$

so that we need only be concerned with $\psi_0^{(1)}$, which is given by (6.6).

We have seen that (6.6) has saddle points at $\bar{\lambda} = \rho \sin \theta$ and $\bar{\lambda} = kp$, where p is given by (6.19). The neighborhood of the shadow boundary is characterized by the fact that these two saddle points approach each other, moving toward the point $\lambda = \beta$. The main contribution to the integral then arises from the neighborhood of $\lambda = \beta$, so that it is convenient to take the path of integration through this point and to split it in the following form:

$$\psi_0^{(1)} = -\left(\frac{\pi}{2\rho} \right)^{1/2} e^{-i\pi/4} \left[\int_{\sigma_1\infty}^{\beta} \frac{H_\lambda^{(2)}(\beta)}{H_\lambda^{(1)}(\beta)} H_\lambda^{(1)}(\rho)Q_{\lambda-1/2}^{(1)}(\cos \theta)e^{i\lambda\pi/2}\lambda \, d\lambda \right.$$

$$+ 2 \int_{\beta}^{\sigma_2\infty} \frac{J_\lambda(\beta)}{H_\lambda^{(1)}(\beta)} H_\lambda^{(1)}(\rho)Q_{\lambda-1/2}^{(1)}(\cos \theta)e^{i\lambda\pi/2}\lambda \, d\lambda \quad (7.22)$$

$$\left. - \int_{\beta}^{\sigma_2\infty} H_\lambda^{(1)}(\rho)Q_{\lambda-1/2}^{(1)}(\cos \theta)e^{i\lambda\pi/2}\lambda \, d\lambda \right] = \psi_{01}^{(1)} + \psi_{02}^{(1)} + \psi_{03}^{(1)},$$

where $\sigma_1\infty$ and $\sigma_2\infty$ denote the beginning and end points of Γ, as illustrated

in Fig. 6, and we have used the identity

$$H_\lambda^{(2)}(\beta)/H_\lambda^{(1)}(\beta) = 2J_\lambda(\beta)/H_\lambda^{(1)}(\beta) - 1. \qquad (7.23)$$

In $\psi_{03}^{(1)}$, we may employ the same approximations that led to (6.9). Restricting ourselves to the main term of (6.11), we find

$$\psi_{03}^{(1)} \approx \left(\frac{\rho}{2\pi \sin \theta}\right)^{1/2} e^{-i\pi/4}$$
$$\cdot \int_{\theta_0}^{\sigma_2'\infty} (\sin w \cos w)^{1/2} \exp \{i\rho[\cos w + (w - \theta) \sin w]\} \, dw. \qquad (7.24)$$

Above the shadow boundary, the integrand still has a saddle point at $\bar{w} = \theta$, as in (6.10). In any case, for $\theta \approx \theta_0$, the main contribution comes from the neighborhood of the lower limit of integration, so that we may expand the integrand around $w = \theta$ and extend the corresponding range of integration to infinity, with the following result:

$$\psi_{03}^{(1)} \approx \left(\frac{kz}{2\pi}\right)^{1/2} e^{-i\pi/4} e^{ikz} \int_{\theta_0}^{\infty} \exp [ikz(w - \theta)^2/2] \, dw, \qquad (7.25)$$

where we have substituted $\rho \cos \theta = kz$.

The condition for the validity of this approximation is that higher-order terms in the expansion of the exponent in (7.24) shall be negligible in the relevant portion of the domain of integration. This leads to the following conditions:

$$kz \gg \beta^{2/3}, \qquad (7.26)$$

$$| \theta - \theta_0 | \ll \beta^{-1/3}. \qquad (7.27)$$

The above result may be rewritten as follows:

$$\psi_{03}^{(1)} \approx e^{ikz - i\pi/4}[F(\infty) - F(-\nu)]/\sqrt{2} \qquad (7.28)$$

where

$$\nu = (kz/\pi)^{1/2}(\theta - \theta_0) \qquad (7.29)$$

and

$$F(\nu) = \int_0^\nu \exp (i\pi\tau^2/2) \, d\tau \qquad (7.30)$$

is the Fresnel integral. Since

$$F(\infty) = e^{i\pi/4}/\sqrt{2}, \qquad (7.31)$$

(7.28) becomes

$$\psi_{03}^{(1)} \approx \frac{1}{2} e^{ikz} - \frac{e^{ikz - i\pi/4}}{\sqrt{2}} F(-\nu). \qquad (7.32)$$

This is analogous to the classical Fresnel diffraction pattern of a straight edge
(19). On the geometrical shadow boundary, where $\nu = 0$ (cf. (7.29)), it would
give one half the amplitude of the incident wave, which is a well-known result.

Now let us consider the two remaining terms of (7.22). Since the main con-
tribution to the integrals comes from the neighborhood of $\lambda = \beta$, we may em-
ploy the approximations (A.17) and (A.18), which give

$$H_\lambda^{(2)}(\beta)/H_\lambda^{(1)}(\beta) \approx e^{2i\pi/3} Ai(xe^{-2i\pi/3})/Ai(xe^{2i\pi/3}) \qquad (\lambda < \beta), \quad (7.33)$$

$$2J_\lambda(\beta)/H_\lambda^{(1)}(\beta) \approx e^{i\pi/3} Ai(x)/Ai(xe^{2i\pi/3}) \qquad (\lambda > \beta), \quad (7.34)$$

where x is defined by (7.10).

For the remaining factors of the integrand, we may employ the same approxi-
mations that led to (7.24), so that we get, with the substitution (6.8),

$$
\begin{aligned}
\psi_{01}^{(1)} + \psi_{02}^{(1)} \approx -&\left(\frac{\rho}{2\pi \sin \theta}\right)^{1/2} e^{-i\pi/4} \left\{ e^{2i\pi/3} \int_{\sigma_1'\infty}^{\theta_0} (\sin w \cos w)^{1/2} \right. \\
&\cdot \frac{Ai(xe^{-2i\pi/3})}{Ai(xe^{2i\pi/3})} \exp \{i\rho[\cos w + (w - \theta) \sin w]\} \, dw \\
&+ e^{i\pi/3} \int_{\theta_0}^{\sigma_2'\infty} (\sin w \cos w)^{1/2} \frac{Ai(x)}{Ai(xe^{2i\pi/3})} \\
&\left. \times \exp \{i\rho[\cos w + (w - \theta) \sin w]\} \, dw \right\}.
\end{aligned}
\qquad (7.35)
$$

In the neighborhood of $\theta = \theta_0$, we may again employ the expansion around
$w = \theta$ that led to (7.25), with the following result:

$$
\begin{aligned}
\psi_{01}^{(1)} + \psi_{02}^{(1)} \approx -&\left(\frac{kz}{2\pi}\right)^{1/2} e^{-i\pi/4} e^{ikz} \left\{ e^{2i\pi/3} \int_{-\infty}^{\theta_0} \exp[ikz(w - \theta)^2/2] \right. \\
&\times \frac{Ai(xe^{-2i\pi/3})}{Ai(xe^{2i\pi/3})} \, dw \\
&\left. + e^{i\pi/3} \int_{\theta_0}^{\infty} \exp[ikz(w - \theta)^2/2] \frac{Ai(x)}{Ai(xe^{2i\pi/3})} \, dw \right\},
\end{aligned}
\qquad (7.36)
$$

where

$$x = \left(\frac{2}{\beta}\right)^{1/3} \rho(\sin w - \sin \theta_0) = 2\left(\frac{2}{\beta}\right)^{1/3} \rho \cos\left(\frac{w + \theta_0}{2}\right) \sin\left(\frac{w - \theta_0}{2}\right). \quad (7.37)$$

The discussion of the asymptotic behavior of the Airy function given in Ap-
pendix D shows that values of $|x| \gg 1$ do not contribute much to the integrals
in (7.36). On the other hand, $\rho/\beta^{1/3} \geq \beta^{2/3} \gg 1$, so that, according to (7.37),
only small values of $|w - \theta_0|$ give a significant contribution. Under these

conditions, we may replace (7.37) by

$$x \approx (2/\beta)^{1/3} \rho \cos \theta_0 (w - \theta_0) \approx (2/\beta)^{1/3} kz(w - \theta_0), \qquad (7.38)$$

where the last approximation follows from $\theta_0 \approx \theta$.

Making the change of variable (7.38) in (7.36), we find

$$\psi_{01}^{(1)} + \psi_{02}^{(1)} \approx -\pi^{-1/2} e^{-i\pi/4} \eta e^{ikz} \exp{(i\pi\nu^2/2)} \left[e^{2i\pi/3} \int_{-\infty}^{0} \exp{(i\xi x + i\eta^2 x^2)} \right.$$
$$\left. \times \frac{Ai(xe^{-2i\pi/3})}{Ai(xe^{2i\pi/3})} \, dx + e^{i\pi/3} \int_{0}^{\infty} \exp{(i\xi x + i\eta^2 x^2)} \frac{Ai(x)}{Ai(xe^{2i\pi/3})} \, dx \right], \qquad (7.39)$$

where ν is given by (7.29), and

$$\xi = (\beta/2)^{1/3} (\theta - \theta_0), \qquad \eta = (\beta/2)^{1/3}/(2kz)^{1/2}. \qquad (7.40)$$

According to (7.26) and (7.27), we have $|\xi| \ll 1$, $\eta \ll 1$, so that, in the significant range of the domain of integration, the exponential function in the integrands of (7.39) may be replaced by unity, with the following result:

$$\psi_{01}^{(1)} + \psi_{02}^{(1)} \approx -Ce^{-i\pi/4} \beta^{1/3} (2\pi kz)^{-1/2} \exp{(ikz + i\pi\nu^2/2)}, \qquad (7.41)$$

where

$$2^{1/3} C = e^{2i\pi/3} \int_{-\infty}^{0} \frac{Ai(xe^{-2i\pi/3})}{Ai(xe^{2i\pi/3})} \, dx + e^{i\pi/3} \int_{0}^{\infty} \frac{Ai(x)}{Ai(xe^{2i\pi/3})} \, dx. \qquad (7.42)$$

The constant C has been evaluated by Rubinow and Wu (20) who found

$$C \approx 0.99615 e^{i\pi/3}. \qquad (7.43)$$

It follows from (7.28) and (7.41) that

$$\psi_0^{(1)} \approx \frac{e^{-i\pi/4}}{\sqrt{2}} e^{ikz} \left[F(\infty) - F(-\nu) - 2^{1/3} C\xi \frac{\exp{(i\pi\nu^2/2)}}{\pi\nu} \right]. \qquad (7.44)$$

The conditions for the validity of this result, besides (7.27), are (7.20) and (7.26), which may be combined into the following condition:

$$\beta^{-1/3} a \ll z \ll \beta^{1/3} a. \qquad (7.45)$$

It is readily seen that, for $|\nu| \gg 1$, either in the lit or in the shadow region, the last term of (7.44) is a small correction, of the order of $|\xi|$, to the amplitude of the diffracted wave.

Thus, if $|\theta - \theta_0| \ll \beta^{-1/3}$, in the domain (7.45), the transition from light to shadow is described by an angular Fresnel diffraction pattern very similar to the classical one for a straight edge. The effects of the curvature of the sphere come in through small correction terms, of the order of $|\xi|$. If $|\theta - \theta_0| \gg \beta^{-1/3}$,

we go over either to the lit region, where (6.23) is valid, or to the shadow region, where (5.6) is valid (cf. (5.10)).

Finally, let us consider the immediate neighborhood of the shadow boundary, where (cf. (7.29))

$$| \nu | \ll 1. \tag{7.46}$$

We may then approximate the Fresnel integral by the first term in its power series expansion,

$$-F(-\nu) \approx \nu = \frac{\rho \cos \theta(\theta - \theta_0)}{(\pi k z)^{1/2}} \approx \frac{\rho(\sin \theta - \sin \theta_0)}{(\pi k z)^{1/2}}, \tag{7.47}$$

and the exponential in the last term of (7.44) may be replaced by unity. Taking into account (7.31), we get

$$\psi_0^{(1)} \approx \frac{1}{2} e^{ikz} \left[1 + \left(\frac{2}{\pi k z} \right)^{1/2} e^{-i\pi/4} k(r \sin \theta - a - C\beta^{-2/3}a) \right]. \tag{7.48}$$

Defining the shadow boundary by the condition that $| \psi | = \frac{1}{2}$ on it, we find from (7.48) that the shadow boundary no longer lies at $r \sin \theta = a$, as in (7.32), but rather at

$$r \sin \theta = a + s, \tag{7.49}$$

where

$$s = a(\operatorname{Re} C + \operatorname{Im} C)/\beta^{2/3} = 1.36077a/\beta^{2/3}. \tag{7.50}$$

This is identical to the result found by Rubinow and Keller (21) for a circular cylinder and by S. O. Rice (22) for a parabolic cylinder, thus confirming, in the present example, Rubinow and Keller's conjecture that the result is true also for three-dimensional obstacles.

There remains to examine the consistency of the various approximations leading to (7.48). According to (7.47), (7.49), and (7.50), the order of magnitude of ν at the (shifted) shadow boundary is given by

$$\nu \sim \frac{ks}{(\pi k z)^{1/2}} \sim \frac{\beta^{1/3}}{(\pi k z)^{1/2}}. \tag{7.51}$$

According to (7.26), this satisfies condition (7.46).

It is readily verified that, in the domain defined by (7.27) and (7.45), the neglected terms in (6.11) and in the approximations that were made in connection with (7.35) give contributions of a higher order of magnitude.

VIII. THE FRESNEL-LOMMEL REGION

A. BASIC APPROXIMATIONS

According to classical diffraction theory, the Fresnel region is the domain, in the neighborhood of the shadow boundary, viewed from which the obstacle

contains a large number of Fresnel zones, i.e., $r \ll a^2/\lambda$, where λ is the wavelength. We shall now consider the behavior of the wave function in this region, at distances larger than those allowed by (7.20), i.e.,

$$\beta^{1/3}a \lesssim r \ll \beta a. \tag{8.1}$$

At the same time, we shall stay within the geometrical shadow, or not too far outside:

$$\theta \lesssim \theta_0 \sim a/r. \tag{8.2}$$

We shall call this the Fresnel-Lommel region, because, as will be seen later, the wave function throughout most of this region can be approximated by Lommel's classical solution to the problem of diffraction by a circular disc (23).

According to (5.8), (5.9), (8.1), and (8.2), condition (7.21) is no longer satisfied in this region, but rather $|\exp(i\lambda_n\delta_0)| \gtrsim 1$. Thus, the integral containing $Q_{\lambda-1/2}^{(2)}(\cos\theta)$ in (6.2) can no longer be expressed as a residue series and we must consider, in the place of (7.22),

$$\psi_0 = -\left(\frac{\pi}{2\rho}\right)^{1/2} e^{-i\pi/4} \left[\int_{\sigma_1\infty}^{\beta} \frac{H_\lambda^{(2)}(\beta)}{H_\lambda^{(1)}(\beta)} H_\lambda^{(1)}(\rho) P_{\lambda-1/2}(\cos\theta) e^{i\lambda\pi/2}\lambda \, d\lambda \right.$$

$$+ 2 \int_\beta^{\sigma_2\infty} \frac{J_\lambda(\beta)}{H_\lambda^{(1)}(\beta)} H_\lambda^{(1)}(\rho) P_{\lambda-1/2}(\cos\theta) e^{i\lambda\pi/2}\lambda \, d\lambda \tag{8.3}$$

$$\left. - \int_\beta^{\sigma_2\infty} H_\lambda^{(1)}(\rho) P_{\lambda-1/2}(\cos\theta) e^{i\lambda\pi/2}\lambda \, d\lambda \right] = \psi_{01} + \psi_{02} + \psi_{03} .$$

The third term of (8.3), like that of (7.22), depends on the scatterer only through its radius appearing in the lower limit of integration. Roughly, it represents the effect of cutting off from the incident wave all the rays that meet the sphere, so that the sphere behaves, in this respect, like an opaque disc of radius a. We shall see that this term gives rise to the classical diffraction pattern of a circular disc. It corresponds to the "shadow-forming wave" mentioned in Section VII.

The main contribution to the integrals in (8.3) still arises from the neighborhood of $\lambda = \beta$, so that $H_\lambda^{(1)}(\rho)$ may be replaced by the expansion (A.16). On the other hand, since we want to consider both the behavior for $\beta\theta \lesssim 1$ and for $\beta\theta \gg 1$, we shall employ the uniform asymptotic expansion (C.11) of $P_{\lambda-1/2}(\cos\theta)$. Finally, in ψ_{01} and ψ_{02}, we may again employ the approximations (7.33) and (7.34). The results are

$$\psi_{01} + \psi_{02} \approx \frac{i}{\rho} \left(\frac{\theta}{\sin\theta}\right)^{1/2} \left\{ e^{2i\pi/3} \int_{\sigma_1\infty}^{\beta} \frac{Ai(xe^{-2i\pi/3})}{Ai(xe^{2i\pi/3})} \exp\left[i(\rho^2 - \lambda^2)^{1/2}\right] \right.$$

$$+ i\lambda \sin^{-1}(\lambda/\rho)] J_0(\lambda\theta)\lambda \, d\lambda + e^{i\pi/3} \int_\beta^{\sigma_2\infty} \frac{Ai(x)}{Ai(xe^{2i\pi/3})} \exp\left[i(\rho^2 - \lambda^2)^{1/2}\right] \tag{8.4}$$

$$\left. + i\lambda \sin^{-1}(\lambda/\rho)] J_0(\lambda\theta)\lambda \, d\lambda \right\} ,$$

where x is given by (7.10) and

$$\psi_{03} \approx -i\rho(\theta/\sin\theta)^{1/2} \int_{a/r}^{\sigma_2 \infty} \exp\,\{i\rho[(1 - \tau^2)^{1/2}$$
$$+ \tau\sin^{-1}\tau]\}J_0(\rho\theta\tau)(1 - \tau^2)^{-1/4}\tau\,d\tau, \tag{8.5}$$

where we have made $\lambda = \rho\tau$.

Since the main contribution to the integral in (8.5) comes from the neighborhood of the lower limit $\tau \sim a/r \lesssim \beta^{-1/3} \ll 1$, we may expand the integrand in powers of τ, keeping only the main terms:

$$\psi_{03} \approx -i\rho(\theta/\sin\theta)^{1/2}e^{i\rho} \int_{a/r}^{\infty} \exp\,(i\rho\tau^2/2)J_0(\rho\theta\tau)\tau\,d\tau, \tag{8.6}$$

where the upper limit has been replaced by ∞.

According to Appendix E, this integral may be expressed in terms of Lommel functions. In fact, it follows from (E.5) that

$$\psi_{03} \approx \left(\frac{\theta}{\sin\theta}\right)^{1/2} \exp\left(i\rho + ik\frac{a^2}{2r}\right)\left[V_0\left(\frac{ka^2}{r}, \beta\theta\right) + iV_1\left(\frac{ka^2}{r}, \beta\theta\right)\right], \tag{8.7}$$

where V_0 and V_1 are Lommel functions of orders zero and one.

Similarly, in (8.4), we may approximate

$$(\rho^2 - \lambda^2)^{1/2} + \lambda\sin^{-1}(\lambda/\rho) \approx \rho + (\lambda^2/2\rho). \tag{8.8}$$

Taking x as new variable of integration, we find

$$\lambda^2/2\rho = ka^2/2r + (\beta/2)^{1/3}ax/r + (\beta/2)^{2/3}x^2/2\rho. \tag{8.9}$$

The main contribution to the integrals comes from $|x| \lesssim 1$, because of the Airy functions. Thus, according to (8.1), the last term of (8.9) is negligible, and we find

$$\psi_{01} + \psi_{02} \approx i\left(\frac{\beta}{2}\right)^{1/3}\frac{a}{r}\left(\frac{\theta}{\sin\theta}\right)^{1/2} \exp\left(i\rho + ik\frac{a^2}{2r}\right)$$
$$\times \left\{e^{2i\pi/3} \int_{-\infty}^{0} \frac{Ai(xe^{-2i\pi/3})}{Ai(xe^{2i\pi/3})} \exp\left[i\left(\frac{\beta}{2}\right)^{1/3}\frac{a}{r}x\right] J_0\left[\beta\theta + \left(\frac{\beta}{2}\right)^{1/3}\theta x\right] dx \right. \tag{8.10}$$
$$\left. + e^{i\pi/3} \int_0^{\infty} \frac{Ai(x)}{Ai(xe^{2i\pi/3})} \exp\left[i\left(\frac{\beta}{2}\right)^{1/3}\frac{a}{r}x\right] J_0\left[\beta\theta + \left(\frac{\beta}{2}\right)^{1/3}\theta x\right] dx \right\}.$$

Putting together (8.7) and (8.10), we finally get

$$\psi_0 \approx \left(\frac{\theta}{\sin\theta}\right)^{1/2} \exp\left(ikr + ik\frac{a^2}{2r}\right)f(s, t, u, v), \tag{8.11}$$

where

$$f(s, t, u, v) = L(u, v) + isF(s, t, v), \qquad (8.12)$$

$$L(u, v) = V_0(u, v) + iV_1(u, v), \qquad (8.13)$$

$$F(s, t, v) = e^{2i\pi/3} \int_{-\infty}^{0} \frac{Ai(xe^{-2i\pi/3})}{Ai(xe^{2i\pi/3})} e^{isx} J_0(v + tx) \, dx \\ + e^{i\pi/3} \int_{0}^{\infty} \frac{Ai(x)}{Ai(xe^{2i\pi/3})} e^{isx} J_0(v + tx) \, dx, \qquad (8.14)$$

and

$$s = (\beta/2)^{1/3} a/r, \qquad t = (\beta/2)^{1/3} \theta,$$
$$u = ka^2/r = \beta a/r, \qquad v = \beta\theta = tu/s. \qquad (8.15)$$

Conditions (8.1) and (8.2) are equivalent to

$$s \lesssim 1, \qquad t \lesssim 1, \qquad u \gg 1. \qquad (8.16)$$

According to classical diffraction theory, the wave function in the Fresnel region due to the diffraction of a plane wave by a circular disc of radius a is (23)

$$\psi_{\rm cl} = \exp\left(ikr + ik\frac{a^2}{2r}\right)\left[V_0\left(\frac{ka^2}{r}, \beta \sin \theta\right) + iV_1\left(\frac{ka^2}{r}, \beta \sin \theta\right)\right], \quad (8.17)$$

in the approximation where $\sin \theta \approx \theta$. In this approximation, (8.17) coincides with (8.7).

Thus, in (8.12), $L(u, v)$ represents Lommel's approximation, while $F(s, t, v)$ is a correction to classical diffraction theory of the same type as the Fock terms discussed in Section VII.

B. Behavior on the Axis (Poisson Spot)

For $\theta = 0$ $(r = z)$, we have, according to (E.3),

$$L(u, 0) = 1, \qquad (8.18)$$

so that

$$\psi_0 \approx \exp\left(ikz + ik\frac{a^2}{2z}\right) f(s), \qquad (8.19)$$

where

$$f(s) = 1 + is\left[e^{2i\pi/3} \int_{0}^{\infty} \frac{Ai(xe^{i\pi/3})}{Ai(xe^{-i\pi/3})} e^{-isx} \, dx + e^{i\pi/3} \int_{0}^{\infty} \frac{Ai(x)}{Ai(xe^{2i\pi/3})} e^{isx} \, dx\right]. \quad (8.20)$$

In Lommel's approximation, the second term would be absent, so that we would have $|\psi_0| = 1$, i.e., the intensity along the axis would be identical to

that of the incident wave. This corresponds to the well-known Poisson spot.

According to Appendix D, $Ai(\zeta e^{i\pi/3})/Ai(\zeta e^{-i\pi/3})$ goes to zero like

$$\exp\left[-\tfrac{4}{3}\,|\,\zeta\,|^{3/2}\sin\,(3\varphi/2)\right]$$

when $\zeta = |\,\zeta\,|\exp\,(i\varphi)$ goes to infinity in the sector $4\pi/3 < \varphi < 2\pi$, so that the path of integration in the first integral of (8.20) may be rotated by $\pi/3$ into the fourth quadrant, with the following result:

$$f(s) = 1 + ise^{i\pi/3}\left[\int_0^\infty \frac{Ai(x)}{Ai(xe^{-2i\pi/3})}\exp\,(-ie^{-i\pi/3}sx)\,dx\right.$$
$$\left. + \int_0^\infty \frac{Ai(x)}{Ai(xe^{2i\pi/3})}\exp\,(isx)\,dx\right]. \quad (8.21)$$

Both integrands now tend to zero like $\exp\,(-\tfrac{4}{3}x^{3/2})$ for $x \to \infty$.

At distances $z \ll \beta^{1/3}a$ $(s \gg 1)$, the residue series representation (5.11) should converge well, so that the wave function must become exponentially small. To recover this result from (8.21), let us note that, by partial integration, (8.21) becomes

$$f(s) = \frac{e^{-i\pi/6}}{2\pi}\int_0^\infty \frac{\exp\,(-ie^{-i\pi/3}sx)}{[Ai(xe^{-2i\pi/3})]^2}\,dx + \frac{e^{i\pi/6}}{2\pi}\int_0^\infty \frac{\exp\,(isx)}{[Ai(xe^{2i\pi/3})]^2}\,dx, \quad (8.22)$$

where we have employed the Wronskian relation (D.2). This result may be rewritten as

$$f(s) = \frac{e^{i\pi/6}}{2\pi}\int_\Gamma \frac{\exp\,(is\zeta)}{[Ai(\zeta e^{2i\pi/3})]^2}\,d\zeta, \quad (8.23)$$

where Γ is the path shown in Fig. 10, going from $\infty e^{2i\pi/3}$ to ∞.

If $s \gg 1$, the integral can be evaluated by reducing it to a series of residues at the poles $\zeta_n = e^{i\pi/3}x_n$, where $-x_n$ is the nth zero of the Airy function. The result is

$$f(s) = e^{-i\pi/6}s\sum_n \frac{\exp\,(ie^{i\pi/3}sx_n)}{[Ai'(-x_n)]^2}. \quad (8.24)$$

Substituting this in (8.19), we find

$$\psi_0 \approx e^{-i\pi/6}\exp\left(ikz + ik\frac{a^2}{2z}\right)\left(\frac{\beta}{2}\right)^{1/3}\frac{a}{z}\sum_n \frac{\exp\,[ie^{i\pi/3}x_n(\beta/2)^{1/3}a/z]}{[Ai'(-x_n)]^2}$$
$$(z \ll \beta^{1/3}a). \quad (8.25)$$

It may readily be verified that this result coincides with the term $m = 0$ of (5.11), with $z \gg a$. Thus, the wave function along the axis is exponentially small for $z \ll \beta^{1/3}a$.
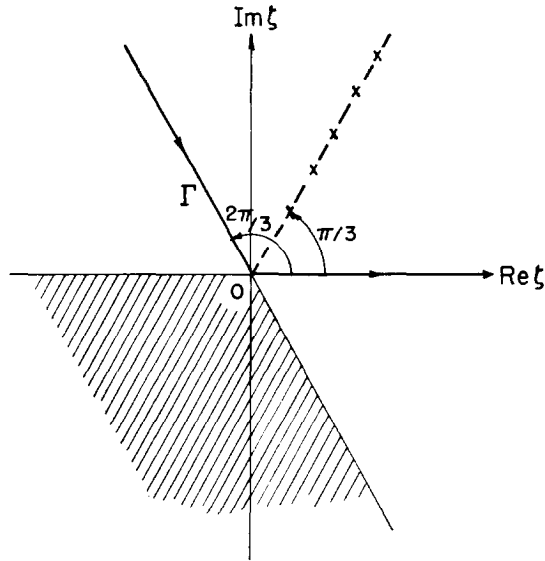
FIG. 10. Path of integration in (8.23). $\times$ $\times$ $\times$—Poles of the integrand. The integrand goes to zero at infinity outside of the shaded sector, except along the line of poles.

On the other hand, for $z \gg \beta^{1/3}a$ ($s \ll 1$), we can expand $f(s)$ in a power series,

$$f(s) = 1 + is\sum_{n=0}^{\infty} i^n M_n s^n/n! \qquad (8.26)$$

where, according to (8.21),

$$M_n = e^{i\pi/3}\int_0^{\infty} \frac{Ai(x)}{Ai(xe^{2i\pi/3})} x^n\,dx + e^{i(2n+1)\pi/3}\int_0^{\infty} \frac{Ai(x)}{Ai(xe^{-2i\pi/3})} x^n\,dx. \quad (8.27)$$

The first few coefficients M_n have been computed by Wu (24). In particular,

$$M_0 = 2^{1/3}C = 1.2551e^{i\pi/3}, \qquad M_1 = 0.5323e^{2i\pi/3}, \qquad (8.28)$$

where C is given by (7.43).

Substituting (8.26) in (8.19), we get

$$\psi_0 \approx \exp\left(ikz + ik\frac{a^2}{2z}\right)\left[1 + iM_0\left(\frac{\beta}{2}\right)^{1/3}\frac{a}{z} - M_1\left(\frac{\beta}{2}\right)^{2/3}\frac{a^2}{z^2} + \cdots\right] \qquad (8.29)$$
$$(z \gg \beta^{1/3}a).$$

Thus, for $z \gg \beta^{1/3}a$, the intensity approaches that of the incident wave.

On comparing (8.29) with (8.25), we see that a Poisson spot of intensity

comparable to that of the incident wave begins to develop at a distance

$$z \sim \beta^{1/3} a \tag{8.30}$$

from the sphere. This is in contrast to the case of a circular disc, where the Poisson spot begins to appear at a distance $z \sim a$ from the plane of the disc (5, p. 103).

C. Behavior Away from the Axis

Let us consider first the term $L(u, v)$, which corresponds to the classical diffraction pattern (cf. (8.13)). The behavior of this term depends on the parameter

$$u/v = a/r\theta \approx \theta_0/\theta. \tag{8.31}$$

In the lit region, $\theta \gg \theta_0$, we can employ the expansion (E.1), which leads to

$$L(u, v) = \exp\left[-\frac{i}{2}\left(u + \frac{v^2}{u}\right)\right] + i\frac{u}{v} J_1(v) + \left(\frac{u}{v}\right)^2 J_2(v) + \cdots \tag{8.32}$$
$$(u \ll v).$$

The corresponding classical wave function, according to (8.11), would be

$$\psi_{\text{cl}} \approx \left(\frac{\theta}{\sin\theta}\right)^{1/2}\left\{\exp\left[i\rho\left(1 - \frac{\theta^2}{2}\right)\right]\right.$$
$$\left. + i\frac{a}{r\theta}\exp\left(i\rho + ik\frac{a^2}{2r}\right) J_1(\beta\theta) + \cdots\right\} \approx \exp\left(i\rho\cos\theta\right) \quad (\theta \gg a/r) \tag{8.33}$$

so that ψ_{cl} approaches the incident wave.

Near the shadow boundary, at $\theta = a/r$, we can employ (E.2), which gives

$$L(u, u) = \tfrac{1}{2}[e^{-iu} + J_0(u)], \tag{8.34}$$

so that

$$\psi_{\text{cl}} \approx \frac{1}{2}\left(\frac{\theta}{\sin\theta}\right)^{1/2}\exp\left(i\rho - ik\frac{a^2}{2r}\right)\left[1 + \exp\left(ik\frac{a^2}{r}\right) J_0\left(\frac{ka^2}{r}\right)\right] \tag{8.35}$$
$$(\theta = a/r).$$

The factor $\tfrac{1}{2}$ corresponds to the classical behavior at the shadow boundary discussed in Section VII. For $r \gg \beta^{1/3}a$, the shift of the shadow boundary is no longer given by (7.50): it increases with r and then oscillates. At distances $r \sim \beta a$, which mark the transition to the Fraunhofer region, the concept of shadow boundary is already meaningless.

Finally, well within the geometrical shadow region, $\theta \ll \theta_0$, we can employ the expansion (E.6):

$$L(u, v) \approx J_0(v) - i\frac{v}{u} J_1(v) - \left(\frac{v}{u}\right)^2 J_2(v) + \cdots \qquad (u \gg v), \quad (8.36)$$

which gives

$$\psi_{cl} \approx \left(\frac{\theta}{\sin \theta}\right)^{1/2} \exp\left(i\rho + ik\frac{a^2}{2r}\right)$$
$$\cdot \left[J_0(\beta\theta) - i\frac{r\theta}{a}J_1(\beta\theta) - \left(\frac{r\theta}{a}\right)^2 J_2(\beta\theta) + \cdots\right] \qquad (\theta \ll a/r). \tag{8.37}$$

Now let us consider the effect of the Fock-type terms $F(s, t, v)$ in (8.12). Just as in (8.21), we can rewrite (8.14) as

$$F(s, t, v) = e^{i\pi/3}\left[\int_0^\infty \frac{Ai(x)}{Ai(xe^{-2i\pi/3})} \exp\left(-ie^{-i\pi/3}sx\right)J_0(v - e^{-i\pi/3}tx)\, dx\right.$$
$$\left. + \int_0^\infty \frac{Ai(x)}{Ai(xe^{2i\pi/3})} \exp\left(isx\right)J_0(v + tx)\, dx\right]. \tag{8.38}$$

In the shadow region, for $r \ll \beta^{1/3}a$ $(s \gg 1)$, it can be shown, as in (8.25), that $isF(s, t, v)$ cancels the main term in $L(u, v)$, leaving as a remainder a residue series corresponding to (5.11).

For $r \gtrsim \beta^{1/3}a$ $(s \lesssim 1)$ and $\theta \ll \beta^{-1/3}$ $(t \ll 1)$, the main contribution to the integrals (8.38) arises from small values of the argument, because of the Airy functions. Therefore, we may employ the expansion

$$J_0(v + tx) = J_0(v) - txJ_1(v) + \cdots \tag{8.39}$$

and similarly for the other term, with the following result:

$$isF(s, t, v) = [f(s) - 1]J_0(v) - tg(s)J_1(v) + \cdots \qquad (s \lesssim 1, t \ll 1), \tag{8.40}$$

where $f(s)$ is given by (8.21) and

$$g(s) = ise^{i\pi/3}\left[\int_0^\infty \frac{Ai(x)}{Ai(xe^{2i\pi/3})} \exp\left(isx\right)x\, dx - e^{-i\pi/3}\right.$$
$$\left. \times \int_0^\infty \frac{Ai(x)}{Ai(xe^{-2i\pi/3})} \exp\left(-ie^{-i\pi/3}sx\right)x\, dx\right]. \tag{8.41}$$

In particular, if also $s \ll 1$, we may expand the exponentials in power series, and we get, with the help of (8.27),

$$F(s, t, v) \approx (M_0 + iM_1s + \cdots)J_0(v)$$
$$- M_1tJ_1(v) + \cdots \qquad (s \ll 1, t \ll 1). \tag{8.42}$$

Taking into account (8.11) and (8.37), this leads to

$$\psi_0 \approx \left(\frac{\theta}{\sin \theta}\right)^{1/2} \exp\left(ikr + ik\frac{a^2}{2r}\right)\left\{\left[1 + iM_0\left(\frac{\beta}{2}\right)^{1/3}\frac{a}{r} - M_1\left(\frac{\beta}{2}\right)^{2/3}\left(\frac{a}{r}\right)^2 + \cdots\right]\right.$$
$$\left. \times J_0(\beta\theta) - i\left[1 + M_1\left(\frac{\beta}{2}\right)^{2/3}\left(\frac{a}{r}\right)^2 + \cdots\right]\frac{r\theta}{a}J_1(\beta\theta) + \cdots\right\} \tag{8.43}$$
$$(r \gg \beta^{1/3}a, \theta \ll a/r).$$

Note that (8.29) is a particular case of this result.

In the neighborhood of the axis, for $r \gg \beta^{1/3}a$, the intensity, according to (8.43), behaves like $J_0^2(\beta\theta)$ times the intensity of the incident wave, so that the Poisson spot actually corresponds to a "Poisson cone" of angular opening

$$\theta \sim \beta^{-1}. \tag{8.44}$$

In this region, the Fock terms give only a small correction, having the same angular dependence as the Fresnel-Lommel approximation.

Finally, if $\theta \gg \beta^{-1/3}$, we must recover the reflected wave, given by (6.23). It can be verified that it arises from a saddle point in one of the Fock terms. However, we shall not discuss this problem here; the analogous but simpler case of the far field will be discussed in the next Section.

IX. THE SCATTERING AMPLITUDE

A. Behavior Away from Forward or Backward Directions

For $r \to \infty$, we have

$$\psi(r,\theta) \approx e^{ikz} + f(k,\theta)e^{ikr}/r, \tag{9.1}$$

where $f(k,\theta)$ is the scattering amplitude. If θ is not too close to 0 or π, $f(k,\theta)$ may be obtained from the expressions derived in Section VI, which remain valid for $r \to \infty$. Actually, the asymptotic form (9.1) is already valid in the "Fraunhofer region" defined by $r \gg \beta a$ (cf. Section VIII).

According to (6.19) and Fig. 7, the angle $\bar{w}$ approaches zero as $r \to \infty$, so that $\zeta \to \theta/2$ in (6.20) and the saddle point approaches

$$\bar{\lambda} = kp = \beta \cos(\theta/2). \tag{9.2}$$

This corresponds to the geometrically reflected ray in the direction θ, as shown in Fig. 11.
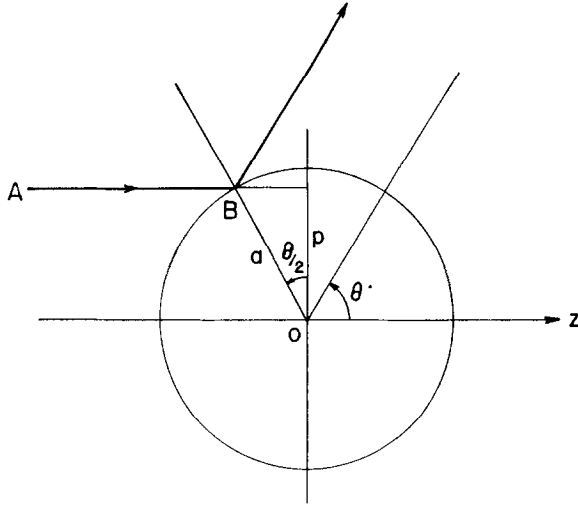
It follows from (6.23) and (6.24) that

$$f(k,\theta) = f_r(k,\theta) + f_{res}(k,\theta), \tag{9.3}$$

where

$$f_r(k,\theta) = -\frac{a}{2} \exp\left(-2i\beta \sin\frac{\theta}{2}\right)\left(1 + \frac{i}{2\beta \sin^3\frac{\theta}{2}} + \cdots\right) \tag{9.4}$$

is the "reflection" amplitude and

$$f_{res}(k,\theta) = e^{-i\pi/6} \frac{a}{2}\left(\frac{2}{\beta}\right)^{1/6}(\pi \sin\theta)^{-1/2}$$

$$\cdot \left\{ e^{-i\pi/4} \sum_n \frac{\exp(i\lambda_n \delta_0')}{[Ai'(-x_n)]^2} + \sum_{m=1}^{\infty}(-1)^m \sum_n \frac{1}{[Ai'(-x_n)]^2} \tag{9.5} \right.$$

$$\left. \cdot \left[\exp\left(i\lambda_n \gamma_m' + i\frac{\pi}{4}\right) + \exp\left(i\lambda_n \delta_m' - i\frac{\pi}{4}\right)\right]\right\},$$

Fig. 11. Geometrically reflected ray in direction θ.

where, according to (5.7) and (5.8),

$$\gamma_m' = 2m\pi - \theta, \qquad \delta_m' = 2m\pi + \theta. \tag{9.6}$$

The main term of (9.4) corresponds to the geometrical optics approximation, whereas (9.5) represents the radiation from the surface waves.

The expression (9.4) was obtained as a limiting case of (6.23), so that it represents the contribution from the neighborhood of the saddle point (9.2) in (6.6) or (6.31). It may also be derived by substituting directly in (6.6) or (6.31) the expansion

$$H_\lambda^{(1)}(\rho) \approx \left(\frac{2}{\pi\rho}\right)^{1/2} \exp\left[i\left(\rho - \lambda\frac{\pi}{2} - \frac{\pi}{4}\right)\right] \qquad (\rho \to \infty), \tag{9.7}$$

which leads to

$$f_r(k, \theta) = \frac{i}{k} \int_\Gamma \frac{H_\lambda^{(2)}(\beta)}{H_\lambda^{(1)}(\beta)} Q_{\lambda-1/2}^{(1)}(\cos\theta)\lambda \, d\lambda. \tag{9.8}$$

As in (6.6) or (6.31), the path Γ crosses the real axis at the saddle point (9.2), at an angle of $-\pi/4$ (Fig. 12). Since the main contribution arises from the neighborhood of this point, the path of integration may be extended to infinity on both sides, provided that the integral converges.

According to Appendix A and (C.7), the integrand of (9.8) behaves at infinity like $\exp[i\lambda(2\pi - \theta)]$ in region C of Fig. 12 and like $\exp(-i\lambda\theta)$ in region A. Thus, for $\theta \neq 0$, the path Γ may begin at infinity in C and end at infinity in
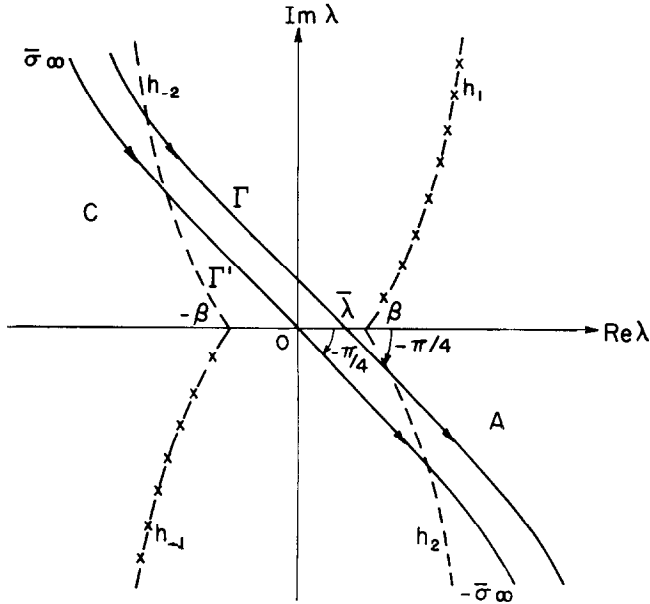
Fɪɢ. 12. Paths of integration for (9.8). × × ×—Poles of $S(\lambda, \beta)$.

A. In particular, it is equivalent to the path Γ' of Fig. 12, which is taken to be symmetrical about the origin. This will be useful later on.

Substituting (6.14) and (C.7) in (9.8) and employing (6.21), we are led again to (9.4).

The result (9.4) can no longer be applied when the correction terms in the expression within brackets become comparable to the main term, i.e., for $\theta \lesssim \beta^{-1/3}$. Furthermore, the asymptotic expansion (C.7) of $Q_{\lambda-1/2}^{(1)}(\cos \theta)$ for $\theta = \pi - \epsilon$ is only valid for $|\lambda\epsilon| \gg 1$ or, with $\lambda = \bar{\lambda} = \beta \sin(\epsilon/2) \approx \beta\epsilon/2$, for $\epsilon \gg \beta^{-1/2}$. Thus the conditions for the validity of the above results are

$$\theta \gg \beta^{-1/3}, \qquad \pi - \theta \gg \beta^{-1/2}. \tag{9.9}$$

In the next sections, we shall examine what happens near the forward and backward directions, when these conditions are no longer satisfied.

B. Tʜᴇ Nᴇɪɢʜʙᴏʀʜᴏᴏᴅ ᴏꜰ ᴛʜᴇ Fᴏʀᴡᴀʀᴅ Dɪʀᴇᴄᴛɪᴏɴ

Let us consider first the neighborhood of the forward direction, defined by $\theta \lesssim \beta^{-1/3}$. In this domain, not only does (9.4) lose its validity, but also the residue series involving δ_0' in (9.5) is no longer rapidly convergent, so that we must make a rearrangement similar to that of Section VIII, namely,

$$f(k, \theta) = f_0(k, \theta) + \tilde{f}_{\text{res}}(k, \theta), \tag{9.10}$$

where, according to Section VIII and (C.11),

$$\tilde{f}_{\text{res}}(k, \theta) = e^{-i\pi/6} a \left(\frac{\beta}{2}\right)^{1/3} \left(\frac{\theta}{\sin \theta}\right)^{1/2} \sum_{m=1}^{\infty} (-1)^m \sum_n \frac{\exp (2im\pi\lambda_n)}{[A\,i'(-x_n)]^2} J_0(\lambda_n \theta), \quad (9.11)$$

and $f_0(k, \theta)$ is defined by

$$\psi_0 \approx e^{ikz} + f_0(k, \theta)e^{ikr}/r \qquad (r \to \infty), \quad (9.12)$$

where ψ_0 is given by (8.3).

Since (8.10) remains valid for $r \to \infty$, we find at once that

$$\psi_{01} + \psi_{02} \approx i \frac{e^{ikr}}{r} a \left(\frac{\beta}{2}\right)^{1/3} \left(\frac{\theta}{\sin \theta}\right)^{1/2} \left\{ e^{2i\pi/3} \int_{-\infty}^{0} \frac{Ai(xe^{-2i\pi/3})}{Ai(xe^{2i\pi/3})} \right.$$
$$\times J_0 \left[\beta\theta + \left(\frac{\beta}{2}\right)^{1/3} \theta x \right] dx + e^{i\pi/3} \int_0^{\infty} \frac{Ai(x)}{Ai(xe^{2i\pi/3})} \qquad (9.13)$$
$$\left. \times J_0 \left[\beta\theta + \left(\frac{\beta}{2}\right)^{1/3} \theta x \right] dx \right\} \qquad (r \to \infty).$$

According to (8.3), we have

$$\psi_{03} = \left(\frac{\pi}{2\rho}\right)^{1/2} e^{-i\pi/4} \left(\int_0^{\sigma_2 \infty} - \int_0^{\beta} \right) H_\lambda^{(1)}(\rho) P_{\lambda-1/2} (\cos \theta) e^{i\lambda\pi/2} \lambda \, d\lambda. \quad (9.14)$$

In the integral from 0 to β, we can replace $H_\lambda^{(1)}(\rho)$ by its asymptotic expansion for $\rho \to \infty$, so that

$$\psi_{03} \approx \frac{i}{k} \frac{e^{ikr}}{r} \int_0^{\beta} P_{\lambda-1/2} (\cos \theta)\lambda \, d\lambda + \left(\frac{\pi}{2\rho}\right)^{1/2} e^{-i\pi/4}$$
$$\times \int_0^{\sigma_2 \infty} H_\lambda^{(1)}(\rho) P_{\lambda-1/2} (\cos \theta) e^{i\lambda\pi/2} \lambda \, d\lambda \qquad (r \to \infty). \quad (9.15)$$

On the other hand, since

$$\tan (\pi\lambda) = i - 2i \frac{e^{2i\pi\lambda}}{1 + e^{2i\pi\lambda}}, \quad (9.16)$$

it follows from (2.34), with $\sigma = \sigma_2$ (cf. Fig. 2 and Fig. 6), that

$$e^{i\rho\cos\theta} = \left(\frac{\pi}{2\rho}\right)^{1/2} e^{-i\pi/4} \int_0^{\sigma_2 \infty} H_\lambda^{(1)}(\rho) P_{\lambda-1/2} (\cos \theta) e^{i\lambda\pi/2} \lambda \, d\lambda - \Delta, \quad (9.17)$$

$$\Delta(\rho, \theta) = \left(\frac{2\pi}{\rho}\right)^{1/2} e^{-i\pi/4} \int_0^{i\infty} H_\lambda^{(1)}(\rho) P_{\lambda-1/2} (\cos \theta) e^{i\lambda\pi/2} \frac{e^{2i\pi\lambda}}{1 + e^{2i\pi\lambda}} \lambda \, d\lambda. \quad (9.18)$$

In the last integral, the path of integration has been shifted to the positive imaginary axis, which is allowed because of the extra convergence factor

exp $(2i\pi\lambda)$. Substituting (9.17) in (9.15), we get

$$\psi_{03} \approx e^{i\rho\cos\theta} + \frac{i}{k}\frac{e^{ikr}}{r}\int_0^\beta P_{\lambda-1/2}\left(\cos\theta\right)\lambda\,d\lambda + \Delta \qquad (r\to\infty). \quad (9.19)$$

The second term of this expression can be evaluated by inserting for $P_{\lambda-1/2}(\cos\theta)$ the uniform asymptotic expansion (C.11) and integrating term by term with the help of the well-known formula

$$\int x^{-n+1}J_n(x)\,dx = -x^{-n+1}J_{n-1}(x). \quad (9.20)$$

The result is

$$\frac{i}{k}\int_0^\beta P_{\lambda-1/2}\left(\cos\theta\right)\lambda\,d\lambda = ika^2\left(\frac{\theta}{\sin\theta}\right)^{1/2}\left[\frac{J_1(\beta\theta)}{\beta\theta} + O(\beta^{-2})\right]. \quad (9.21)$$

On the other hand, making $\lambda = i\mu$ in (9.18), we find

$$|\Delta| < \left(\frac{2\pi}{\rho}\right)^{1/2}\int_0^\infty e^{-\mu\pi/2}\left|H_{i\mu}^{(1)}(\rho)\right|\left|P_{i\mu-1/2}\left(\cos\theta\right)\right|e^{-2\pi\mu}\mu\,d\mu. \quad (9.22)$$

According to Watson (25), we may employ, for all $\mu \geqq 0$ and $\rho \gg 1$, the asymptotic expansion

$$H_{i\mu}^{(1)}(\rho) \approx \left(\frac{2}{\pi}\right)^{1/2}(\rho^2 + \mu^2)^{-1/4}$$
$$\cdot\exp\left\{i\left[(\rho^2 + \mu^2)^{1/2} - \mu\sinh^{-1}\frac{\mu}{\rho} - \frac{\pi}{4}\right] + \frac{\pi\mu}{2}\right\}, \quad (9.23)$$

so that

$$|H_{i\mu}^{(1)}(\rho)| \lesssim \left(\frac{2}{\pi\rho}\right)^{1/2}e^{\pi\mu/2}. \quad (9.24)$$

Furthermore, according to (C.12),

$$|P_{i\mu-1/2}(\cos\theta)| \leqq (\cos\theta)^{-1/2}e^{\pi\mu/2} \qquad (0 \leqq \theta < \pi/2). \quad (9.25)$$

Substituting (9.24) and (9.25) in (9.22), we find

$$|\Delta| < \frac{8}{9\pi^2}(\cos\theta)^{-1/2}\rho^{-1} \qquad (r\to\infty). \quad (9.26)$$

Since we are only interested in the domain $\theta \lesssim \beta^{-1/3}$, it follows from (9.19), (9.21), and (9.26) that

$$\psi_{03} \approx e^{i\rho\cos\theta} + ika^2\left(\frac{\theta}{\sin\theta}\right)^{1/2}\left[\frac{J_1(\beta\theta)}{\beta\theta} + O(\beta^{-2})\right]\frac{e^{ikr}}{r} \qquad (r\to\infty). \quad (9.27)$$

Combining this with (9.13), we finally obtain

$$f_0(k, \theta) \approx \frac{ika^2}{2} \left(\frac{\theta}{\sin \theta}\right)^{1/2} [g_{cl}(k, \theta) + g_F(k, \theta)], \qquad (9.28)$$

where

$$g_{cl}(k, \theta) = 2J_1(\beta\theta)/\beta\theta, \qquad (9.29)$$

$$g_F(k, \theta) = (2/\beta)^{2/3} F(0, t, v), \qquad (9.30)$$

$F(s, t, v)$ being defined in (8.14).

Except for the substitution $\sin \theta \to \theta$, which is allowed in this order of approximation, (9.29) coincides with the classical Fraunhofer diffraction pattern of a circular disc or aperture (26). The other term g_F may be called the Fock correction term (27).

The forward scattering amplitude is obtained by setting $\theta = 0$ in (9.28):

$$f_0(k, 0) \approx \tfrac{1}{2} ika^2(1 + 2C\beta^{-2/3} + \cdots), \qquad (9.31)$$

where C is given by (7.42) and (7.43). This result also follows from (8.29), by taking $z \gg \beta a$.

The total cross section is obtained from (9.31) with the help of the well-known "optical theorem"

$$\sigma = \frac{4\pi}{k} \operatorname{Im} f(k, 0) = \pi a^2(2 + 1.9923\beta^{-2/3} + \cdots), \qquad (9.32)$$

where we have employed (7.43).

This result was first derived by Rubinow and Wu (20). Higher-order terms in the expansion in powers of $\beta^{-2/3}$ have been computed by Wu (24) and by Beckmann and Franz (28). They involve the coefficients M_n defined in (8.27).

If $\theta \ll \beta^{-1/3}$, we may employ (8.42) with $s = 0$. The result is

$$
\begin{aligned}
f_0(k, \theta) &= \frac{1}{2} ika^2 \left(\frac{\theta}{\sin \theta}\right)^{1/2} \left\{ 2 \frac{J_1(\beta\theta)}{\beta\theta} + \left(\frac{2}{\beta}\right)^{2/3} \right. \\
&\quad \cdot \left. \left[M_0 J_0(\beta\theta) - M_1 \left(\frac{\beta}{2}\right)^{1/3} \theta J_1(\beta\theta) + \cdots \right] \right\} \\
&= \frac{1}{2} ika^2 \left\{ 2 \frac{J_1(\beta\theta)}{\beta\theta} + e^{i\pi/3}\beta^{-2/3}[1.9923 J_0(\beta\theta) \right. \\
&\quad \left. + 0.6706\beta^{1/3}\theta J_1(\beta\theta) + \cdots] \right\} \qquad (\theta \ll \beta^{-1/3}),
\end{aligned}
\qquad (9.33)
$$

where we have employed (8.28). This is also a limiting form of (8.43) for $r \gg \beta a$.

The first term of (9.33), which gives rise to the well-known forward diffraction

peak, dominates throughout the region $\theta \ll \beta^{-1/3}$. The corrections are of the order $\beta^{1/3}\theta$.

If θ becomes $\gg \beta^{-1/3}$, we must recover (9.3). To show this, let us rewrite $F(0, t, v)$ as follows (cf. (8.14) and (8.21)):

$$e^{-i\pi/3}F(0, t, v) = \int_0^\infty \frac{Ai(x)}{Ai(xe^{-2i\pi/3})} J_0(v - te^{-i\pi/3}x) \, dx$$

$$+ \int_0^\infty \frac{Ai(x)}{Ai(xe^{2i\pi/3})} J_0(v + tx) \, dx. \tag{9.34}$$

Let us make the decomposition: $J_0 = [H_0^{(1)} + H_0^{(2)}]/2$ and substitute $x = e^{-2i\pi/3}x'$ in the first integral in $H_0^{(1)}$, employing also the relation (D.3).

The result is

$$2e^{-i\pi/3}F(0, t, v) = \int_0^\infty \frac{Ai(x)}{Ai(xe^{-2i\pi/3})} H_0^{(2)}(v - te^{-i\pi/3}x) \, dx$$

$$+ \int_0^\infty \frac{Ai(x)}{Ai(xe^{2i\pi/3})} H_0^{(2)}(v + tx) \, dx + \int_\Gamma \frac{Ai(x)}{Ai(xe^{2i\pi/3})} H_0^{(1)}(v + tx) \, dx \tag{9.35}$$

$$+ \frac{e^{-i\pi/3}}{t} \int_v^{\infty e^{2i\pi/3}} H_0^{(1)}(x) \, dx,$$

where Γ is the path of integration shown in Fig. 10. This path can be closed at infinity, reducing the integral to a residue series

$$\int_\Gamma \approx -e^{-i\pi/4} \left(\frac{2}{\pi v}\right)^{1/2} e^{iv} \sum_n \frac{\exp(ie^{i\pi/3}tx_n)}{[Ai'(-x_n)]^2}, \tag{9.36}$$

where $-x_n$ are the zeros of the Airy function and we have replaced $H_0^{(1)}$ by its asymptotic expansion.

Since $v \gg t \gg 1$, the Hankel functions may be replaced by their asymptotic expansions also in the other terms of (9.35). By partial integration, we find

$$\int_v^{\infty e^{2i\pi/3}} H_0^{(1)}(x) \, dx = e^{i\pi/4} \left(\frac{2}{\pi v}\right)^{1/2} e^{iv}[1 + O(v^{-1})]. \tag{9.37}$$

The asymptotic expansion of the second term of (9.35) can also be obtained by partial integration. The first term has a saddle point at

$$\bar{x} = e^{i\pi/3}t^2/4, \tag{9.38}$$

as can be verified by replacing the Airy functions by their asymptotic expansion

(D.4). In addition to the saddle point, we must take into account the contribution from the lower limit of integration. The result is

$$\int_0^\infty \frac{Ai(x)}{Ai(xe^{-2i\pi/3})} \, H_0^{(2)}(v - te^{-i\pi/3}x) \, dx$$

$$+ \int_0^\infty \frac{Ai(x)}{Ai(xe^{2i\pi/3})} \, H_0^{(2)}(v + tx) \, dx \approx \left(\frac{2t}{v}\right)^{1/2} e^{i\pi/6} \exp\left(-iv + \frac{it^3}{12}\right) \quad (9.39)$$

$$+ \left(\frac{2}{\pi v}\right)^{1/2} \frac{e^{-i\pi/3}}{t} \exp\left[-i\left(v + \frac{\pi}{4}\right)\right] + \cdots ,$$

where the first term represents the contribution from the saddle point and the second one those from the lower limits of integration.

It follows from (9.35) to (9.39) that

$$F(0, t, v) \approx i\left(\frac{t}{2v}\right)^{1/2} \exp\left(-iv + \frac{it^3}{12}\right) - \frac{1}{t}\left(\frac{2}{\pi v}\right)^{1/2} \cos\left(v - \frac{3\pi}{4}\right)$$

$$- \frac{e^{i\pi/12}}{(2\pi v)^{1/2}} \sum_n \frac{\exp\,(iv + ie^{i\pi/3}tx_n)}{[Ai'(-x_n)]^2} + \cdots \quad (v \gg t \gg 1). \quad (9.40)$$

Substituting this result in (9.28) to (9.30), and replacing $J_1(\beta\theta)$ by its asymptotic expansion, it is found that the main term of this expansion is cancelled by the second term of (9.40), leaving us with

$$f_0(k, \theta) \approx -\frac{a}{2}\left(\frac{\theta}{\sin \theta}\right)^{1/2} \exp\left\{-2i\beta\left[\frac{\theta}{2} - \frac{1}{3!}\left(\frac{\theta}{2}\right)^3\right]\right\}$$

$$+ e^{-5i\pi/12} \frac{a}{2}\left(\frac{2}{\beta}\right)^{1/6} \frac{1}{(\pi \sin \theta)^{1/2}} \sum_n \frac{\exp\,(i\lambda_n\theta)}{[Ai'(-x_n)]^2} \quad (\theta \gg \beta^{-1/3}). \quad (9.41)$$

The second term is identical to the residue series involving δ_0' in (9.5). The exponent of the first term is the expansion of $-2i\beta \sin (\theta/2)$ up to the term of order $\beta\theta^3$. Thus, in the domain where $\beta\theta^3 \gg 1$ but the next term in this expansion can be neglected (and at the same time $\theta/\sin \theta \approx 1$), the first term of (9.40) coincides with the main term of the reflection amplitude (9.4).

Therefore, (9.10) goes over smoothly into (9.3) when θ becomes $\gg \beta^{-1/3}$ but, just as was found in Section VIII, the Fock functions cannot be employed for too large values of θ. Their angular domain of validity is just sufficient to make a smooth transition.

The transition from the forward diffraction peak to the region of geometrical reflection takes place in the domain $\theta \sim \beta^{-1/3}$. In this domain, we must employ

the expression (cf. (9.10), (9.11), (9.28) to (9.30) and (9.34)):

$$
\begin{aligned}
f(k, \theta) = \frac{1}{2} ika^2 \left(\frac{\theta}{\sin \theta}\right)^{1/2} &\left\{ 2 \frac{J_1(\beta\theta)}{\beta\theta} + \left(\frac{2}{\beta}\right)^{2/3} \left[\int_0^\infty \frac{Ai(x)}{Ai(xe^{-2i\pi/3})} \right.\right. \\
&\cdot J_0\left(\beta\theta - e^{-i\pi/3}\left(\frac{\beta}{2}\right)^{1/3}\theta x\right) dx + \int_0^\infty \frac{Ai(x)}{Ai(xe^{2i\pi/3})} \\
&\left.\cdot J_0\left(\beta\theta + \left(\frac{\beta}{2}\right)^{1/3}\theta x\right) dx \right] + \cdots \right\} + e^{-i\pi/6}a\left(\frac{\beta}{2}\right)^{1/3} \qquad (9.42)\\
&\cdot \left(\frac{\theta}{\sin \theta}\right)^{1/2} \sum_{m=1}^\infty (-1)^m \sum_n \frac{\exp(2im\pi\lambda_n)}{[Ai'(-x_n)]^2} J_0(\lambda_n\theta)\\
&\hspace{6cm} (0 \leqq \theta \lesssim \beta^{-1/3}),
\end{aligned}
$$

where, for $\theta \sim \beta^{-1/3}$, the Fock-type functions should be computed by numerical methods. Some related functions have already been tabulated (22, 29), but there seem to exist no tables for those appearing in (9.42).

C. THE NEIGHBORHOOD OF THE BACKWARD DIRECTION

There remains to consider only the neighborhood of the backward direction, i.e., according to (9.9), the domain

$$\theta = \pi - \epsilon, \qquad \epsilon \lesssim \beta^{-1/2}. \qquad (9.43)$$

The expression for $f(k, \theta)$ in this domain may be obtained similarly to (9.8), by substituting (9.7) in (6.30) and (6.35):

$$f(k, \theta) = f_r(k, \theta) + f_{res}(k, \theta), \qquad (9.44)$$

where

$$f_r(k, \theta) = \frac{i}{k} \int_0^{\bar\sigma\infty} \frac{H_\lambda^{(2)}(\beta)}{H_\lambda^{(1)}(\beta)} P_{\lambda-1/2}(-\cos \theta) \tan(\pi\lambda)e^{-i\pi\lambda}\lambda \, d\lambda, \qquad (9.45)$$

$$f_{res}(k, \theta) = -i \frac{\pi}{k} \sum_n \frac{\lambda_n r_n(\beta)}{\cos \pi\lambda_n} P_{\lambda_n-1/2}(-\cos \theta). \qquad (9.46)$$

The path of integration in (9.45) is the upper half of the path Γ' shown in Fig. 12. Actually, (9.45) can also be obtained from (9.8), by taking the integral along the symmetric path Γ' and then applying the same transformation that led from (6.30) to (6.31).

Substituting (2.18), (3.16), and (9.43) in (9.46), and employing the uniform asymptotic expansion (C.11), we get

$$f_{\text{res}}(k, \pi - \epsilon) \approx -e^{i\pi/3}a \left(\frac{\beta}{2}\right)^{1/3} \left(\frac{\epsilon}{\sin \epsilon}\right)^{1/2}$$
$$\cdot \sum_{m=0}^{\infty} (-1)^m \sum_n \frac{\exp\left[i(2m + 1)\pi\lambda_n\right]}{[Ai'(-x_n)]^2} J_0(\lambda_n \epsilon),$$
(9.47)

which is also a limiting case of (6.38). In particular, if $\epsilon \gg \beta^{-1}$, we may replace $J_0(\lambda_n\epsilon)$ by its asymptotic expansion and (9.47) goes over into (9.5), as may easily be verified.

In (9.45), we may employ the expansion (6.14), which remains valid even for $|\lambda| \ll \beta$. According to (9.2), the main contribution to the integral arises from the neighborhood of the lower limit, i.e. from the domain

$$|\lambda| \lesssim \beta^{-1/2}.$$
(9.48)

Thus, we can expand the exponent and the other terms of (6.14) in powers of λ/β, with the following result

$$e^{-i\pi\lambda}H_\lambda^{(2)}(\beta)/H_\lambda^{(1)}(\beta) = ie^{-2i\beta} \exp\left(-i\lambda^2/\beta\right)\left(1 + \frac{i}{4\beta} - \frac{i\lambda^4}{12\beta^3} + \cdots\right),$$
(9.49)

where we have kept all correction terms up to the order β^{-1}, according to (9.48).

On the other hand, $P_{\lambda-1/2}(-\cos\theta) = P_{\lambda-1/2}(\cos\epsilon)$ and, according to (9.43) and (9.48), the relevant portion of the domain of integration corresponds to $|\lambda\epsilon| \lesssim 1$, so that we may employ the expansion (C.9).

Making the change of variable appropriate to the steepest descent path (cf. Fig. 12)

$$\lambda = e^{3i\pi/4}\beta^{1/2}x = \alpha x,$$
(9.50)

we finally get from (9.45)

$$f_r(k, \pi - \epsilon) = iae^{-2i\beta}\left[\left(1 + \frac{i}{4\beta}\right)\int_0^{\infty} \exp\left(-x^2\right)J_0(\omega x) \tan\left(\pi\alpha x\right)x \, dx\right.$$
$$+ \frac{i}{12\beta}\int_0^{\infty} \exp\left(-x^2\right)J_0(\omega x) \tan\left(\pi\alpha x\right)x^5 \, dx + \frac{\omega}{6} \sin^2\frac{\epsilon}{2}$$
$$\times \int_0^{\infty} \exp(-x^2)J_3(\omega x) \tan\left(\pi\alpha x\right)x^2 \, dx - \sin^2\frac{\epsilon}{2}$$
$$\times \int_0^{\infty} \exp(-x^2)J_2(\omega x) \tan\left(\pi\alpha x\right)x \, dx + \frac{1}{2\omega} \sin^2\frac{\epsilon}{2}$$
$$\left.\times \int_0^{\infty} \exp\left(-x^2\right)J_1(\omega x) \tan\left(\pi\alpha x\right) \, dx + O(\beta^{-2})\right],$$
(9.51)

where

$$\omega = 2e^{3i\pi/4}\beta^{1/2} \sin (\epsilon/2) = 2\alpha \sin (\epsilon/2) \tag{9.52}$$

and the upper limit of integration has been extended to ∞, since large values of x give no significant contribution. Note that $|\omega| \lesssim 1$ according to (9.43).

The evaluation of the integrals appearing in (9.51) is taken up in Appendix F. The result is given by (F.13). Expanding $\omega^2 = -4i\beta \sin^2 \epsilon/2$ in powers of ϵ^2 and taking into account (9.43), we finally get

$$f_r(k, \pi - \epsilon) = -\frac{a}{2} \exp \left[-2i\beta \left(1 - \frac{\epsilon^2}{8} \right) \right] \left[1 + \frac{i}{2\beta} - \frac{i\beta\epsilon^4}{192} + O(\beta^{-2}) \right] \tag{9.53}$$
$$(0 \leqq \epsilon \lesssim \beta^{-1/2}).$$

As may readily be verified, this result coincides with the expansion of (9.4) in powers of ϵ^2, within the domain $\epsilon \lesssim \beta^{-1/2}$. Thus, (9.4) is uniformly valid up to $\theta = \pi$. This had often been assumed in previous work, on account of the regularity of (9.4) up to $\theta = \pi$. Obviously, however, such regularity constitutes no proof of the validity of (9.4), since the asymptotic expansion (C.7), employed in its derivation, is no longer applicable in this domain.

Since (9.47) also remains valid for $\epsilon \gg \beta^{-1}$, we conclude that

$$f(k, \theta) = -\frac{a}{2} \exp \left(-2i\beta \sin \frac{\theta}{2} \right) \left(1 + \frac{i}{2\beta \sin^3 \dfrac{\theta}{2}} + \cdots \right)$$
$$- e^{i\pi/3} a \left(\frac{\beta}{2} \right)^{1/3} \left(\frac{\pi - \theta}{\sin \theta} \right)^{1/2} \tag{9.54}$$
$$\times \sum_{m=0}^{\infty} (-1)^m \sum_n \frac{\exp [i(2m + 1)\pi\lambda_n]}{[A i'(-x_n)]^2} J_0[\lambda_n(\pi - \theta)]$$

uniformly throughout the whole domain

$$\beta^{-1/3} \ll \theta \leqq \pi. \tag{9.55}$$

Together with (9.42), this determines the behavior of $f(k, \theta)$ for $0 \leqq \theta \leqq \pi$.

D. DIRECT TRANSFORMATION OF THE SCATTERING AMPLITUDE

The expressions for $f(k, \theta)$ employed in the above discussion were obtained by letting $r \to \infty$ in the representations previously derived for $\psi(r, \theta)$. The advantage of this method is to make clear the connection between the behavior of the wave function in the near and in the far regions, as well as the physical interpretation of the various terms. However, one may ask whether it is possible to bypass the limiting procedure and to derive the same results directly from

the partial-wave expansion of $f(k, \theta)$,

$$f(k, \theta) = \sum_{l=0}^{\infty} \frac{(2l + 1)}{2ik} [S_l(k) - 1] P_l(\cos \theta), \qquad (9.56)$$

where S_l is given by (2.3).

It is well known (30) that Watson's transformation, in the form usually applied to Yukawa-type potentials, cannot be applied to (9.56) in the case of a cutoff potential (including, in particular, the case of a hard sphere). This is essentially due to the asymptotic behavior of the S-function as $|\lambda| \to \infty$, $|\arg \lambda| \to \pi/2$.

Modified versions of Watson's transformation have been employed for this purpose (31, 32). However, the proposed modifications still lead to singular integrals,[5] so that the difficulty is not overcome.

It will now be shown that it is indeed possible to derive all the representations for $f(k, \theta)$ employed above directly from (9.56).

Let us start by applying Poisson's sum formula (2.12):

$$f(k, \theta) = \frac{i}{k} \sum_{m=-\infty}^{\infty} (-1)^m \int_0^{\infty} [1 - S(\lambda, k)] P_{\lambda-1/2}(\cos \theta) e^{2im\pi\lambda} \lambda \, d\lambda, \quad (9.57)$$

where $S(\lambda, k)$ is given by (3.1). It follows from (2.15) that

$$S(-\lambda, k) = e^{2i\pi\lambda} S(\lambda, k), \qquad (9.58)$$

so that, making $\lambda \to -\lambda$ in the sum from $m = -1$ to $-\infty$, we get

$$f(k, \theta) = \frac{i}{k} \sum_{m=0}^{\infty} (-1)^m \left\{ \int_{-\infty}^0 [e^{2i\pi\lambda} - S(\lambda, k)] P_{\lambda-1/2}(\cos \theta) e^{2im\pi\lambda} \lambda \, d\lambda \right.$$
$$\left. + \int_0^{\infty} [1 - S(\lambda, k)] P_{\lambda-1/2}(\cos \theta) e^{2im\pi\lambda} \lambda \, d\lambda \right\}. \qquad (9.59)$$

Note that

$$e^{2i\pi\lambda} - S(\lambda, k) = 2e^{i\pi\lambda} J_{-\lambda}(\beta)/H_{\lambda}^{(1)}(\beta). \qquad (9.60)$$

According to Appendix A and (C.8), the integrand of the first integral in (9.59), for all $m \geqq 0$, goes to zero at least exponentially for $|\lambda| \to \infty$ in the second quadrant. Thus, we may shift the path of integration to the positive imaginary axis, from $i\infty$ to 0. Writing

$$e^{2i\pi\lambda} - S(\lambda, k) = e^{2i\pi\lambda} - 1 + 1 - S(\lambda, k)$$

[5] Cf. Eqs. (26)–(27) and the related discussion on p. 328 of (31) and Eqs. (5)–(8) and (48) of (32).

in the corresponding terms for $m \geq 1$, and employing the identity

$$\sum_{m=1}^{\infty} (-1)^m (e^{2i\pi\lambda} - 1) e^{2im\lambda\pi} = e^{2i\pi\lambda} \left(\frac{2}{1 + e^{2i\pi\lambda}} - 1 \right), \qquad (9.61)$$

we get

$$f(k, \theta) = f_0(k, \theta) + \tilde{f}_{\text{res}}(k, \theta), \qquad (9.62)$$

where

$$f_0(k, \theta) = \frac{i}{k} \int_0^{\infty} [1 - S(\lambda, k)] P_{\lambda-1/2}(\cos \theta) \lambda \, d\lambda$$

$$- \frac{i}{k} \int_{i\infty}^0 S(\lambda, k) P_{\lambda-1/2}(\cos \theta) \lambda \, d\lambda + \Delta_1 , \qquad (9.63)$$

$$\Delta_1 = \frac{2i}{k} \int_{i\infty}^0 \frac{e^{2i\pi\lambda}}{1 + e^{2i\pi\lambda}} P_{\lambda-1/2}(\cos \theta) \lambda \, d\lambda, \qquad (9.64)$$

$$\tilde{f}_{\text{res}}(k, \theta) = \frac{i}{k} \sum_{m=1}^{\infty} (-1)^m \int_C [1 - S(\lambda, k)] P_{\lambda-1/2}(\cos \theta) e^{2im\pi\lambda} \lambda \, d\lambda, \qquad (9.65)$$

and C is the path shown in Fig. 13, going from $i\infty$ to 0 and from 0 to ∞.

It follows from Appendix A that this path may be closed at infinity in the first quadrant, so that

$$\tilde{f}_{\text{res}}(k, \theta) = \frac{2\pi}{k} \sum_{m=1}^{\infty} (-1)^m \sum_{n=1}^{\infty} \lambda_n r_n \exp (2im\pi\lambda_n) P_{\lambda_n-1/2}(\cos \theta), \quad (9.66)$$

where λ_n are the poles of $S(\lambda, k)$ and r_n are the corresponding residues, given by (3.14). This corresponds exactly to (9.11).

On the other hand, we may rewrite (9.63) as

$$f_0(k, \theta) = f_{01} + f_{02} + f_{03} , \qquad (9.67)$$

where

$$f_{01} + f_{02} = \frac{i}{k} \left(\int_{i\infty}^0 + \int_0^{\beta} \right) \frac{H_\lambda^{(2)}(\beta)}{H_\lambda^{(1)}(\beta)} P_{\lambda-1/2}(\cos \theta) \lambda \, d\lambda$$

$$+ \frac{2i}{k} \int_{\beta}^{\infty} \frac{J_\lambda(\beta)}{H_\lambda^{(1)}(\beta)} P_{\lambda-1/2}(\cos \theta) \lambda \, d\lambda \qquad (9.68)$$

and

$$f_{03} = \frac{i}{k} \int_0^{\beta} P_{\lambda-1/2}(\cos \theta) \lambda \, d\lambda + \Delta_1 . \qquad (9.69)$$

The first integral in (9.68) may also be taken along the path C' from $\sigma_1 \infty$ to
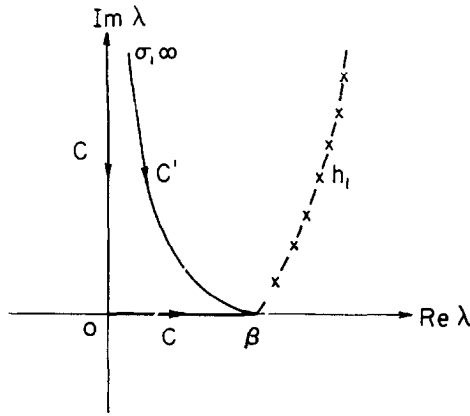
Fig. 13. Paths of integration in the λ plane. $\times$ $\times$ $\times$—Poles of $S(\lambda, \beta)$.

β shown in Fig. 13. Since the main contribution to both integrals arises from the neighborhood of $\lambda = \beta$, where we may employ the approximations (7.33) and (7.34), we see that (9.68) corresponds to (9.13). Similarly, (9.69) corresponds to (9.19). Just as in (9.26), it can be shown that

$$| \Delta_1 | \leqq \frac{8}{9\pi^2 k (\cos \theta)^{1/2}} , \tag{9.70}$$

so that the contribution from Δ_1, which is independent of a, would be included in the correction term of order β^{-2} in (9.27).

Thus, (9.62) leads to the same results as (9.10) and is the appropriate splitting of $f(k, \theta)$ in the domain $\theta \lesssim \beta^{-1/3}$.

Now let us consider the domain $\theta \gg \beta^{-1/3}$. In this case, the integrals containing $Q_{\lambda-1/2}^{(2)}(\cos \theta)$ in (9.63) can also be reduced to residue series. For this purpose, let us add and subtract the (convergent) integral

$$\int_{i\infty}^{0} Q_{\lambda-1/2}^{(2)} (\cos \theta) \lambda \, d\lambda$$

and rewrite (9.62) to (9.65) as follows:

$$f(k, \theta) = f_r(k, \theta) + f_{\text{res}}(k, \theta), \tag{9.71}$$

where

$$f_{\text{res}}(k, \theta) = \tilde{f}_{\text{res}}(k, \theta) + (2\pi/k) \sum_{n=1}^{\infty} \lambda_n r_n Q_{\lambda_n-1/2}^{(2)}(\cos \theta), \tag{9.72}$$

$\tilde{f}_{\text{res}}$ being given by (9.66), and

$$f_r(k, \theta) = -\frac{i}{k} \int_{i\infty}^{0} [S(\lambda, k)Q_{\lambda-1/2}^{(1)}(\cos \theta) + Q_{\lambda-1/2}^{(2)}(\cos \theta)]\lambda \, d\lambda$$

$$+ \frac{i}{k} \int_{0}^{\infty} [1 - S(\lambda, k)]Q_{\lambda-1/2}^{(1)}(\cos \theta)\lambda \, d\lambda + \Delta_1 . \tag{9.73}$$

From the discussion given in connection with (9.8) and (9.59) and from (C.7) it follows that the path of integration in the first integral of (9.73) may be deformed away from the imaginary axis into the second quadrant, so as to coincide with the upper half of the path Γ' in Fig. 12. Similarly, according to Appendix A and (C.7), the path of integration in the second integral may be deformed within the region A of Fig. 12, so as to coincide with the lower half of Γ'. This leads to

$$f_r(k, \theta) = -\frac{i}{k} \int_{\bar{\sigma}\infty}^{-\bar{\sigma}\infty} S(\lambda, k)Q_{\lambda-1/2}^{(1)}(\cos \theta)\lambda \, d\lambda$$

$$- \frac{i}{k} \int_{\bar{\sigma}\infty}^{0} \left[Q_{\lambda-1/2}^{(2)}(\cos \theta) + Q_{-\lambda-1/2}^{(1)}(\cos \theta) - 2 \frac{e^{2i\pi\lambda}}{1+e^{2i\pi\lambda}} P_{\lambda-1/2}(\cos \theta) \right] \lambda \, d\lambda, \tag{9.74}$$

where the integrals are taken along the path Γ'. We have also made $\lambda \to -\lambda$ in the integral of $Q_{\lambda-1/2}^{(1)}$ and employed (9.64) (with the path of integration shifted to Γ').

It follows from (C.5) and (C.6) that the expression within square brackets in (9.74) is identically zero, so that we are left with

$$f_r(k, \theta) = -\frac{i}{k} \int_{\bar{\sigma}\infty}^{-\bar{\sigma}\infty} S(\lambda, k)Q_{\lambda-1/2}^{(1)}(\cos \theta)\lambda \, d\lambda, \tag{9.75}$$

in exact agreement with (9.8). Since (9.72) also corresponds to (9.5), we see that the splitting (9.71) is equivalent to (9.3).

Furthermore, just as in (9.45), we may rewrite (9.75) as

$$f_r(k, \theta) = -\frac{i}{k} \int_{0}^{\bar{\sigma}\infty} S(\lambda, k)P_{\lambda-1/2}(-\cos \theta) \tan (\pi\lambda)e^{-i\pi\lambda}\lambda \, d\lambda \tag{9.76}$$

and, with the help of the identity (6.33), we may rewrite (9.72) as

$$f_{\text{res}}(k, \theta)$$

$$= -(2\pi i/k) \sum_{m=0}^{\infty} (-1)^m \sum_{n=1}^{\infty} \lambda_n r_n \exp [i(2m + 1)\pi\lambda_n]P_{\lambda_n-1/2}(-\cos \theta), \tag{9.77}$$

which, according to (2.18), is equivalent to (9.46).

The results (9.76) and (9.77) remain valid up to $\theta = \pi$ and correspond to those employed in (9.44). In this form, the splitting (9.71) may be employed for $\beta^{-1/3} \ll \theta \leqq \pi$.

In conclusion, according to (9.62), (9.64), (9.66), (9.67) to (9.69), (9.71), (9.76), and (9.77), the modified Watson transformation may be expressed as follows:

$$f(k, \theta) = -\frac{i}{k} \int_{C'} S(\lambda, k) P_{\lambda-1/2}(\cos \theta) \lambda \, d\lambda + \frac{i}{k} \int_{\beta}^{\infty} [1 - S(\lambda, k)]$$

$$\times P_{\lambda-1/2}(\cos \theta) \lambda \, d\lambda + \frac{i}{k} \int_{0}^{\beta} P_{\lambda-1/2}(\cos \theta) \lambda \, d\lambda + \frac{2i}{k} \int_{i\infty}^{0} \frac{e^{2i\pi\lambda}}{1 + e^{2i\pi\lambda}} \quad (9.78)$$

$$\times P_{\lambda-1/2}(\cos \theta) \lambda \, d\lambda + \frac{2\pi}{k} \sum_{m=1}^{\infty} (-1)^m \sum_{n=1}^{\infty} \lambda_n r_n \exp (2im\pi\lambda_n) P_{\lambda_n-1/2}(\cos \theta),$$

where the path C' is shown in Fig. 13, and

$$f(k, \theta) = \frac{i}{k} \int_{\hat{\sigma}\infty}^{0} S(\lambda, k) P_{\lambda-1/2}(-\cos \theta) \tan (\pi\lambda) e^{-i\pi\lambda} \lambda \, d\lambda$$

$$- \frac{2\pi i}{k} \sum_{m=0}^{\infty} (-1)^m \sum_{n=1}^{\infty} \lambda_n r_n \exp [i(2m + 1)\pi\lambda_n] P_{\lambda_n-1/2}(-\cos \theta),$$

$$(9.79)$$

where the integral may also be expressed in the equivalent form (9.75).

Both of these representations are exact and their terms have a direct physical interpretation, as discussed above. They may be employed to obtain higher-order corrections to the results derived in the present section: (9.78) should be employed for $0 \leq \theta \lesssim \beta^{-1/3}$ and (9.79) for $\beta^{-1/3} \ll \theta \leq \pi$.

X. CONCLUSION

The main results obtained in the present work may be summarized as follows:

(i) The high-frequency behavior of the wave function in scattering by a totally reflecting sphere may be completely determined, both in the near and in the far regions of space, by means of a modified Watson transformation, based upon Poisson's sum formula. Each term in the transformed series has a direct physical interpretation. This procedure has the advantage that it does not require a reevaluation of the whole residue series in going over from the shadow to the lit region, but only of that part of the lowest-order term that would not correspond to a rapidly converging series, thus showing clearly the connection between shadow and lit region.

(ii) It is necessary to apply different representations in the forward and backward half-spaces. It is already clear from the singularity of $P_{\lambda-1/2}(x)$ at $x = -1$ that one cannot have a single representation for all values of θ: one needs a representation in terms of $P_{\lambda-1/2}(\cos \theta)$ near $\theta = 0$ and one in terms of $P_{\lambda-1/2}(-\cos \theta)$ near $\theta = \pi$. The present treatment is based upon the integral representations (2.34) and (2.35) of the primary wave. In the forward half-
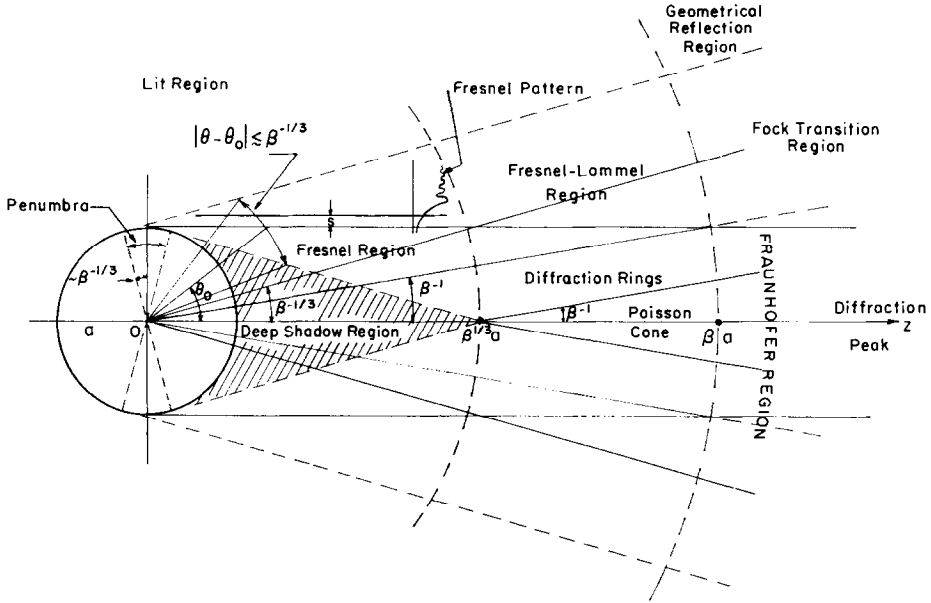
Fig. 14. Division into regions (the angles are greatly exaggerated). The separation between regions is indicated by the broken lines.

space, we employ (2.16) and (2.17); in the backward half-space, we must employ (6.29), (6.30) and (6.34).

(iii) A rigorous proof of Watson's transformation is based upon a study of the behavior of the integrand for $|\lambda| \to \infty$, $\arg \lambda \to \pi/2$, as well as of the asymptotic behavior of the poles and their residues. It follows from this discussion that the residue series (4.15) converges in the whole forward half-space $0 \leqq \theta < \pi/2$, but it is only useful in this form in the domain where it is rapidly convergent, i.e. within the shadow region. This happens in the domain $r \ll \beta^{1/3}a$, $\theta_0 - \theta \gg \beta^{-1/3}$, where $\theta_0 = \sin^{-1}(a/r)$ is the shadow boundary angle. This domain, which may be called the deep shadow region, is represented by the shaded area in Fig. 14.

(iv) The wave function in the deep shadow region is given by (5.7), which represents a superposition of "diffracted rays" arising from the surface waves associated with the poles of the S-function in the complex angular momentum plane. These poles do not show the typical Regge behavior associated with Yukawa-type potentials. The physical interpretation of these terms is in agreement with Keller's geometrical theory of diffraction: they give rise to an exponentially damped wave function in the angular variable. However, this interpretation can be applied, at a given frequency, only to the lowest-order

poles, and loses its validity when the damping within one wavelength becomes appreciable. The higher-order poles, however, give a negligible contribution. The exponential damping in the deep shadow should be contrasted with the much weaker damping found in the case of a circular disc: the shadow of the sphere is much darker than that of the disc (27, p. 463). Physically, the reason for this result is that the intensity thrown into the shadow by diffraction at the edge of the disc is much greater than that due to diffraction around a curved surface. Classical diffraction theory, which predicts the same behavior for the sphere and the disc, fails in this domain.

(v) In the lit region, sufficiently far from the shadow boundary $(\theta - \theta_0 \gg \beta^{-1/3})$, the WKB expansion for the wave function has been confirmed up to the second order. The expression (6.23) for the reflected wave is valid both in the forward and in the backward half-space, although the derivation is different in the two cases. In this region, we also find the continuation of the surface waves, but they are masked by the much greater contribution from the incident and reflected waves, except in the immediate vicinity of the shadow boundary.

(vi) On the surface of the sphere, Kirchhoff's approximation (7.1)–(7.2) for the normal derivative of the wave function is accurate, except within the penumbra region, $|\theta - (\pi/2)| \lesssim \beta^{-1/3}$ (Fig. 14). The behavior in this region is described by Fock's function (7.11)–(7.13), which interpolates smoothly between the values on the lit and on the shadow regions. However, it cannot be employed too far beyond the penumbra. The penumbra or, equivalently, the corresponding angular momentum domain $|\lambda - \beta| \lesssim \beta^{-1/3}$, is responsible, in the sense of Huygens' Principle, for the main corrections to classical diffraction theory.

(vii) The neighborhood of the shadow boundary, $|\theta - \theta_0| \ll \beta^{-1/3}$, at distances $\beta^{-1/3}a \ll z \ll \beta^{1/3}a$, is denoted as the Fresnel region in Fig. 14. In this region, the main term of the angular diffraction pattern corresponds to the classical Fresnel pattern of a straight edge, with small corrections, representing the effect of the curvature of the sphere (cf. (7.44)). One of these corrections is the shift of the shadow boundary, denoted by s in Fig. 14. It is given by (7.50), in agreement with a conjecture made by Rubinow and Keller (21).

The solution in this region is still not in agreement with the result given by classical diffraction theory, which would be analogous to the Fresnel pattern of a slit, rather than an edge. In fact, it would contain, in addition to (7.28), a contribution from the diametrically opposite edge, corresponding to $\Psi_0^{(2)}$, which is actually replaced by a rapidly convergent residue series (cf. (7.21)).

(viii) In the Fresnel-Lommel region, $\theta \lesssim \theta_0$, $\beta^{1/3}a \ll r \ll \beta a$ (Fig. 14), the main term of the wave function corresponds to Lommel's classical solution (8.17) for the diffraction of a plane wave by a circular disc. The main correction term is given by the Fock-type function (8.14), which also gives rise to a smooth

transition to the deep shadow and to the lit region. Along the axis, starting at a distance $z \sim \beta^{1/3}a$, we find the well-known Poisson spot, which actually corresponds to a cone (Fig. 14) of angular opening $\sim\beta^{-1}$, surrounded by diffraction rings (cf. (8.43)).

(ix) In the Fraunhofer region, $r \gg \beta a$, the wave function is given by (9.1). For $\beta^{-1/3} \ll \theta \leqq \pi$, the scattering amplitude is given by (9.54), the main term of which corresponds to geometrical reflection. For $\theta \ll \beta^{-1/3}$, the amplitude is dominated by the forward diffraction peak (cf. (9.33)), which corresponds to the classical result for a circular disc. In the transition domain $\theta \sim \beta^{-1/3}$, we have to employ (9.42), which again may be continued smoothly up to the region of geometrical reflection. Higher-order corrections may be obtained from the exact representations (9.78) and (9.79), which result from applying the modified Watson transformation directly to the scattering amplitude.

(x) Fock-type functions such as (7.13), (7.39), (8.14), (8.20), and (9.34) play an important role in linking the domains of geometrical optics and classical diffraction theory. In view of this role, which probably is not restricted to the present example, but is of more general validity, it would be desirable to construct tables and graphs of these functions. Only in a few cases is this material presently available.

Possible applications and extensions of the present treatment include the problem of a transparent sphere (square well potential in quantum mechanics), which will be discussed in a subsequent paper.

APPENDIX A. ASYMPTOTIC BEHAVIOR OF THE CYLINDRICAL FUNCTIONS

The asymptotic behavior of the cylindrical functions $Z_\lambda(x)$, $x > 0$, in the complex λ plane may be derived from the formulae given by Watson (25, p. 262). The results are graphically presented in Fig. 15.[6] The notation is as follows:

$$A(\lambda, x) = (2/\pi)^{1/2}(\lambda^2 - x^2)^{-1/4}, \tag{A.1}$$

$$\alpha(\lambda, x) = (\lambda^2 - x^2)^{1/2} - \lambda \ln\left[\frac{\lambda}{x} + \frac{(\lambda^2 - x^2)^{1/2}}{x}\right], \tag{A.2}$$

where the branch of $(\lambda^2 - x^2)^{1/2}$ to be taken is specified by the condition

$$(\lambda^2 - x^2)^{1/2} \to \lambda = |\lambda| \exp(i\varphi) \qquad (-\pi < \varphi \leqq \pi) \quad \text{for } |\lambda| \to \infty. \tag{A.3}$$

Thus,

$$A \to \left(\frac{2}{\pi\lambda}\right)^{1/2}, \qquad e^\alpha \to \left(\frac{ex}{2\lambda}\right)^\lambda \quad \text{for } |\lambda| \to \infty. \tag{A.4}$$

The asymptotic behavior of $H_\lambda^{(1)}(x)$, $H_\lambda^{(2)}(x)$ changes (Stokes' phenomenon)

[6] Similar figures appear in (33). However, they contain several mistakes.

λ-plane

$\eta \to 3\pi/2$ $\eta \to \pi/2$

$\underline{C}$
(Re $\alpha > 0$)

$H_\lambda^{(1)} = Ae^\alpha$

$H_\lambda^{(2)} = -Ae^{\alpha + 2i\pi\lambda}$

$J_\lambda = \frac{A}{2}e^\alpha$

$J_{-\lambda} = \frac{iA}{2}e^{-(\alpha+i\pi\lambda)}$

$J_{-\lambda} \to 0$

$\underline{BC}$

$H_\lambda^{(2)} \to 0$

h'_{-2}

Re$(\alpha+i\pi\lambda)=0$

$\underline{B}$
(Re $\alpha > 0$)

$H_\lambda^{(1)} = Ae^\alpha$

$H_\lambda^{(2)} = iAe^{-\alpha}$

$J_\lambda = \frac{A}{2}e^\alpha$

$J_{-\lambda} = \frac{iA}{2}e^{-(\alpha+i\pi\lambda)}$

$H_\lambda^{(2)} \to 0$

$\eta \to -\pi/2$

$\underline{AB}$

h_1

Re $\alpha = 0$

$\underline{A}$
(Re $\alpha < 0$)

$H_\lambda^{(1)} = -iAe^{-\alpha}$

$H_\lambda^{(2)} = iAe^{-\alpha}$

$J_\lambda = \frac{A}{2}e^\alpha$

$J_\lambda \to 0$

$\underline{I}$ $\underline{CD}$ $\underline{O}$ $\underline{BE}$ $-x$ x $\pi/3$

Re $\alpha = 0$

$\underline{D}$
(Re $\alpha > 0$)

$H_\lambda^{(1)} = -Ae^{\alpha - 2i\pi\lambda}$

$H_\lambda^{(2)} = Ae^\alpha$

$J_\lambda = \frac{A}{2}e^\alpha$

$J_{-\lambda} = \frac{-iA}{2}e^{-(\alpha-i\pi\lambda)}$

$J_{-\lambda} \to 0$

$\underline{DE}$ Re$(\alpha-i\pi\lambda)=0$

h_{-1}

$H_\lambda^{(1)} \to 0$

$\eta \to -3\pi/2$ $\eta \to -\pi/2$

$\underline{E}$
(Re $\alpha > 0$)

$H_\lambda^{(1)} = -iAe^{-\alpha}$

$H_\lambda^{(2)} = Ae^\alpha$

$J_\lambda = \frac{A}{2}e^\alpha$

$J_{-\lambda} = -\frac{iA}{2}e^{-(\alpha-i\pi\lambda)}$

$H_\lambda^{(1)} \to 0$
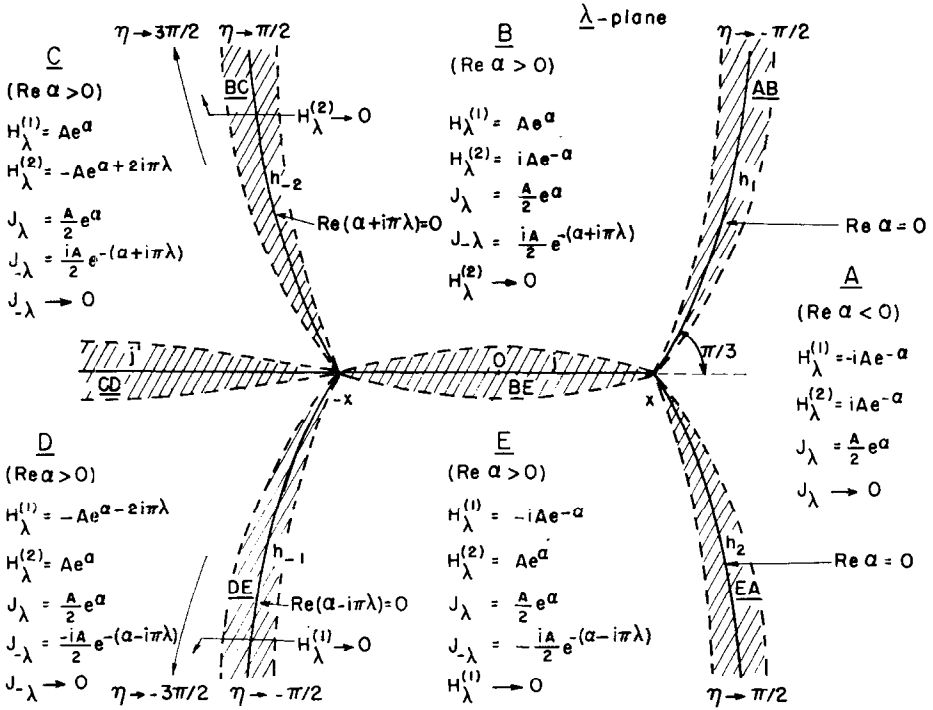
$\underline{EA}$

h_2

Re $\alpha = 0$

$\eta \to \pi/2$

Fig. 15. Asymptotic behavior of the cylindrical functions $Z_\lambda(x)$ in the index plane ($x > 0$). The zeros of $H_\lambda^{(1)}(x)$ are asymptotically located on curves h_1 and h_{-1}; those of $H_\lambda^{(2)}(x)$, on h_2 and h_{-2}; those of $J_\lambda(x)$, on j and j'.

across certain branch lines, shown as thick lines in Fig. 15. For $H_\lambda^{(1)}(x)$, we have the curves h_1 (Re $\alpha = 0$, Im $\lambda > 0$) and h_{-1} (Re $(\alpha - i\pi\lambda) = 0$, Im $\lambda < 0$). These curves are symmetrical with respect to the origin and the zeros of $H_\lambda^{(1)}(x)$ are asymptotically located on them. The curve h_1 cuts the real axis at $\lambda = x$ at an angle of $\pi/3$. The tangent to this curve tends to the vertical direction for $|\lambda| \to \infty$. Asymptotically, the curve approaches $\lambda = \sigma|\lambda|$, $\eta \to -\pi/2$, where σ and η are defined by (2.26) and (2.27) with ρ replaced by x:

$$\sigma = \exp\left[i\left(\frac{\pi}{2} + \epsilon\right)\right], \qquad \eta = \epsilon \ln |2\lambda/ex|. \qquad (A.5)$$

For $H_\lambda^{(2)}(x)$, we have the branch lines h_2 (Re $\alpha = 0$, Im $\lambda < 0$) and h_{-2} (Re $(\alpha + i\pi\lambda) = 0$, Im $\lambda > 0$), which are complex conjugate to h_1 and h_{-1}, respectively, and where the zeros of $H_\lambda^{(2)}(x)$ are asymptotically located. In addition, we have the portions of the real axis denoted in Fig. 15 by j' (from $-\infty$ to $-x$) and j (from $-x$ to x), where the zeros of $J_\lambda(x)$ are located.

These curves divide the λ plane into 5 regions, A to E in Fig. 15, and the asymp-

totic behavior of $H_\lambda^{(1)}(x)$, $H_\lambda^{(2)}(x)$, $J_\lambda(x)$, and $J_{-\lambda}(x)$ in these regions is shown in this figure. Note that

$$J_\lambda(x) \to (2\pi\lambda)^{-1/2}(ex/2\lambda)^\lambda \qquad (|\lambda| \to \infty) \quad (A.6)$$

in all regions.

For each function, there is a domain where it tends to zero for $|\lambda| \to \infty$, whereas it tends to infinity outside of this domain. For $J_\lambda(x)$, this domain is region A. For $H_\lambda^{(1)}(x)$, it is the domain between h_2 and the curve $\lambda = -\sigma|\lambda|$, $\eta \to -3\pi/2$ in the lower half-plane. For $H_\lambda^{(2)}(x)$, it is the domain between h_1 and the curve $\lambda = \sigma|\lambda|$, $\eta \to 3\pi/2$ in the upper half-plane.[7] Finally, $J_{-\lambda}(x) \to 0$ in regions C and D.

These results have to be modified in the neighborhood of each of the branch lines, where the two representations for the same function on different sides become of comparable order of magnitude. We then must take for the function the sum of the two representations. This is indicated by the shaded regions in Fig. 15.

Thus, we have

$$H_\lambda^{(1)}(x) \approx 2A e^{i\pi/4} \sinh\left(\alpha - i\frac{\pi}{4}\right) \qquad \text{in } AB, \tag{A.7}$$

$$H_\lambda^{(1)}(x) \approx -2A \exp\left(-i\pi\lambda - i\frac{\pi}{4}\right) \sinh\left(\alpha - i\pi\lambda + i\frac{\pi}{4}\right) \qquad \text{in } DE, \quad (A.8)$$

$$H_\lambda^{(2)}(x) \approx -2A \exp\left(i\pi\lambda + i\frac{\pi}{4}\right) \sinh\left(\alpha - i\pi\lambda - i\frac{\pi}{4}\right) \qquad \text{in } BC, \qquad (A.9)$$

$$H_\lambda^{(2)}(x) \approx 2A e^{-i\pi/4} \sinh\left(\alpha + i\frac{\pi}{4}\right) \qquad \text{in } EA. \tag{A.10}$$

What is the width of the shaded regions? In AB, for instance, we have

$$H_\lambda^{(1)}(x) \approx A(e^\alpha - ie^{-\alpha}),$$

while outside of AB one of the two terms dominates, so that $\exp(2|\operatorname{Re}\alpha|) \gg 1$. Thus, the boundary curves of AB, shown by broken lines in Fig. 15, can be defined by

$$\operatorname{Re}\alpha = \pm C, \tag{A.11}$$

where C is a constant such that

$$e^{2C} \gg 1, \tag{A.12}$$

i.e., e^{-2C} may be neglected within the required degree of approximation.

[7] Franz (5, p. 36) incorrectly states that E and B are the domains where $H_\lambda^{(1)}(x) \to 0$, $H_\lambda^{(2)}(x) \to 0$, respectively.

Asymptotically, with $\lambda = \sigma|\lambda|$, we find that (A.11) corresponds to

$$\left(\frac{\pi}{2} + \eta\right)|\lambda| = \pm C, \tag{A.13}$$

where σ and η are given by (A.5). Thus, the angular width of the region AB is

$$\Delta\epsilon = 2C/|\lambda| \ln (2|\lambda|/ex) \tag{A.14}$$

and the corresponding arc length $|\lambda|\Delta\epsilon$ tends to zero like $(\ln |\lambda|)^{-1}$. Similar results are valid for the other shaded regions.

It must be noted that, due to our choice of the phase in (A.3), A goes over into $-A$ and the phase of α changes by $2i\pi\lambda$ on crossing the line j', so that, in spite of appearances to the contrary, the representations for $H_\lambda^{(1)}(x)$, $H_\lambda^{(2)}(x)$ and $J_{-\lambda}(x)$ given in Fig. 15 are continuous across j', while that for $J_\lambda(x)$ changes. In particular, on j' itself, with $\lambda = -\mu$, we find

$$J_{-\mu}(x) \approx A(\mu, x)\{\sin (\pi\mu) \exp [-\alpha(\mu, x)]$$
$$+ \tfrac{1}{2} \cos (\pi\mu) \exp [\alpha(\mu, x)]\} \ (\mu > x), \tag{A.15}$$

where A and α are given by (A.1) and (A.2). Thus, $J_\lambda(x)$ has infinitely many zeros on j', located asymptotically very close to the negative integers.

The asymptotic expansions given in Fig. 15 should be employed for $|\lambda| \gg x$. For smaller values of $|\lambda|$, additional regions have to be considered (25). We shall require only a few additional results.

In region BE, in the neighborhood of the real axis, we may employ the Debye asymptotic expansions

$$H_\lambda^{(1,2)}(x) = (2/\pi)^{1/2}(x^2 - \lambda^2)^{-1/4}$$
$$\cdot \exp\left\{\pm i\left[(x^2 - \lambda^2)^{1/2} - \lambda \cos^{-1}\frac{\lambda}{x} - \frac{\pi}{4}\right]\right\} \tag{A.16}$$
$$\times \left[1 \mp \frac{i}{8(x^2 - \lambda^2)^{1/2}}\left(1 + \frac{5}{3}\frac{\lambda^2}{(x^2 - \lambda^2)} + \cdots\right) + \cdots\right],$$

where the upper signs refer to $H_\lambda^{(1)}(x)$ and the lower ones to $H_\lambda^{(2)}(x)$, and $(x^2 - \lambda^2)^{-1/4} > 0, 0 < \cos^{-1}(\lambda/x) < \pi/2$ for $-x < \lambda < x$.

These expansions fail in the neighborhood of $\lambda = \pm x$. If $|\lambda - x|$ becomes comparable with $|\lambda|^{1/3}$, we must employ the expansions (34, pp. 367, 446)

$$H_\lambda^{(1,2)}(x) = 2 \exp (\mp i\pi/3)(2/\lambda)^{1/3} A i[\exp (\pm 2i\pi/3)(2/\lambda)^{1/3}(\lambda - x)] + O(\lambda^{-1}), \tag{A.17}$$

$$J_\lambda(x) = (2/\lambda)^{1/3} A i[(2/\lambda)^{1/3}(\lambda - x)] + O(\lambda^{-1}), \tag{A.18}$$

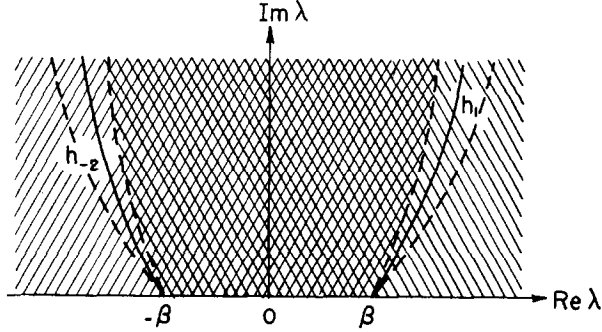where $Ai(z)$ denotes the Airy function, defined in Appendix D.

FIG. 16. Division of the λ plane into regions; ▧ Region 1 ▨ Region 2. The two regions overlap in the cross-hatched domain. The curves in broken line correspond to those of Fig. 15.

APPENDIX B. ASYMPTOTIC BEHAVIOR OF $g(\lambda, \beta, \rho)$

In order to prove (4.2), we note first that, according to (2.9) and (2.15),

$$g(-\lambda, \beta, \rho) = g(\lambda, \beta, \rho), \tag{B.1}$$

so that it suffices to study the asymptotic behavior in the upper half-plane. For this purpose, we shall subdivide it into two overlapping regions, as shown in Fig. 16.

In region 1, we may rewrite $g(\lambda, \beta, \rho)$ as

$$g(\lambda, \beta, \rho) = 2[J_\lambda(\beta)H_\lambda^{(2)}(\rho) - H_\lambda^{(2)}(\beta)J_\lambda(\rho)]. \tag{B.2}$$

Substituting J_λ and $H_\lambda^{(2)}$ by their asymptotic expansions, valid in regions A, AB and B of Fig. 15, we find

$$g(\lambda, \beta, \rho) \approx iA(\lambda, \beta)A(\lambda, \rho)\{\exp[\alpha(\lambda, \beta) - \alpha(\lambda, \rho)] \\ - \exp[-\alpha(\lambda, \beta) + \alpha(\lambda, \rho)]\}. \tag{B.3}$$

In region 2, $g(\lambda, \beta, \rho)$ may be rewritten as

$$g(\lambda, \beta, \rho) = 2e^{i\pi\lambda}[H_\lambda^{(1)}(\beta)J_{-\lambda}(\rho) - J_{-\lambda}(\beta)H_\lambda^{(1)}(\rho)]. \tag{B.4}$$

Substituting $H_\lambda^{(1)}$ and $J_{-\lambda}$ by their asymptotic expansions, valid in regions C, BC, and B of Fig. 15, we are led again to the same result (B.3). Taking into account (A.4), this yields

$$g(\lambda, \beta, \rho) \approx \frac{2i}{\pi\lambda}\left[\left(\frac{a}{r}\right)^\lambda - \left(\frac{r}{a}\right)^\lambda\right] \tag{B.5}$$

for $|\lambda| \to \infty$ in the whole upper half-plane. It then follows from (B.1) that

the same result is valid in the lower half-plane. This proves the validity of (4.2) in the whole λ plane.

APPENDIX C. ASYMPTOTIC BEHAVIOR OF THE LEGENDRE FUNCTIONS

The functions $Q_\nu^{(1)}(\cos\theta)$ and $Q_\nu^{(2)}(\cos\theta)$ employed in the present work are defined by

$$Q_\nu^{(1,2)}(\cos\theta) = \frac{1}{2}\left[P_\nu(\cos\theta) \pm \frac{2i}{\pi}Q_\nu(\cos\theta)\right], \tag{C.1}$$

where P_ν and Q_ν are Legendre functions of the first and second kind, respectively. We have the following relations (35):

$$P_\nu(\cos\theta) = Q_\nu^{(1)}(\cos\theta) + Q_\nu^{(2)}(\cos\theta), \tag{C.2}$$

$$Q_{\lambda-1/2}^{(1)}(-\cos\theta) = ie^{-i\pi\lambda}Q_{\lambda-1/2}^{(2)}(\cos\theta), \tag{C.3}$$

$$Q_{\lambda-1/2}^{(2)}(-\cos\theta) = -ie^{i\pi\lambda}Q_{\lambda-1/2}^{(1)}(\cos\theta), \tag{C.4}$$

$$P_{\lambda-1/2}(-\cos\theta) = ie^{-i\pi\lambda}P_{\lambda-1/2}(\cos\theta) - 2i\cos(\pi\lambda)Q_{\lambda-1/2}^{(1)}(\cos\theta), \tag{C.5}$$

$$P_{\lambda-1/2}(-\cos\theta) = -ie^{i\pi\lambda}P_{\lambda-1/2}(\cos\theta) + 2i\cos(\pi\lambda)Q_{\lambda-1/2}^{(2)}(\cos\theta). \tag{C.6}$$

Both $Q_{\lambda-1/2}^{(1)}$ and $Q_{\lambda-1/2}^{(2)}$ have poles at the negative half-integers, which are cancelled in $P_{\lambda-1/2}$.

If $\epsilon \leqq \theta \leqq \pi - \epsilon$, $|\lambda| \gg 1$, $|\lambda|\epsilon \gg 1$, the following asymptotic expansions are valid (35, pp. 237, 240):

$$Q_{\lambda-1/2}^{(1,2)}(\cos\theta) = \frac{\exp[\mp i(\lambda\theta - \pi/4)]}{(2\pi\lambda\sin\theta)^{1/2}}\left[1 \pm \frac{i\cot\theta}{8\lambda} + O(\lambda^{-2})\right], \tag{C.7}$$

$$P_{\lambda-1/2}(\cos\theta) = \left(\frac{2}{\pi\lambda\sin\theta}\right)^{1/2}$$
$$\cdot\left[\cos\left(\lambda\theta - \frac{\pi}{4}\right) + \frac{\cot\theta}{8\lambda}\sin\left(\lambda\theta - \frac{\pi}{4}\right) + O(\lambda^{-2})\right]. \tag{C.8}$$

If $0 \leqq \theta \leqq \epsilon$, $|\lambda|\epsilon \lesssim 1$, $|\lambda| \gg 1$, we may employ the expansion (35, p. 243)

$$P_{\lambda-1/2}(\cos\theta) = J_0(u) + \sin^2\frac{\theta}{2}\left[\frac{u}{6}J_3(u) - J_2(u) + \frac{J_1(u)}{2u}\right]$$
$$+ O\left(\sin^4\frac{\theta}{2}\right), \tag{C.9}$$

where

$$u = 2\lambda\sin\frac{\theta}{2}. \tag{C.10}$$

A uniform asymptotic expansion of the Legendre function[8] has been given by Szegö (36):

$$P_{\lambda-1/2}(\cos\theta) = \left(\frac{\theta}{\sin\theta}\right)^{1/2}$$

$$\cdot\left[J_0(\lambda\theta) + \frac{1}{8}(\theta\cot\theta - 1)\frac{J_1(\lambda\theta)}{\lambda\theta} + O(\lambda^{-2})\right]. \tag{C.11}$$

This reduces to (C.8) when $|\lambda|\theta \gg 1$ and remains valid for $\theta \to 0$.

In Section IX we made use of the inequality

$$|P_{i\mu-1/2}(\cos\theta)| \leqq (\cos\theta)^{-1/2}\exp(\pi\mu/2) \quad (\mu \geqq 0, 0 \leqq \theta < \pi/2). \tag{C.12}$$

To prove this inequality, we start from the integral representation (25, p. 387)

$$P_\nu(\cos\theta) = \frac{1}{\Gamma(\nu+1)}\int_0^\infty \exp(-t\cos\theta)J_0(t\sin\theta)t^\nu\,dt \tag{C.13}$$

$$(0 < \theta < \pi/2, \mathrm{Re}\,(\nu+1) > 0),$$

where $\Gamma(z)$ is the Gamma function. It follows that

$$|P_{i\mu-1/2}(\cos\theta)| \leqq \frac{1}{|\Gamma(i\mu+\frac{1}{2})|}\int_0^\infty \exp(-t\cos\theta)t^{-1/2}\,dt$$

$$= (\cos\theta)^{-1/2}\frac{\Gamma(\frac{1}{2})}{|\Gamma(i\mu+\frac{1}{2})|} = \left[\frac{\cosh(\pi\mu)}{\cos\theta}\right]^{1/2} \leqq \frac{e^{\pi\mu/2}}{(\cos\theta)^{1/2}}\left(0 \leqq \theta < \frac{\pi}{2}\right),$$

which proves (C.12).

APPENDIX D. THE AIRY FUNCTION

The Airy function is defined by

$$Ai(z) = \frac{3^{1/3}}{\pi}\int_0^\infty \cos(t^3 + 3^{1/3}zt)\,dt. \tag{D.1}$$

It can also be expressed in terms of Bessel functions of order $\frac{1}{3}$ (34, p. 446). We have

$$W[Ai(z), Ai(ze^{\pm2i\pi/3})] = e^{\mp i\pi/6}/2\pi, \tag{D.2}$$

where W denotes the Wronskian. Also,

$$Ai(z) + e^{2i\pi/3}Ai(ze^{2i\pi/3}) + e^{-2i\pi/3}Ai(ze^{-2i\pi/3}) = 0. \tag{D.3}$$

The asymptotic expansion of $Ai(z)$ for large $|z|$ is given by (34, p. 448)

---

[8] Cf. also (37). However, there are several mistakes in the expansion given in this reference.

$$Ai(z) \approx \frac{e^{-\zeta}}{2\pi^{1/2}z^{1/4}} [1 + O(\zeta^{-1})] \qquad\qquad (|\arg z| < \pi), \quad (D.4)$$

$$Ai(-z) \approx \pi^{-1/2}z^{-1/4} \left\{ \sin\left(\zeta + \frac{\pi}{4}\right) [1 + O(\zeta^{-2})] - \cos\left(\zeta + \frac{\pi}{4}\right) O(\zeta^{-1}) \right\} \quad (D.5)$$

$$(|\arg z| < 2\pi/3).$$

where

$$\zeta = \tfrac{2}{3}z^{3/2}. \tag{D.6}$$

The zeros of the Airy function are all located on the negative real axis. If $-x_n$ denotes the nth zero, we have, for large n (*34*, p. 450),

$$x_n = \left[\frac{3\pi}{2}\left(n - \frac{1}{4}\right)\right]^{2/3} [1 + O(n^{-2})] \qquad (n \gg 1), \quad (D.7)$$

$$Ai'(-x_n) \approx (-1)^{n-1}\pi^{-1/2}\left[\frac{3\pi}{2}\left(n - \frac{1}{4}\right)\right]^{1/6} \qquad (n \gg 1). \quad (D.8)$$

The first five values of x_n and the corresponding values of $Ai'(-x_n)$ are listed in Table I (*34*, p. 478).

APPENDIX E. THE LOMMEL FUNCTIONS

Lommel's functions of two variables (*25*, pp. 537–550) are defined by

$$V_\nu(u, v) = \cos\left(\frac{u}{2} + \frac{v^2}{2u} + \frac{\nu\pi}{2}\right) + \sum_{m=0}^{\infty} (-1)^m \left(\frac{u}{v}\right)^{2m-\nu+2} J_{2m-\nu+2}(v). \quad (E.1)$$

In particular,

$$V_0(u, u) = \tfrac{1}{2}[J_0(u) + \cos u], \qquad V_1(u, u) = -\tfrac{1}{2}\sin u, \quad (E.2)$$

$$V_0(u, 0) = 1, \qquad V_1(u, 0) = 0. \quad (E.3)$$

The following integral representation is valid:

$$V_\nu(u, v) + iV_{\nu-1}(u, v) = -\frac{v^{\nu-1}}{u^{\nu-2}} \int_1^\infty J_{1-\nu}(vt) \exp[iu(1 - t^2)/2]t^{-\nu+2}\, dt \quad (E.4)$$

$$(u > 0, v > 0, \operatorname{Re} \nu > \tfrac{1}{2}).$$

In particular,

$$\int_1^\infty J_0(vt) \exp(iut^2/2)t\, dt = (i/u) \exp(iu/2)[V_0(u, v) + iV_1(u, v)]. \quad (E.5)$$

For large $|u|$ and fixed v and ν, we may employ the asymptotic expansion

$$V_\nu(u, v) \approx \sum_{m=0}^{\infty} (-1)^m (v/u)^{\nu+2m} J_{-\nu-2m}(v). \quad (E.6)$$

TABLE I

THE FIRST FIVE ZEROS OF $Ai(-x)$

n	x_n	$Ai'(-x_n)$
1	2.33811	$+0.70121$
2	4.08795	-0.80311
3	5.52056	$+0.86520$
4	6.78671	-0.91085
5	7.94413	$+0.94734$

APPENDIX F. EVALUATION OF $f_r(k, \pi - \epsilon)$

To evaluate the first integral in (9.51), we may employ the expansion

$$\tan (\pi\alpha x) = i + 2i\sum_{n=1}^{\infty} (-1)^n \exp (2in\pi\alpha x), \qquad (\text{F.1})$$

which gives

$$\int_0^{\infty} \exp (-x^2)J_0(\omega x) \tan (\pi\alpha x)x \, dx = i \int_0^{\infty} \exp (-x^2)J_0(\omega x)x \, dx$$

$$+ 2i \sum_{n=1}^{\infty} (-1)^n \int_0^{\infty} \exp (-x^2 + 2in\pi\alpha x)J_0(\omega x)x \, dx. \qquad (\text{F.2})$$

According to Weber's integral formula (25, p. 393),

$$\int_0^{\infty} \exp (-x^2)J_0(\omega x)x \, dx = \tfrac{1}{2} \exp (-\omega^2/4). \qquad (\text{F.3})$$

On the other hand, by partial integration,

$$\int_0^{\infty} \exp (-x^2 + 2in\pi\alpha x)J_0(\omega x)x \, dx = -\frac{1}{(2n\pi\alpha)^2} + O(\beta^{-2}), \qquad (\text{F.4})$$

so that, finally,

$$\int_0^{\infty} \exp (-x^2)J_0(\omega x) \tan (\pi\alpha x)x \, dx = \frac{i}{2} \exp \left(\frac{-\omega^2}{4}\right) + \frac{i}{24\alpha^2} + O(\beta^{-2}), \qquad (\text{F.5})$$

where we have employed the well-known formula

$$\sum_{n=1}^{\infty} \frac{(-1)^{n+1}}{n^2} = \frac{\pi^2}{12}. \qquad (\text{F.6})$$

It is clear from the above calculation that, since we are neglecting terms of the order of β^{-2}, we may replace $\tan (\pi\alpha x)$ by i in all remaining integrals of (9.51).

To compute these integrals, we employ Hankel's formula (25, p. 393):

$$
\int_0^\infty \exp(-x^2) J_n(\omega x) x^{m-1} \, dx
$$
$$
= \frac{\Gamma((m+n)/2)}{2\Gamma(n+1)} \left(\frac{\omega}{2}\right)^n \exp\left(\frac{-\omega^2}{4}\right) \Phi\left(\frac{n-m}{2}+1, n+1, \frac{\omega^2}{4}\right), \tag{F.7}
$$

where $\Phi(a, b, z)$ is Kummer's confluent hypergeometric function.

Substituting the above results in (9.51), we get

$$
f_r(k, \pi - \epsilon) = -\frac{a}{2} e^{-2i\beta} \left\{ \left(1 + \frac{i}{4\beta}\right) \left[\exp\left(\frac{-\omega^2}{4}\right) + \frac{1}{12\alpha^2}\right] \right.
$$
$$
+ \frac{i}{6\beta} \exp\left(\frac{-\omega^2}{4}\right) \Phi\left(-2, 1, \frac{\omega^2}{4}\right) + \frac{1}{4} \sin^2 \frac{\epsilon}{2} \exp\left(\frac{-\omega^2}{4}\right) \tag{F.8}
$$
$$
\left. \cdot \left[\frac{\omega^4}{36} \Phi\left(1, 4, \frac{\omega^2}{4}\right) - \frac{\omega^2}{2} \Phi\left(1, 3, \frac{\omega^2}{4}\right) + \Phi\left(1, 2, \frac{\omega^2}{4}\right)\right] + O(\beta^{-2}) \right\}.
$$

It follows from the definition of $\Phi(a, b, z)$ that

$$
\Phi\left(-2, 1, \frac{\omega^2}{4}\right) = 1 - \frac{\omega^2}{2} + \frac{\omega^4}{32}. \tag{F.9}
$$

On the other hand, we have (38)

$$
\Phi(1, n+1, z) = n e^z z^{-n} \gamma(n, z), \tag{F.10}
$$

where $\gamma(n, z)$ is the incomplete gamma function, and

$$
\gamma(n, z) = (n-1)! \left(1 - e^{-z} \sum_{m=0}^{n-1} \frac{z^m}{m!}\right), \tag{F.11}
$$

so that

$$
\Phi(1, n+1, z) = \frac{n!}{z^n} \left(e^z - \sum_{m=0}^{n-1} \frac{z^m}{m!}\right). \tag{F.12}
$$

Substituting (F.9) and (F.12) in (F.8) and taking into account (9.52), we finally get

$$
f_r(k, \pi - \epsilon) = -\frac{a}{2} \exp\left(-2i\beta - \frac{\omega^2}{4}\right) \left[1 + \frac{i}{2\beta} - \frac{i\omega^4}{64\beta} + O(\beta^{-2})\right]. \tag{F.13}
$$

REFERENCES

1. G. N. WATSON, *Proc. Roy. Soc. (London)* **A 95,** 83 (1918).
2. H. BREMMER, "Terrestrial Radio Waves." Elsevier, Amsterdam, 1949.
3. V. A. FOCK, *J. Phys. (U.S.S.R.)* **9,** 255 (1945). Cf. also "Diffraction of Radio Waves Around the Earth's Surface." Publishers of the Academy of Sciences, U.S.S.R., Moscow, 1946.
4. W. FRANZ, *Z. Naturforsch.* **9a,** 705 (1954).
5. W. FRANZ, "Theorie der Beugung Elektromagnetischer Wellen." Springer, Berlin, 1957.
6. E. J. SQUIRES, "Complex Angular Momentum and Particle Physics." Benjamin, New York, 1964.
7. E. C. TITCHMARSH, "Introduction to the Theory of Fourier Integrals," 2nd ed., p. 60. Oxford Univ. Press, 1937.
8. W. FRANZ AND R. GALLE, *Z. Naturforsch.* **10a,** 374 (1955).
9. W. MAGNUS AND L. KOTIN, *Numerische Math.* **2,** 228 (1960).
10. J. B. KELLER, S. I. RUBINOW, AND M. GOLDSTEIN, *J. Math. Phys.* **4,** 829 (1963).
11. E. PFLUMM, New York Univ., Courant Inst. of Math. Sci., Div. Electromag. Res., Res. Rep. BR-35 (1960).
12. A. SOMMERFELD, "Partial Differential Equations in Physics," p. 215. Academic Press, New York, 1949.
13. B. R. LEVY AND J. B. KELLER, *Commun. Pure Appl. Math.* **12,** 159 (1959).
14. F. G. FRIEDLANDER, "Sound Pulses." Cambridge Univ. Press, 1958.
15. R. K. LUNEBURG, "The Mathematical Theory of Optics." Lecture Notes, Brown University, 1944.
16. M. KLINE, *Commun. Pure Appl. Math.* **4,** 225 (1951).
17. J. B. KELLER, R. M. LEWIS, AND B. D. SECKLER, *Commun. Pure Appl. Math.* **9,** 207 (1956).
18. P. M. MORSE AND H. FESHBACH, "Methods of Theoretical Physics," Vol. II, p. 1554. McGraw-Hill, New York, 1953.
19. A. SOMMERFELD, "Optics," p. 245. Academic Press, New York, 1954.
20. S. I. RUBINOW AND T. T. WU, *J. Appl. Phys.* **27,** 1032 (1956).
21. S. I. RUBINOW AND J. B. KELLER, *J. Appl. Phys.* **32,** 814 (1961).
22. S. O. RICE, *Bell System Tech. J.* **33,** 417 (1954).
23. E. C. J. VON LOMMEL, *Abh. der Bayer. Akad. Wiss., München* **15,** 233, 531 (1884–86); cf. also J. WALKER, "The Analytical Theory of Light." Cambridge, 1904; and G. PETIAU, "La Théorie des Fonctions de Bessel." CNRS, Paris, 1955.
24. T. T. WU, *Phys. Rev.* **104,** 1201 (1956).
25. G. N. WATSON, "Theory of Bessel Functions," 2nd ed., p. 268. Cambridge Univ. Press, 1962.
26. M. BORN AND E. WOLF, "Principles of Optics," p. 394. Pergamon Press, London, 1959.
27. D. S. JONES, "The Theory of Electromagnetism," p. 516. Pergamon Press, Oxford, 1964.
28. P. BECKMANN AND W. FRANZ, *Z. Naturforsch.* **12a,** 533 (1957).

29. N. A. Logan, "General Research in Diffraction Theory, I–II" (Lockheed Missiles and Space Co., Sunnyvale, California, 1959).

30. A. O. Barut and F. O. Calogero, *Phys. Rev.* **128,** 1383 (1962).

31. S. I. Rubinow, *Ann. Phys.* (*N.Y.*) **14,** 305 (1961).

32. S. Ciulli, Gr. Ghika, and M. Stihi, *Nuovo Cimento* **32,** 955 (1964).

33. "Handbuch der Physik," Bd. **25**/1, pp. 503, 504. Springer, Berlin, 1961.

34. "Handbook of Mathematical Functions." National Bureau of Standards, Washington, 1964.

35. L. Robin, "Fonctions Sphériques de Legendre et Fonctions Sphéroïdales," Tome II. Gauthier-Villars, Paris, 1958.

36. G. Szegö, *Proc. London Math. Soc.* (**2**) **36,** 427 (1934).

37. R. C. Thorne, *Phil. Trans. Roy. Soc. London* **A 249,** 597 (1957).

38. A. Erdélyi, W. Magnus, F. Oberhettinger, and F. G. Tricomi, "Higher Transcendental Functions," Vol. II, p. 136. McGraw-Hill, New York, 1953.